ESTIMATING LEAF AREA INDEX (LAI) OF BLACK WATTLE (*ACACIA MEARNSII*) USING LANDSAT ETM+ SATELLITE IMAGERY

Selamawit T. Ghebremicael

Submitted in

partial fulfillment of the academic requirements for the degree of

Master of Science

in Applied Environmental Sciences

School of Applied Environmental Sciences,

Faculty of Science and Agriculture

University of Natal, Pietermaritzburg

May, 2003

DECLARATION

The work described in this dissertation was carried out in the School of Applied Environmental Sciences, University of Natal, Pietermaritzburg, with the assistance of Institute for Commercial Forestry Research (ICFR) from August 2001 to February 2003, under the supervision of Dr Fethi Ahmed and co-supervision of Dr Colin Smith.

I hereby certify that the research work reported in this dissertation is the result of my own original investigation except where acknowledged.

Selamawit T. Ghebremicael
Pietermaritzburg.

Abstract

Leaf area index (LAI) is an important variable in models that attempt to simulate carbon, nutrient, water and energy fluxes for forest ecosystems. LAI can be measured either directly (destructive sampling) or by using indirect techniques that involve estimation of LAI from light penetration through canopies. Destructive sampling techniques are laborious, expensive and can only be carried out for small plots. Although indirect techniques are non-destructive and less time consuming, they assume a random foliage distribution that rarely occurs in nature. Thus a technique is required that would allow for rapid estimation of LAI at the stand level. A means of getting this information is via remotely sensed measurements of reflected energy with an airborne or satellite-based sensor. Such information on an important plant species such as *Acacia mearnsii* (Black Wattle) is vital as it provides an insight into its water use.

Landsat ETM+ images covering four study sites in KwaZulu-Natal midlands encompassing pure stands of *Acacia mearnsii* were processed to obtain four types of vegetation indices (VIs). The indices included: normalized difference vegetation index (NDVI), ratio vegetation index (RVI), transformed vegetation index (TVI) and vegetation index 3 (VI3). Ground based measurements of LAI were made using destructive sampling (actual LAI) and LAI-2000 optical instrument, (plant area index, PAI). Specific leaf area (SLA) and leaf area (LA) were measured in the field for the entire sample stands to estimate their LAI values. The relationships between the various VIs and SLA, actual LAI and PAI values measured by LAI-2000 were evaluated using correlation and regression statistical analyses.

Results showed that the overall mean SLA value of *Acacia mearnsii* was 8.28 m^2kg^{-1}. SLA showed strong correlations with NDVI ($r=0.71$, $\rho<0.01$) and RVI ($r=0.76$, $\rho<0.01$) and a moderate correlation with TVI ($r=0.66$, $\rho<0.05$). Regression analysis revealed that SLA had significant relationship with RVI ($R^2=0.59$) and NDVI ($R^2=0.51$). Actual LAI values showed strong correlation with PAI values ($r=0.86$) and the analysis revealed that 74 % of the variation in the relationship between actual LAI and PAI values could be explained by regression. PAI values were strongly correlated with NDVI ($r=0.75$,

$\rho<0.01$) and moderately correlated with RVI ($r=0.63$, $\rho<0.05$) and TVI ($r=0.58$, $\rho<0.05$). Actual LAI was strongly correlated with NDVI ($r=0.79$, $\rho<0.01$) and moderately correlated with RVI ($r=0.61$, $\rho<0.05$). Out of the various VIs examined in this study, NDVI was found to have a better relationship with actual LAI values ($R^2=0.62$) and with PAI values ($R^2=0.56$); while VI3 didn't show any significant relationship with SLA, PAI or actual LAI.

In conclusion, preliminary estimate of SLA of *Acacia mearnsii* could be obtained from RVI or NDVI. The relationship obtained between PAI and actual LAI values was satisfactory, thus the regression equation can be used to calibrate the LAI-2000 plant canopy analyzer. Because NDVI was observed to have a good relationship with actual LAI and PAI, LAI of *Acacia mearnsii* can be estimated from Landsat ETM+ satellite imagery with a reasonable degree of accuracy. These results can satisfactorily be used as inputs into models that attempt to estimate water use by *Acacia mearnsii*.

Acknowledgements

First of all I would like to thank Dr. Fethi Ahmed for supervising the entire project over the past two years. His friendly and enthusiastic approach has made this study a thoroughly enjoyable experience. His confidence in my ability has motivated and inspired me to always aim high, believe in myself and to specialize in GIS and Remote Sensing starting from scratch.

I would like to thank Dr Colin Smith of ICFR, co-supervisor of this project, for always making time available to assist and advice me throughout the project. I am really grateful for his words of encouragement, experience and knowledge of forestry proved to be valuable.

I would like to acknowledge the Human Resources Development (HRD) Program of the Government of Eritrea for sponsoring this project.

I would like to acknowledge ICFR, the Director and staff, for assisting me in locating suitable study sites, covering all my field data collection expenses and providing all the materials and labor needed for fieldwork. The time and effort of all ICFR staff in providing this information is appreciated. I am especially indebted to Steven Dovey for his assistance and cooperation during the tedious field data collection and through out the project.

I would like to thank Mondi Forests and the South African Wattle Growers Union (SAWGU) for providing me the digital maps of the study sites and for allowing me to do my research in their forest plantations and fell trees for sampling. Special thanks goes to Mr Mark Norris Rogers of Mondi Forests.

All the staff members of the Discipline of Geography of the University of Natal, Pietermaritzburg are thanked for their continuous professional support and encouragement throughout the course of the project in a very friendly approach.

Finally, I would like to thank my parents for their love, support and encouragement. Thanks for all the friends that I made during this masters course for their continued love and support.

Table of Contents

List of Tables

List of Figures

List of Abbreviations

3-PG	Physiological Processes Predicting Growth Model
3-PGS	Physiological Processes Predicting Growth Model (Spatial Version)
ABS	Absolute Value
ANOVA	Analysis of Variance
AVHRR	Advanced Very High Resolution Radiometer
CCWR	Computer Center for Water Research
CSIR	Council for Scientific and Industrial Research
CTVI	Corrected Transformed Vegetation Index
DBH	Diameter at Breast Height
DEM	Digital Elevation Model
DN	Digital Number
DWAF	Department of Water Affairs and Forestry
EM	Electromagnetic Spectrum
ETM+	Enhanced Thematic Mapper Plus
FOREST-BGC	Forest-Bio-Geo-Chemical
GIS	Geographic Information Systems
GPS	Global Positioning System
GVI	Green Vegetation Index
LA	Leaf Area
LAI	Leaf Area Index
LAI_e	Effective Leaf Area Index
Landsat 7	Satellite System Used to Gather Information about the Earth Surface
LSD	Least Significant Difference
MAI	Mean Annual Increment
MAP	Mean Annual Precipitation
MAT	Mean Annual Temperature
MGVI	Misra's Green Vegetation Index
MIR	Middle Infrared
MSS	Multi-Spectral Scanner
NDVI	Normalized Difference Vegetation Index

NIR	Near Infrared
NOAA	National Oceanographic and Atmospheric Administration
NRVI	Normalized Ratio Vegetation Index
NTE	Natal Tanning Extract
PAI	Plant Area Index
PAR	Photosynthetically Active Radiation
PCA	Principal Component Analysis
pET	Potential Evapotranpiration
PVI	Perpendicular Vegetation Index
REP	Red-Edge Position
RMSE	Root Mean Square Error
RVI	Ratio Vegetation Index
SAC	Satellite Applications Center
SARVI2	Soil and Atmosphere Resistant Vegetation Index
SAWGU	South African Wattle Growers Union
SEL	Standard Error of LAI
SEM	Standard Error of Mean Tip Angle
SLA	Specific Leaf Area
SMA	Spectral Mixture Analysis
SNR	Signal to Noise Ratio
SPOT	Systeme Pour l'Observation de la Terre
SQT	Square Root
SR	Simple Ratio
STDERR	Standard Errors of the Contact Frequencies
TM	Thematic Mapper
TMS	Thematic Mapper Simulator
TTVI	Thiam's Transformed Vegetation Index
TVI	Transformed Vegetation Index
VI	Vegetation Index
VI3	Vegetation Index 3
WAG	Water Use and Growth Model

Chapter 1: General Introduction

1.1 Introduction

Models provide ecologists with tools for extrapolating field measurements and integrating complex ecological information over space and time. This ability has become increasingly important as ecologists work at the broader scales of landscape and the globe, because the scale of most ecological measurements is millimeters to meters. Furthermore, an individual measurement provides only one piece of ecological information and cannot account for the complexity, interaction, and dynamic nature of an entire ecosystem or landscape (Johnston, 2000). The integration of geographic information system (GIS) with environmental models is emerging as a significant new area of GIS development and has been the topic of major conferences (Goodchild *et al.,* 1996). Other scientific tools, such as air photo interpretation, remote sensing, field measurements, laboratory experiments and multivariate or spatial statistics can be integrated with GIS to enhance the modeling (Goodchild *et al.,1993).*

As one of the several relatively simple simulation models that are based on major physiological processes behind water use and growth of forest stands that emerged recently physiological processes predicting growth (3PG), point model, is claimed to be a useful tool for water use by planners and forest managers (Dye, 2001a). Its potential usefulness for predicting water use and growth of forest plantations is currently being extensively tested around the world on a wide range of sites in Australia, New Zealand, Brazil, China, United Kingdom, USA, Portugal, Denmark, Vietnam and Chile (Dicks, 2001). In South Africa the decision of the Council for Scientific and Industrial Research (CSIR) to investigate the model led to several validation studies on *Pinus patula* and *Eucalyptus species.* Dye (2001a) assessed the ability of the model to predict growth and water use of *Pinus patula* at four widely separated test sites and the simulation results were very encouraging. A preliminary validation of the point model for *Acacia mearnsii* was also done by Dicks (2001).

The work already done on 3-PG is all on a point model. But a key to the ecological use of remote sensing has become the application of process models to derive a spatial ecosystem simulation model over large areas of terrain. This enables us to understand the interaction of radiation with a leaf and a canopy (Curran *et al.*, 1999). The ability of remote sensing to predict LAI, biomass and eventually water use over a large area is sought after by the forestry companies. Currently it is being tested by many researchers and the evaluation made by Mthembu (2001) on the use of remotely sensed VIs to estimate LAI of *Eucalyptus grandis x camaldulensis* can be mentioned as an example. In addition, the original 3-PG model has been modified to allow remotely sensed observations to be utilized as inputs to it. The modified model is called 3-PGS, the S symbolizing the use of satellite data in the model framework (Coops *et al.,* 1998). Currently this model is being tested for its validity in South Africa by the CSIR on *Eucalyptus grandis x camaldulensis* (Dye, 2001b).

Acacia mearnsii is one of the important commercial tree species in KwaZulu-Natal and has established itself as an aggressive invader throughout South Africa most notably in riparian zones (James, 1983). According to Dobson (2001) there are currently 130,000 ha of commercial plantation and an estimated 2,000,000 ha of weed wattle in South Africa. This species is a category two species that may henceforth only be grown in an area demarcated for that purpose (regulation 15B, DWAF, 1996).

LAI is defined as the total one-sided green leaf area per unit soil area ("number of leaf layers"), and it is regarded as a very important plant characteristic because photosynthesis takes place in the green plant parts (Clevers, 1988). LAI is a critical variable in models that attempt to simulate carbon, nutrient, water and energy fluxes for forest ecosystems, and specifically in modeling water use of *Acacia mearnsii* through 3-PGS. Thus techniques to rapidly estimate LAI over large areas are in great demand.

Formerly, most of the LAI measurements were done directly by tree cutting (destructive sampling). But these direct measurements are laborious, expensive and can only be carried out for small plots. In addition, using non-site-specific allometric equations to estimate

LAI and foliage production can cause large errors because carbon allocation to foliage is influenced by numerous environmental and ecological factors (Gower *et al.*, 1999).

There are also a number of techniques that are based on an interactive relationship between canopy structure and radiation interception. These techniques measure the gap fraction, i.e. the proportion of radiation that is not blocked by foliage in a range of azimuthal directions. LA is estimated using mathematical models with the gap fraction as an input parameter. These mathematical models often assume a random foliage distribution that rarely occurs (Cherry *et al.*, 1998). In addition, light sensors need to be placed within and above the forest canopy in order to measure the gap fraction. This limits the scale of sampling and its utilization. These instruments (one of them is LAI-2000) and techniques do not also provide timely or cost-effective ways to obtain this information over larger areas (Wolpert, 1999). Thus, a cost effective and accurate technique is required that would allow for rapid estimation of LAI at the stand level so that a large number of stand-level estimates of LAI could be collected in a relatively short period of time. A means of getting this information is via remotely sensed measurements of reflected energy with an airborne or satellite-based sensor.

Advances in the field of remote sensing presented possible methods for evaluating canopy characteristics including LA, density and canopy architecture. The most commonly used method of remote data acquisition is the use of multi-spectral images that are collected by satellites (e.g., Landsat ETM+) and processed to produce a measure of canopy reflectance (e.g., a vegetation index).

The LAI values obtained from remotely sensed data could be used to produce thematic maps of, for example, rates of photosynthesis, transpiration, respiration and nutrient uptake. Such thematic maps could then be combined with other spatial data in a GIS so that modeling can be performed. The ability to rapidly assess LAI using VIs from remotely sensed satellite imagery provides a means of establishing a correlation between LA and site factors. For example, it may be possible to predict improved growth returns from silvicultural practices such as fertilization, or irrigation predicting the extent to which LAI can be increased. LAI estimated from VI could be useful for examining seasonal changes in LAI and differences between treatments imposed on plantations. LAI is an important attribute of ecosystems and forest stands that are related to productivity (Franklin *et al.*, 2000). Above all LAI is a major input parameter for 3-PGS to estimate water use and growth of different species.

Water is one of the most important natural resources. Although water is a renewable resource it is also a finite resource and is distributed unevenly geographically and temporally. South Africa has a mean annual precipitation (MAP) of 475 mm., which is low in comparison with the world average of 868 mm (Department of Water Affairs, 1986). Runoff, South Africa's main source of water is even more variable, both seasonally and regionally (Anon, 2001). Quantification of the amount of water being consumed by commercial forests is very important since prediction of forest water use is necessary to measure its impact on catchment water yields. With rising concern over diminishing water resources, it is becoming ever more important to predict such impacts accurately, not only on a broad national scale, but also at the plantation scale where local site conditions may exert profound influence on long-term patterns of water use.

Dye (2001a) explained that current methods for estimating forest or plant water use are based on two different approaches. The first involves extrapolation of stream flow reduction from research catchments (Le Maitre *et al.,* 1996) that tried to model the consequences of uncontrolled invasion on water yields using geographic information system. The second approach involves simulation of forest water use using models (e.g., ACRU) that determine the rate of evaporation (Jewitt and Schulze, 1999). But this model is designed for use at a catchment scale rather than at forest stand scale, and its usefulness to natural resource managers and particularly forest managers is limited. The recent emergence of physiological process-based models like 3-PGS can overcome some of these limitations. Therefore, these models should be parameterized and validated over a wide range of important species and *Acacia mearnsii* is one of them. In the long term this will contribute to a fulfillment of the Water Act of No. 36 of 1998 (Government Gazette 20615, 1999) which makes provisions for the classification of various crops and land use practices as stream flow reduction activities, which are then subject to controls to ensure equity in water allocation.

On the other hand, according to Versfeld *et al.* (1998) one of the biggest threats to the water resources in South Africa is invasion of alien plants. Versfeld *et al.* (1998) indicated that a small subset of the invasion is responsible for most of the water use by invaders in this country. The most important species, by this standard, is *Acacia mearnsii* followed by *Acacia cyclops*. A recent estimate is that invading aliens cover 10 million ha, and use 3.3 billion cubic meters of water in excess of that used by native vegetation every year. This estimate for water use is based on models that make a number of assumptions and can therefore be regarded as only preliminary (Stein, 1999).

Therefore the importance of LAI, as a first and decisive step in estimating water use from 3-PGS, necessitates the need to use standard methods to obtain accurate ground truth estimates of LAI that are correlated to satellite-derived estimates. Thus the aim of this study is to explore the utility of Landsat ETM+ satellite imagery data for accurately estimating LAI of *Acacia mearnsii.*

1.2 Aim and Objectives

Despite the controversial status of *Acacia mearnsii* as a potential commercial tree that is cultivated for its bark and pulp and as an aggressive invader that needs to be removed by conservationists, little has been known about its biology, ecology and water use at stand and landscape scales. Most of the studies that have been done before focus at tree or regional level thus there is a great need for information about this species in particular its water use as estimated from 3-PGS through LAI by environmentalists, government agencies and commercial producers.

The aim of this study was to explore the utility of Landsat ETM+ by optimizing the relationship between the various VIs determined from the remotely sensed data, LAI values determined from direct field-based measurements (destructive sampling) and indirect field-based measurements (through the use of LAI-2000 optical instrument) for one specific species, *Acacia mearnsii*. Because LAI is a key variable in ecological models the results thereof, will assist in providing inputs to models such as 3-PGS.

The following are the specific objectives of the study.

a. To determine the SLA, LA and LAI of *Acacia mearnsii* (Black wattle) stands from four sites in KwaZulu-Natal province by destructive sampling.
b. To measure the PAI at the same sites using the LAI-2000 optical instrument.
c. To determine four different VIs by transforming remotely sensed Landsat ETM+ satellite imagery.
d. To assess the relationships between the various VIs obtained from remotely sensed imagery and SLA.
e. To assess the relationships between the various VIs obtained from remotely sensed imagery and LAI estimates from direct and indirect field-based measurements (destructive sampling and the LAI-2000 respectively).
f. To identify the best vegetation index for estimating LAI of *Acacia mearnsii* from remotely sensed data and develop a predictive equation for future use.

1.3 The Structure of the Thesis

The first chapter has introduced the rationale for undertaking this study by looking at the controversy of the status of *Acacia mearnsii* among environmentalists and forest managers. This formed a theoretical framework of why it is necessary to quantify the water use of *Acacia meansii* at stand-level. It was also explained why it is necessary to develop a sound methodology for estimating LAI first. Chapter two reviews the literature on the biological and physical characteristics of *Acacia mearnsii*, how it has been introduced and spread in South Africa with more emphasis on its advantages and disadvantages. Furthermore, the chapter gives the theoretical basis on how to estimate LAI using different techniques and the concept of different types of VIs is discussed briefly. Chapter three describes the study areas in terms of climate, topography, natural vegetation and soils. Chapter four discusses the methodology used in this study including the direct and indirect field based estimation of LAI and how to obtain remotely sensed VIs. In Chapter five the results of the three methods of estimating LAI are presented and discussed. Chapter six deals with conclusions and recommendations from this study.

Chapter 2: Literature Review

2.1 Introduction

This chapter provides an understanding of how *Acacia mearnsii* benefits society and how it impacts the environment and especially water resources of South Africa. Relevant remote sensing and LAI literature is presented, with specific emphasis on the estimation of LAI. Techniques for estimating LAI to be used in the study are reviewed, and lastly, the concepts of process-based ecological models and site quality are discussed.

2.2 Characteristics of *Acacia mearnsii*

Acacias belong to the family *Mimosaceae*. The name *Acacia* is derived from the Greek word 'akis' meaning "a sharp point" and relates to the sharp thorned species of tropical Africa and Western Asia that were the only known *Acacias* at the time that the name was published (Simmons, 1999).

There are three species of 'Wattle', *Acacia dealbata* (Silver Wattle), *Acacia decurrens* (Green Wattle) and *Acacia mearnsii* (Black Wattle) that originate from Australia and are now serious invaders in South Africa (Bromilow, 1995). *Acacia mearnsii* is an evergreen exotic species that grows above 20m in height (Sherry, 1971). It has dark-green, bi-pinnate leaves that have many raised glands; the bark is usually grey-brown to black, becoming rough in older trees (De Beer, 1986). The plant produces scented, pale yellow flowers between August and November (Stirton, 1987) followed by black seeds that have a whitish-yellow seed stalk.

Acacia mearnsii occurs naturally in southeastern Australia, where it forms part of the undergrowth in *Eucalyptus* forests, or grows in dense stands along roads (De Beer, 1986). It grows very well in high rainfall areas on deep, well-drained soils but establishes on shallow soils if there is sufficient water (Stirton, 1987). Literature explains that the first *Acacia mearnsii* seed was brought to South Africa from Australia in 1864 by John van der Plank, an English seafarer who settled on a farm in the Camperdown area in Natal

(De Beer, 1986; Stirton, 1987). The seed was distributed to travelers by van der Plank, which led to *Acacia mearnsii* spreading far from the original introduction locality (De Beer, 1986). It is not certain whether the trees in the Cape descended from the original van der Plank progeny, as there are other records of seed being received from Australia, in Cape Town, around the late 1800s. Records show that it was already in the Cape Town Botanical Gardens by 1858 (Stirton, 1987).

By 1880, *Acacia mearnsii* bark had been analyzed and discovered to be rich in tannins, compounds used in the process of tanning leather (Stirton, 1987). This information led to *Acacia mearnsii* being cultivated in vast plantations as a source for both firewood and the extraction of tannins from the bark. The commercial plantations in Natal soon became the center of a large and profitable export industry (De Beer, 1986). *Acacia mearnsii* is still grown for these purposes in Natal, where the industry thrive with additional markets for the wood in the paper manufacturing, charcoal, and parquet flooring industries (De Beer, 1986; Stirton, 1987). *Acacia mearnsii* is also extensively cultivated in East Africa, Zimbabwe, India, Japan, Brazil and China (James, 1987).

Acacia mearnsii is considered as one of the world's highest yielding sources of condensed tannins. The tannin extract has an array of other current and potential uses. These water-soluble phenolic compounds extracted from the bark have traditionally been used for converting animal skins into leather (Anon, 1998). They are also used for wood bonding adhesives, treatment for preventing the corrosion of metals (Anon, 1998; Duke, 1981) and as a conditioning agent for drilling mud.

Acacia mearnsii became popular for its quality pulp in recent years (Anon, 2000a). Apart from its commercial value, it could produce poles for fencing and house building, windbreaks or shade for stock, firewood for cooking and sale. In addition, as a legume it enriches the soil through the fixing of atmospheric nitrogen (James, 1983; Bromilow, 1995). Smith *et al.* (1992) identified *Acacia mearnsii* as a potentially useful species in mine site rehabilitation, because water use by trees on mining sites is viewed as a strategy for the reduction of acid rock drainage.

On the other hand, according to recent statistics, out of the hundreds of plant species, which have been introduced into South Africa, 161 are regarded invasive and many more are anticipated to become weeds. Of these, a number of species have been declared or proposed for declaration as noxious weeds (i.e., their removal is required by law), while others have been declared or proposed for declaration as invaders (i.e. their spread has to be controlled), (Stein, 1999). *Acacia mearnsii* is among those declared as invaders and it is categorized as category two species that may henceforth only be grown in areas demarcated for that purpose (regulation 15B, DWAF, 1996). James (1983) mentioned that *Acacia mearnsii* is regarded as a "green cancer" in places where it is spreading vigorously as a weed citing from (Little, 1983). It is a problem along watercourses where it can alter stream morphology (Rowntree, 1991) and reduce runoff. DWAF (1996) regard *Acacia mearnsii* as one of the species that have the most impact on the water resources of South Africa.

Acacia mearnsii propagates by means of seeds that can remain viable for at least 50 years in the upper soil horizons where they accumulate and can form densities as high as 20,000 seeds per square meter (De Beer, 1986). Due to its bark, a mature tree is fire resistant and its seeds are resistant to both disease and insects (Greenfell, 1976). Seeds are dispersed by birds and are waterborne and they can thus spread rapidly down streams, often forming dense, impenetrable thickets that obstruct watercourses (Henderson *et al.,* 1987). These thickets may also impede access, smoother indigenous vegetation, reduce grazing land and render areas aesthetically unpleasing (Macdonald and Jarman, 1985). Germination of the seeds is stimulated by fire, a common characteristic of plant species found in the Fynbos Biome, and form dense thickets in the burnt areas (De Beer, 1986; Macdonald, 1984). It has also been linked to extreme bank erosion and creation of debris dams. In addition it competes with natural vegetation for water, light, nutrients and space (Rowntree, 1991).

In view of the aim of the present research and the lack of information on water use by *Acacia mearnsii*, the following sections will discuss techniques and related studies on the water use of *Acacia mearnsii* at tree, stand and catchment scale.

2.3 Plant Water Use

Because water use varies widely from plant to plant, estimates are usually first derived for a single situation and then adapted for other plants. Furthermore, true water use varies depending upon many other factors. When calculated daily, the accuracy of estimates will change from day to day. However, these will usually average out over a week to ten days, and the sum over that period may be quite accurate.

There are many techniques used to measure or estimate plant water use. The use of water by plants can be estimated by calculating what is known as potential evapotranspiration (pET). This is the possible loss of water through evaporation and transpiration. Transpiration is the movement of water through a plant from the soil into the roots, up the stem, and out through the leaves. Simple calculations of pET can be based on sunshine, wind, temperature, and humidity. Soil type is also crucial in using pET to estimate water use and schedule irrigation (Anon, 1997). Many researchers attempted to measure or estimate the loss of water through evaporation and transpiration using different techniques for example the Penman Calculator. Dye *et al.* (2001) carried out a comparative study on the water use of wattle thickets and indigenous plant communities at riparian sites in the Western Cape and KwaZulu-Natal. They showed that annual evapotranspiration varies considerably in different riparian plant communities, and that one must consider the structural and physiological characteristics of both the pre-clearing and post-clearing vegetation in order to predict the net change in evapotranspiration.

Another simple way of measuring plant water use is the gravimetric method. Here the technique is to stop watering the plants and follow the change in weight over time. This is not quite equivalent to measuring transpiration, although it is interesting to express water consumption relative to the LAs that can be measured (Wullschleger *et al.*, 1998).

The Heat Pulse Velocity technique is also a practical means of measuring water uptake through the stems of trees. This technique uses a data logger with four sets of paired Teflon probes, each of which is capable of giving a point estimate of sap flux. Here it is possible to measure sap flow rates, and thus transportation, for individual trees. Smith *et al.* (1992)

estimated the average water use for an *Acacia mearnsii* tree (diameter 9.2cm) using this technique at approximately 30 l/day.

Apart from the above-mentioned techniques of estimating single plant water use, another indicator of plant water use is LA or leaf vigor. Total LA has significant effects on plant water loss. Leaf production or shedding is an important way by which plant species adjust their demand for water to current availability in a time scale of days (Passiura, 1982). As plants grow they increase their LA and consequently their water use.

Even though LA can be a good indicator of plant water use, it varies from species to species and depends on the environmental conditions. If plants would have the same allocation programs, the size of a plant would be the only determinant of LA and species effects on LA would be negligible. But this is not the case, because plant species show a large variation in their allocation of carbon to leaves, stems, and roots. Also the amount of carbon required for building a unit of LA, or SLA, varies across species. In general, species that have higher growth rates in terms of biomass have higher allocation to leaves and their leaves are thinner (higher SLA) resulting in even higher rates of LA increase (Cornelissen *et al.,* 1996).

The relationship between biomass and leaf vigor and water use is well understood and researchers have been trying to extrapolate them to a larger scale. As a result, recent international advances in understanding of physiological processes governing water use and growth in forest plantations have led to the development of relatively simple process-based models that offer great potential for advancing the knowledge of the hydrological impacts of forests. For example, a study was carried out in Hosakote, India and showed that in soil moisture limited conditions, the growth of Eucalyptus, expressed in terms of stand volume increment was essentially linearly related to the volume of water transpired (Calder and Dye, 2000). This allowed development of a simple water use and growth model (WAG), based not only on knowledge of the linearity between growth rate and water use, but also on knowledge of the soil moisture and tree size limits and controls (Calder and Dye, 2000).

Even though it is possible to measure the SLA and LA of individual trees, it is tedious and time consuming. Recent developments in the field of remote sensing have created a possibility of estimating leaf vigor or biomass production of plantations. Solar radiation reflected from a vegetation canopy and measured by satellite sensors results from interaction of photons traversing through the foliage medium, bounded at the bottom by a relatively participating surface. Therefore to estimate the canopy radiation regime, three important features must be carefully formulated. They are (1) the architecture of individual plants or trees and the entire canopy; (2) optical properties on physiological conditions (water status, pigment concentration); and (3) atmospheric conditions which determine the incident radiation field (Knyazikhin *et al.*, 1999).

2.4 Leaf Area Index

LAI is defined as the total single-side LA per unit ground area (Deblonde *et al.,* 1994; Gower and Norman, 1991; Pierce and Running, 1988) and as such is a dimensionless index (Watts *et al.,* 1976; Wells, 1990). LAI is a biophysical variable that describes canopy structure and is related to functional process rates of energy and mass exchange. These products are essential in calculating terrestrial energy, carbon, water cycle processes, and biogeochemistry of vegetation (Boyd *et al.,* 2000). Thus it is a variable, which is frequently used by forest managers, agronomists, crop physiologists and crop modelers.

The importance of LAI as a surface variable is seen in widespread applications ranging from biomass productivity models (McLeod and Running, 1988) to radiative transfer studies (Lang, 1987; Norman and Campbell, 1989), site water balance (Grier and Running, 1977) and to studies involving remotely sensed data (Spanner *et al.*, 1990). The determination of LAI is especially important in the context of the recent shift to large-scale intensive studies attempting to link remotely sensed data to ground-based measurements (Eklundh *et al.,* 2001; Fassanacht *et al.*, 1997).

Many relationships have been established between LAI and a range of ecological processes: rates of photosynthesis (Beadle *et al.*, 1998), transpiration and evapotranspiration (Grier and Running, 1977), rainfall interception (Beymer, 2001), aboveground net primary production (Gholz, 1982) and rates of energy exchange between plants and the atmosphere (Botkin, 1986). Measurements of LAI have been used to predict future growth and yield and to monitor changes in canopy structure due to pollution and climate change (Waring, 1985). Accurate estimates of LA are required if changes in LA or growth efficiency resulting from acid deposition are to be detected (Burton *et al.*, 2000). The LAI product is an input to Biome-BGC (Biogeochemical) models, it is also a state parameter in all models describing the exchange of fluxes of energy, mass (water and carbon dioxide), and momentum between the surface and the planetary boundary layer (Boyd *et al.*, 2000). The ability to estimate LAI is therefore a valuable tool in modeling the ecological processes occurring within a forest and in predicting ecosystem responses. Leaves are the primary sites of energy and mass exchange within the forest environment, and therefore the interception of radiation and the process of evapotranspiration are proportional to LAI (Pierce and Running, 1988). McNaughton and Jarvis (1983) have shown that LAI is important in canopy scale estimates of evapotranspiration.

In general terms, all leaves have similar features- an epidermis, mesophyll, vascular tissue and stomata. However, the arrangement of these four components is, to a large extent, dictated by the physical environment- water availability, light intensity and ecological niche. Thus it is the interplay of these environmental parameters that serve to modify leaf structure. Therefore having detailed information about LAI can help characterize the physical environment and plants' reaction to it (Anon, 2000b).

2.4.1 Methods of Estimating LAI

Accurate estimates of LAI are needed in ecosystem analysis because of the importance of canopy structure in gas, water, carbon and energy exchange. Methods to rapidly obtain accurate estimates of LAI in forests are needed as ecologists attempt to scale-up ecosystem processes from the stand to the landscape level to address pressing regional and ecological questions.

2.4.1.1 Direct Field-based LAI Estimation (Destructive Sampling)

Many methods are available to measure LAI directly and are variations of either leaf sampling or litter fall collection techniques (Chason *et al.,* 1991; Clough *et al.,* 1997). There are problems associated with both however: leaf sampling involves the destructive harvesting of representative branches and trees, and using allometric relationships between LA and stem characteristics and measurement of LA for all leaves within a vertical quadrat down through the entire canopy. LA is usually determined directly for individual leaves using automatic leaf area meters, leaf area-leaf dimensions relations, or leaf area-weight ratios (Norman and Campbell, 1989). Litter fall collection is better suited to deciduous forests that have a single leaf fall as opposed to evergreen canopies. All direct methods are similar in that they are difficult, extremely labor intensive, require many replicates to account for spatial variability in the canopy and are therefore costly in terms of time and money.

2.4.1.2 Indirect Field-based LAI Estimation (Optical Instruments)

Indirect methods of determining LAI relate total LA to the radiation environment below the canopy and are generally less time consuming as well as non-destructive. Many indirect methods of measuring LAI have been developed (Nel and Wessman, 1993) because of the difficulties with direct methods. These methods are based on the Beer-Lambert Law or gap fraction theory (Miller, 1967). Techniques based on gap-fraction analysis assume that LA can be calculated from the canopy transmittance (the fraction of direct solar radiation which penetrates the canopy). This approach to measuring LAI uses data collected from along transects beneath the forest canopy (Nel and Wessman, 1993). Most analytical methods for determining LAI assume that canopy elements are randomly dispersed in space. In reality, canopies exhibit some degree of clumping and the assumption of randomness results in a large source of error (Norman and Campbell, 1989). Some of the instruments commonly used in these analytical methods are AccuPAR Ceptometer, CI-100 plant canopy analyzer (McPherson and Peper, 1998), Ag vision pseudo-color system (Lindsey and Bassuk, 1992), multiband vegetation imager (Kucharik *et al.*, 1997), and LAI-2000 plant canopy analyzer. LAI-2000 was used in this study and will be described in detail below in the following paragraphs.

LAI-2000 Plant Canopy Analyzer

The LAI-2000 (LI-COR, 1990) is a portable integrating radiometer, which provides a non-destructive means of intercepted light not only by the leaves but also by branches, stems and reproductive structures. Such measures estimate PAI, (Cermăk, 1989) thus it is called an effective LAI (LAI_e) rather than LAI (Chen and Black, 1992).

The LAI-2000 calculates PAI for broad canopies, foliage density for isolated canopies, mean foliage inclination angle and the fraction of the sky visible from beneath the canopy from radiation measurements made with a "fish-eye" optical sensor (148° field-of-view). Measurements made above the canopy and below the canopy are used to determine canopy light interception at 5 angles, from which PAI is computed using a model of radiative transfer in vegetative canopies (LI-COR, 1990).

Measures of PAI can provide continuous estimates of actual LAI, enabling time-series studies not possible with destructive sampling. The PAI measured using the LAI-2000 is generally lower than actual LAI and this is probably due to deviations from four theoretical assumptions used in calculating PAI. The most critical assumption made is that no radiation is reflected or transmitted by the foliage. Optical filters incorporated in the LAI-2000 sensors reject light above 490 nm and in the portion of the spectrum seen by the sensors; there is relatively little reflection or transmission by the foliage. The second assumption is that the foliage is randomly distributed. The third and fourth assumptions are, respectively, that the foliage elements are small and that the foliage is azimuthally randomly oriented (LI-COR, 1990). Forest and plantation canopies do not conform exactly to these assumptions because branches and leaves are clumped and are not optically black, leading to the underestimation of LAI. Because of these deviations from the theoretical assumptions, it is necessary to calibrate the LAI-2000 so that measured PAI can be used to predict true LAI (Cherry *et al.*, 1998).

The simplest way to derive factors to convert LAI_e to actual LAI is by comparing LAI-2000 output with LAI values derived from foliar biomass measurements. It is also possible to derive empirical formulae that relate LAI_e to actual LAI. For instance, to obtain LAI in conifer stands using LAI 2000, Chen (1996) derived factors to convert readings from the LAI-2000 to actual LAI estimates. LAI_e was related to LAI according to the following equation.

$$LAI = [(1-\alpha)\, LAI_e\, (\gamma_E/\Omega_E)] \quad \text{[Eq. 2.1]}$$

Where α is the ratio of woody surface area (i.e. boles, branches and cones) to total surface area; γ_E is the shoot clumping factor (ratio of total needle to shoot area); Ω_E is the proportion of foliage clumping at large scales than the shoot (i.e. branches and whorls); and γ_E/Ω_E is the total stand clumping index (Ω)[1] accounting for foliage clumping at all scales and equals unity when foliage distribution is random (Barclay *et al.*, 2000). The factors are difficult to measure directly and the output of the LAI-2000 is an integrated measurement over all these factors. Therefore, the simplest way to derive factors to convert LAI-2000 output to actual LAI is by comparing LAI-2000 output with LAI values derived from foliar biomass measurements.

The LAI-2000 is well suited for taking large numbers of samples in short time periods, even in tall canopies. It has been used in a number of studies: Chason *et al.* (1991) oak-hickory forest; Fassnacht *et al.* (1994) coniferous canopies; Grantz *et al.* (1993) cotton; Runyon *et al.* (1994) coniferous and deciduous stands; Wang *et al.* (1992) oak forest and Yang *et al.* (1993) oak forest. The ability to rapidly assess LAI using LAI-2000 provides a means of establishing a correlation between LA and site factors. For example, it may be possible to predict improved growth returns from silvicultural practices such as fertilization or irrigation by predicting the extent to which LAI can be increased (Battaglia *et al.*, 1997). LAI estimated by the LAI-2000 is also useful for examining seasonal changes in LAI and differences between treatments imposed on plantations. The instrument also offers the opportunity of time-series measurements for following impacts of defoliation

[1] Clumping index is an index that accounts for foliage clumping at all scales and clumping is the gathering of leaves into clusters along the branches.

and the effectiveness of pesticides or other measures in controlling defoliation. Several factors, for example, plot size, tree height and the distribution of canopy gaps should be considered prior to measurement, which must be undertaken under diffuse light conditions.

2.5 Remote Sensing and Image Analysis

Remote sensing in a broad sense is the acquisition of information about an entity without being in physical contact with it and it includes photography and videography as well as other imaging systems (Johnston, 2000). Remote sensing techniques measure the intensity of sunlight reflected from the Earth at different wavelengths. Radiation that is not reflected is absorbed or transmitted and thus each object has its own unique spectrum (Barrett and Curtis, 1976; Cracknell and Hayes, 1991).

All remote sensing methods detect electromagnetic energy, which includes familiar forms as visible light, x-rays, ultraviolet rays, television waves, and radio waves (Sabins, 1997). However all the electromagnetic spectrum is very broad and not all wavelengths are equally effective for remote sensing purposes. Green, red and near infrared wavelengths provide good opportunities for gauging earth surface interactions (Eastman, 1995).

Remotely sensed data from satellite can show larger land areas and, as a satellite regularly passes over the same plot of land capturing new data each time, changes in the land can be monitored (Evans, 1997). Remote sensing systems are of two general types: passive (optical) and active (radar) depending on the sensor. In order to classify vegetation, optical sensors measuring the visible and near/middle infrared spectrum are commonly used (Lillesand and Kiefer, 2000).

Satellite imagery is digital and made of pixels, the size of which determines the spatial resolution. The pixel size differs for different satellites depending on the sensor and the characteristics of the orbit (Luckie, 1990; Perryman, 1996). Satellite images can provide data about plant communities and environmental conditions, but are unsuitable for individual plants (Leysen and Goosens, 1991).

A number of countries have launched satellites for image acquisition; some of the commonly known satellite systems include Landsat multi-spectral scanner (MSS) imagery (80 m resolution), Landsat thematic mapper (TM) imagery (30 m resolution), Landsat ETM+ panchromatic (15 m resolution) and multi-spectral imagery (30 m resolution), SPOT panchromatic (10 m resolution) and multi-spectral imagery (20 m resolution) and national oceanographic and atmospheric administration (NOAA) advanced very high resolution radiometer (AVHRR) imagery (1.1 km resolution). Because Landsat ETM+ was used in this study, its detailed background information is presented.

2.5.1 Landsat Satellites and Imagery

Landsat was the first non-military satellite image acquisition program. The U.S. launched Landsat-1, -2, and -3 in 1972, 1975, and 1978, respectively, and each was decommissioned about 5 years after launch. These early Landsat satellites carried MSS sensors. Subsequent Landsat satellites carried TM scanners in addition to MSS scanners. TM imagery has also much finer spatial resolution than its Landsat predecessors, which is desirable for ecological applications and vegetation discrimination. In particular, the incorporation of the middle infrared bands (bands 5 and 7) has greatly increased the vegetation discrimination of TM data. Landsat satellites have sun-synchronous orbits with a 16-day repeat cycle for each satellite, but the orbits of Landsat-4 and Landsat-5 were established 8 days out of phase, such that an 8-day cycle could be maintained with alternating coverage by each satellite (Lillesand &Kiefer, 2000).

Landsat-7 was launched on April 15, 1999. The earth-observing instrument onboard in this spacecraft is the enhanced thematic mapper Plus (ETM+). General characteristics of Landsat ETM+ and TM satellites and imageries are described in Table 2.1.

Table 2.1 General characteristics of Landsat ETM+ and TM satellites

Property		**Landsat ETM+**	**Landsat TM**
Ground Sampling Interval (GSI) (pixel size)	Bands 1-5 & 7 Band 6 Band 8	30 x 30 m 60 x 60 m 15 x 15 m pixel size (18 x 18m GSI)*	30 x 30 m 120 X 120 m N/A
Swath width		185 km	185 km
Repeat coverage interval		16 days (233 orbits)	16 days (233 orbits)
Altitude		705 km	705 km
Quantisation		Best 8 of 9 bits	8 bits (256 levels)
On-board data storage		375 Gb (solid state)	Magnetic tape failed
Orbit type		Sun-synchronous	Sun-synchronous
Inclination		98.2°	98.2°
Equatorial Crossing		Descending node: 10:00am	Descending node: 10:10am

Source: Anon, 2002

*ETM+ band 8 (panchromatic) was designed to be acquired at 15m resolution, but post-launch testing shows a ground sampling interval closer to 18m.

The design of ETM+ stresses the provision of data continuity with Landsat-4 and 5. Similar orbits and repeat patterns are used, as is the system designed to collect 15-m-resolution "panchromatic" data and six bands of data in the red, near infrared, and middle infrared spectral regions at a resolution of 30m. A seventh thermal band is incorporated with a resolution of 60m (Lillesand &Kiefer, 2000). Table 2.2 shows the spectral range and general application of the different bands of Landsat TM and ETM+ satellite images.

Table 2.2 Radiometric characteristics of the ETM+ and TM sensors

Band Number	Spectral Range (Microns)	EM Region	Generalized Application Details
1	0.45 - 0.52	Blue	Coastal water mapping, differentiation of vegetation from soils
2	0.52 - 0.60	Green	Assessment of vegetation vigor
3	0.63 - 0.69	Red	Chlorophyll absorption for vegetation differentiation
4	0.76 - 0.90	Near Infrared	Biomass surveys and delineation of water bodies
5	1.55 - 1.75	Middle Infrared	Vegetation and soil moisture measurements; differentiation between snow and cloud
6	10.40- 12.50	Thermal Infrared	Thermal mapping, soil moisture studies and plant heat stress measurement
7	2.08 - 2.35	Middle Infrared	Hydrothermal mapping
8	0.52 - 0.90 (panchromatic)	Green, Red, Near Infrared	Large area mapping, urban change studies

Source: Anon, 2002

The application of Landsat image interpretation has been demonstrated in many fields, such as agriculture, botany, cartography, civil engineering, environmental monitoring, forestry, geography, geology, geophysics, land resource analysis, land use planning, oceanography, and water resource analysis (Campbell, 1987).

2.5.2 Vegetation Indices

VIs are derived from multi-spectral data based on the differences in absorption, transmittance and reflectance of energy by vegetation in the red and near infrared bands (Fung and Siu, 2000). They are dimensionless, radiometric measures usually involving a ratio and/ or linear combination of the red and near infrared portions of the spectrum.

VIs have been employed in two separate types of research. The first type is used to establish use of VIs as a means of remote monitoring of the growth (Sellers, 1985) and productivity of specific crops (Asrar *et al.*, 1985) or of seasonal and yearly fluctuations in productivity. Results of such studies have in general confirmed the usefulness of quantitative uses of VIs, but details vary with the specific crop considered, atmospheric conditions, and local agricultural practices. The second type of application uses VIs as a mapping device, much more of a qualitative, rather than a quantitative tool. Such applications use VIs to assist in image classification, to separate vegetated from non-vegetated areas, and to distinguish between different types and densities of vegetation (Price, 1992), and to monitor seasonal variations in vegetative vigor, abundance and distribution (Campbell, 1987). For example, Weber and Dunno (2001) used VIs for evaluating riparian vegetation vigor and spatial extent in north central Arizona.

Because of the strong effects of eco-climatic variables on vegetation parameters, the relationship between VIs and eco-climatic variables such as precipitation, temperature, a series of soil properties and crop transpiration have also been studied in numerous locations (Davenport and Nicholson, 1993; Farrar *et al.*, 1994; Nicholson and Farrar, 1994). In addition, research has shown that VIs can also be used for effective monitoring of rainfall and drought situations and they might also have indirect relationship with water discharge and sediment transport (Lu *et al.,* 2000). Factors such as precipitation, vegetation, soil type and soil moisture that influence spectral reflectance of the vegetation cover also affect soil erosion dynamics. This also suggests that it may be possible to directly monitor soil erosion and sediment transport using remotely sensed data.

Sets of VIs have been designed to provide a quantitative assessment of green vegetation biomass. The proposed VIs are applicable to both low and high spatial resolution satellite images, such as NOAA AVHRR, Landsat TM and MSS, Landsat ETM+, SPOT HRV/XS, and any other similar systems that sense in the red and near infrared regions of the electromagnetic spectrum.

2.5.3 Classification of Vegetation Indices

VIs can be grouped into two categories: as slope-based and distance-based VIs. To appreciate this distinction, it is necessary to consider the position of individual vegetation pixels in a two-dimensional graph (or bi-spectral plot) of red versus infrared reflectance (Eastman, 1999).

2.5.3.1 Slope-based Vegetation Indices

The slope-based VIs are simple arithmetic combinations that focus on the contrast between the spectral response patterns of vegetation in the red and near infrared portions of the electromagnetic spectrum. They are so named because any particular value of the index can be produced by a set of red/infrared reflectance values that form a line emanating from the origin of a bi-spectral plot. Thus different levels of the index can be envisioned as producing a spectrum of such lines that differ in their slope (Eastman, 1999). In slope-based VIs the values indicate both the status and abundance of green vegetation cover and biomass. The Slope-based VIs include NDVI, RVI, TVI, normalized ratio vegetation index (NRVI), corrected transformed vegetation index (CTVI), and Thiam's transformed vegetation index (TTVI). In this study the main focus is on the most commonly used slope-based VIs that were used to ascertain the use of satellite imagery for estimating LAI values. Therefore some of them will be discussed in detail.

Ratio Vegetation Index

The RVI was proposed by Rouse *et al.* (1974) to separate green vegetation from soil background using Landsat MSS imagery. Simply dividing the reflectance values contained in the near infrared band by those contained in the red band produces the RVI. Thus the index is computed using the following formula:

$$RVI = NIR/RED \qquad [Eq. 2.2]$$

Where NIR and RED are the near infrared and red bands, respectively. The result clearly captures the contrast between the red and near infrared bands for vegetated pixels, with high index values being produced by combinations of low red and high near infrared reflectance. In addition, because the index is constructed as a ratio, problems of variable illumination as a result of topography are minimized. However the index is susceptible to division by zero errors and the resulting measurement scale is not linear. As a result, RVI images do not have a normal distribution, making it difficult to apply some statistical procedures (Eastman, 1999).

Normalized Difference Vegetation Index

The NDVI is one of the earliest and perhaps most popular VIs. It is an ideal index, as it is sensitive to the green part of the plant canopy only. To gain accurate VIs, reflectance values may be corrected to reduce the effects of atmosphere. This index was also defined by Rouse *et al.* (1974) and it compensates for changing illumination conditions, surface slope, aspect and other extraneous factors. For example, forest and agricultural land will display medium to dark grey, and soil will show as light grey. High values will be displayed for vegetation, because of the high near infrared reflectance and the low red reflectance. Furthermore, the measurement scale has a desirable property of ranging from –1 to 1 with 0 representing the approximate value of no vegetation and thus negative values represent non-vegetated surfaces. Mathematically, NDVI can be expressed as follows:

$$NDVI = (NIR-RED) / (NIR+RED) \qquad \text{[Eq. 2.3]}$$

Where NIR and RED represent the near infrared and red bands, respectively.

Transformed Vegetation Index

The TVI proposed by Deering *et al.* (1975) modifies the NDVI by adding a constant of 0.5 to all its values and taking the square root (SQT) of the results. The constant 0.5 is introduced in order to avoid operating with negative NDVI values. The calculation of the SQT is intended to correct NDVI values that approximate a poisson distribution and introduce a normal distribution. The use of the TVI requires that the minimum input values be greater than –0.5 to avoid aborting the operation. Negative values will still remain if values less than –0.5 are found in the NDVI. Also there is no technical difference between NDVI and TVI in terms of image output or active vegetation detection (Campbell, 1987).

$$TVI = SQT\ [(NIR-RED) / (NIR+RED) + 0.5] \qquad \text{[Eq. 2.4]}$$

Corrected Transformed Vegetation Index

The CTVI proposed by Perry and Lautenschlager (1984) aims at correcting the TVI. Clearly adding a constant of 0.5 to all NDVI values does not always eliminate all negative values as NDVI values may have the range –1 to 1. Values that are lower than –0.5 will leave small negative values after the addition operation. Thus the CTVI is intended to resolve this situation by dividing (NDVI+0.5) by its absolute value (ABS) (NDVI+0.5) and multiplying the result by the square root of the absolute value. This suppresses the negative sign. The correction is intended to eliminate negative values and generate a VI image that is similar to, if not better than, the NDVI (Lillesand and Keifer, 2000).

$$CTVI= \frac{(NDVI+0.5)}{ABS\ (NDVI+0.5)} \times SQT\ [ABS(NDVI+0.5)] \qquad [Eq.\ 2.5]$$

Where ABS is the absolute value and SQT the square root.

2.5.3.2 Distance-based Vegetation Indices

In contrast to the slope-based category, the distance-based category measures the degree of vegetation present by gauging the difference of any pixel's reflectance from the reflectance of bare soil. A key concept here is that a plot of the positions of bare soil pixels of varying moisture level in a bi-spectral plot will tend to form a line (known as a soil line). All the members of this category (such as the perpendicular vegetation index, PVI) thus require that the slope and intercept of the soil line be defined for the image being analyzed. These VIs are particularly important in arid and semi-arid environments.

The PVI suggested by Richardson and Wiegand (1977) is the parent index from which the entire category is derived. The PVI uses the perpendicular distance from each pixel coordinate to the soil line. Attempts to improve the performance of the PVI have yielded three other VIs suggested by Perry and Lautenschlager (1984), and Qi *et al.* (1994). In order to avoid confusion, the derived PVIs are indexed 1 to 3, (PVI_1, PVI_2 and PVI3).

In addition to the slope-based and distance-based categories of VIs, a third category can be added called orthogonal transformation VIs. Orthogonal indices undertake a transformation of the available spectral bands to form a new set of uncorrelated bands within which a green vegetation band can be defined. VIs under this category include principal component analysis (PCA), green vegetation index (GVI) of the tasseled cap (Kauth and Thomas, 1976) and Misra's green vegetation index (MGVI), which was proposed by Misra *et al.* (1977).

The validity of VIs can be evaluated in the same way as any instrument with the help of a single number, called "Signal to Noise Ratio" (SNR). This numerical value is estimated by dividing the typical range of variation in the signal by the typical amount of noise of variation due to one or more causes, the higher the number the better (Campbell, 1987).

Other than the above-mentioned VIs, which are derived from the red and near infrared bands of the spectrum, recently it has been suggested that including middle infrared band may improve the ability to remotely sensing the LAI values of forests. It is believed that the middle infrared helps to reduce errors caused by understorey and soil types (Nemani *et al.*, 1993). Thus different researchers are trying to come up with new VIs or are modifying the existing ones by replacing the red by middle infrared band. For instance, Kaufman and Remer (1994) cited by Boyd *et al.* (2000) developed a new VI called VI3. It is computed by the formula:

$$VI3 = (NIR - MIR) / (NIR + MIR) \quad \text{[Eq. 2.6]}$$

Where NIR and MIR represent the near infrared and middle infrared bands respectively.

In the middle infrared, light absorption by plants is relatively high, and the optical properties of a canopy can be compared with that of the red region (Miller *et al.*, 1984). Saturation of the reflectance is observed at relatively low LAI in both red and middle infrared wavelength intervals (Ahlrichs and Bauer, 1983; Leamer *et al.*, 1978). There is greater contrast between leaf and soil in the red than in middle infrared if the soil is dry and less if it is wet. Consequently, variations in surface moisture have a larger effect on the response of a plant canopy in the middle infrared than in the red.

Despite the large number of VIs currently in use, it is clear that much needs to be learnt about the application of these indices in different environments and in addition to the near infrared and red bands other bands (e.g., middle infrared band) should be assessed for their capability in estimating biophysical characteristics. It is because of this that the VI3 have been proposed. However, it needs further work and modification.

2.6 Previous Works on Vegetation Indices and LAI

The use of a near infrared to red ratio method for estimating biomass and LAI was first reported by Jordan (1969) who used a radiance ratio of 0.800/0.675 μm to derive the LAI for forest canopies in a tropical rain forest. Subsequent work was reported by Pearson and Miller (1972) who developed a hand-held spectral radiometer for estimating grass canopy biomass. The near infrared to red ratio method has been applied to Landsat image analysis of range biomass by Rouse *et al.* (1973, 1974) and Maxwell (1976), among others. Wiegand *et al.* (1974) tried to relate spectral observations to LAI and concluded that Landsat MSS (7-5) and MSS (5/7) in addition to MSS 7 and MSS 6 bands would be practical indicators of plant cover and density. Model simulation done by Bunnik (1981) show that VIs may be useful for estimating plant cover, but are only slightly sensitive for variations in LAI after complete plant cover has been reached. This is also confirmed by the results of Asrar *et al.* (1984), Hatfield *et al.* (1984), and Holben *et al.* (1980).

VIs have long been used for change detection purposes. Angelici *et al.* (1997) used the difference of band ratio data and the threshold technique to identify changed areas. Banner and Lynham (1981) used a VI difference and the threshold technique to locate forest clear cuts. Nelson (1983) tested the VI difference method quantitatively in the study of gypsy moth defoliation in Pennsylvania. In a comparative study by Singh (1989), the NDVI differencing technique was identified as among the few most accurate change detection techniques. Lyon *et al.* (1998) used Landsat MSS data for land-cover change detection in part of the state of Chiapas, Mexico.

The use of AVHRR NDVI has also provided a powerful tool to monitor the phenology of ecosystems in large regions (Running *et al.*, 1995) and Di Bella *et al.* (2000) showed that

AVHRR NDVI might provide a reliable estimate of photosynthetically active radiation (PAR) interception, a variable closely related to biophysical rates such as primary production and evapotranspiration. In 1989, the U.S. Geological Survey used AVHRR data to conduct a bi-weekly assessment of vegetation conditions in 17 western States. The assessments of NDVI at bi-weekly intervals were found to be adequate for monitoring seasonal growth patterns in types of rangeland, forests, or agricultural areas.

Other than the red and near infrared bands, the middle infrared was also proved for its complimentarity for monitoring wheat canopies by Baret *et al.* (1988). Baret *et al.* (1988) showed that middle infrared provides valuable complementary information on the geometrical structure of the canopy and on the optical properties of the underlying soil. Measurements of middle infrared radiance, when used in conjunction with measurements of near infrared and red radiance, are theoretically suitable for estimating LAI. This can be attributed to three factors: (1) There is strong negative relationship between middle infrared radiance and both leaf and canopy moisture content (Carlson, 1971; Thomas *et al.*, 1971); (2) for unstressed canopies there is a strong positive relationship between canopy moisture content and vegetation amount, of which LAI is a measure (Elvidge and Lyon, 1985; Tucker, 1977); and (3) over a mixture of land covers, middle infrared radiance is poorly correlated to, and therefore carries different information to that carried by red, and near infrared radiance (Townshend *et al.*, 1983).

A large number of relationships have been established between VIs and LAI. Major *et al.* (1986) have shown the usefulness of some VIs to estimate some LAI, biomass and grain production for cereals from radiometric measurements. Generally the VIs approach a saturation level asymptotically for LAI ranging from 2 to 6, depending on the type of VI used, the crop studied, and experimental conditions. Most VIs are dependent on internal factors such as canopy geometry, leaf and soil optical properties, or external factors such as sun position and nebulosity to provide good estimates of LAI. Coops *et al.* (1997) compared field LAI to the NDVI and the simple ratio (SR) derived from the MSS data. Linear relationships were shown to be appropriate to relate both transformations to the LAI data with R^2 values of 0.71 and 0.53, respectively. Using the NDVI relationship, LAI values were estimated along a transect originating from the monitoring site and these were compared to percentage canopy cover values derived from aerial photography.

2.7 Soil Effect

Soil reflectance influences the relation between scene reflectance and LAI. At low plant cover, soil reflectance contributes strongly to the different spectral bands. For a given soil type, soil moisture will be the main factor determining soil reflectance (Clevers, 1989). Reflectance decreases with increasing moisture content of the soil, but the relative effect of soil moisture on the reflectance at distinct wavelengths is similar (Bowers and Hanks, 1965).

Perry and Lauenschlager (1984) had described the mathematical relationships among a number of VIs. In these mathematical relationships there are two cases, which are called the 'field' case and 'mixed pixel' case. In the field case, assumptions are made that vegetation cover is uniform within a pixel so that spatial heterogeneity may be neglected, and consider the canopy as a spatially uniform layer above the soil. This case generally applies to Landsat and SPOT observations. In the mixed pixel case, spatial variability is assumed, corresponding to an AVHRR observation of a number of fields with varying amounts of vegetation and bare soil, but with details of individual fields unknown (Price, 1992). In the current study because Landsat ETM+ was utilized the first field case assumption that vegetation cover is uniform within pixels was followed and the slope-based VIs were used.

To minimize the effect of the soil background, Richardson and Wiegand (1977) have proposed the PVI. It represents the orthogonal distance from a point corresponding to canopy reflectance to the soil line, in red-infrared space. Experimental and theoretical investigations show that PVI is also affected by the optical properties of soil background: brighter soils result in higher index values for a given quantity of incomplete vegetation cover. For this reasons some new indices, which are less influenced by the soil brightness have been proposed and were discussed under distance-based VIs (section 2.5.3.2).

2.8 GIS and Process-based Models

A key to the ecological use of remote sensing has become the application of process-based models that enable us to understand the interaction of radiation with a leaf and a canopy and to use remotely sensed data to derive a spatial ecosystem simulation model over large areas of terrain (Curran *et al.*, 1999). Some of the common process models that can be mentioned as examples are forest-bio-geo-chemical (FOREST-BGC) and 3-PGS. The FOREST-BGC model enables, via the coupling of remotely sensed data with ecosystem understanding, the spatial estimation of vegetation productivity. Similarly, 3-PGS can be run from remotely sensed estimates of LAI coupled with weather data and basic, rapidly available information about soils and stand characteristics (Landsberg and Waring, 1997).

The 3-PG model is a relatively simple process-based model describing the growth and water use of forest stands. It was developed by Landsberg and Waring (1997). The model calculates total fixed carbon from absorbed photosynthetically active radiation, taking into account such factors as tree age, soil droughts, soil fertility and atmospheric vapor pressure deficits in modifying potential growth. 3-PG uses simple allometric relationships to estimate the amount of carbon allocated to roots, stem and branches. A fertility rating describes the influence of nutrients on carbon assimilator and allocation strategy. Self-thinning of forest stands is predicted using –3/2 power law (Landsberg and Waring, 1997), while water use is calculated using the Penman-Monteith equation.

Coops *et al.* (1998) stated that the original 3-PG model has been modified to allow remotely sensed observations to be utilized as inputs to it. The modified model is called 3-PGS, the S symbolizing the use of satellite data in the model framework.

Typical input variables relevant to processes with terrestrial models include land cover type (as influenced by natural factors as well as human use), LAI, the function of PAR that is absorbed by the canopy and other leaf structural and chemical attributes such as SLA and percent of nitrogen (Coops *et al.*, 1998) 3-PG/3-PGS run on monthly time steps, driven by weather data, and avoid the problem of over-parameterization and the requirements for a great deal of input data that limit the practical value of most carbon balance models.

The utility of process-based models to predict forest growth variables at specific stand ages, and their capacity to be extrapolated across the landscape using GIS technology, now offer operational potential for use in routine forest management and planning (Battaglia *et al.*, 1998).

2.9 Site Quality/ Site Index

Site quality is defined as the collective characteristic of a site that influences plant growth. It is therefore a function of temperature, radiation, moisture and nutrients as well as species (McLeod and Running, 1988). Site index is a tree variable, which is related to site quality and is defined as the height of a dominant tree(s) at some reference age, in an even-aged stand of trees (Schönaus, 1969 cited by Smith, 2002a). It is widely used as a measurement of site quality or site productivity because there exists a choice correlation between volume and dominant height growth, and it is generally accepted that height of dominant trees only slightly affected by competition (Beaumont *et al.*, 1999).

The top height (height of dominant trees) of a given species at a reference age is more closely related to the capacity of a given site to produce wood of that species than any other one measure (MacFarlance *et al.*, 2000; Spurr and Burnes, 1980). Height growth is generally the most stable, directly measured stand growth statistics. Top height growth is independent of stocking over a fairly wide range of stand density and thus is often used as a measure of site productivity (Monserud, 1984).

As it has been discussed at the beginning, this chapter presented a brief overview of the theoretical background of *Acacia mearnsii*, LAI, VIs and process-based models. The next two sections deal with the description of the study sites and the materials and methods utilized.

Chapter 3: Study Sites

3.1 Introduction

The study was conducted in four commercial forestry plantations within KwaZulu-Natal province (Figure 3.1). The sites are Bloemendal, Mistley, Seele and Mountain Home. All the study sites are in KwaZulu-Natal midlands and lie between 29°09' and 29°35' South and between 30°14' and 30°42' East. Bloemendal is an experimental station of the ICFR while the others are estates of Mondi Forests. These sites, specifically the sample stands, were selected to represent varying productivity potentials so as to provide a full range of estimated LAI values for the calibration and correlations of the different LAI estimation methods. The sites had *Acacia mearnsii* stands of different age groups.

Trees of four different ages were selected from each study site starting from the time of canopy closure to close to harvest. These were four, six, eight and ten year old in Bloemendal and three, five, seven and eleven year old in Mistley. In the case of Seele and Mountain Home only two ages were selected from each of them and were considered as one site. Four and seven year old stands were selected from Seele and eight and eleven year old stands from Mountain Home. This was done because it was not possible to get trees of four different ages in one of these sites. In each of the sites trees of different ages were chosen because it was not possible to get trees of the same age throughout the four sites.

Within each of the compartments that comprised one age a plot of 19 m by 17 m with an area of 323 m^2 was chosen to represent the whole compartment. The compartments chosen cover at least 5 ha each. In addition to the size of the plots, uniformity of the canopy, condition of understorey vegetation and tree condition were taken into consideration during site selection. Every effort was taken to avoid trees which were diseased or had signs of bagworm infestation and to minimize variation in terrain characteristics, when choosing the plots.

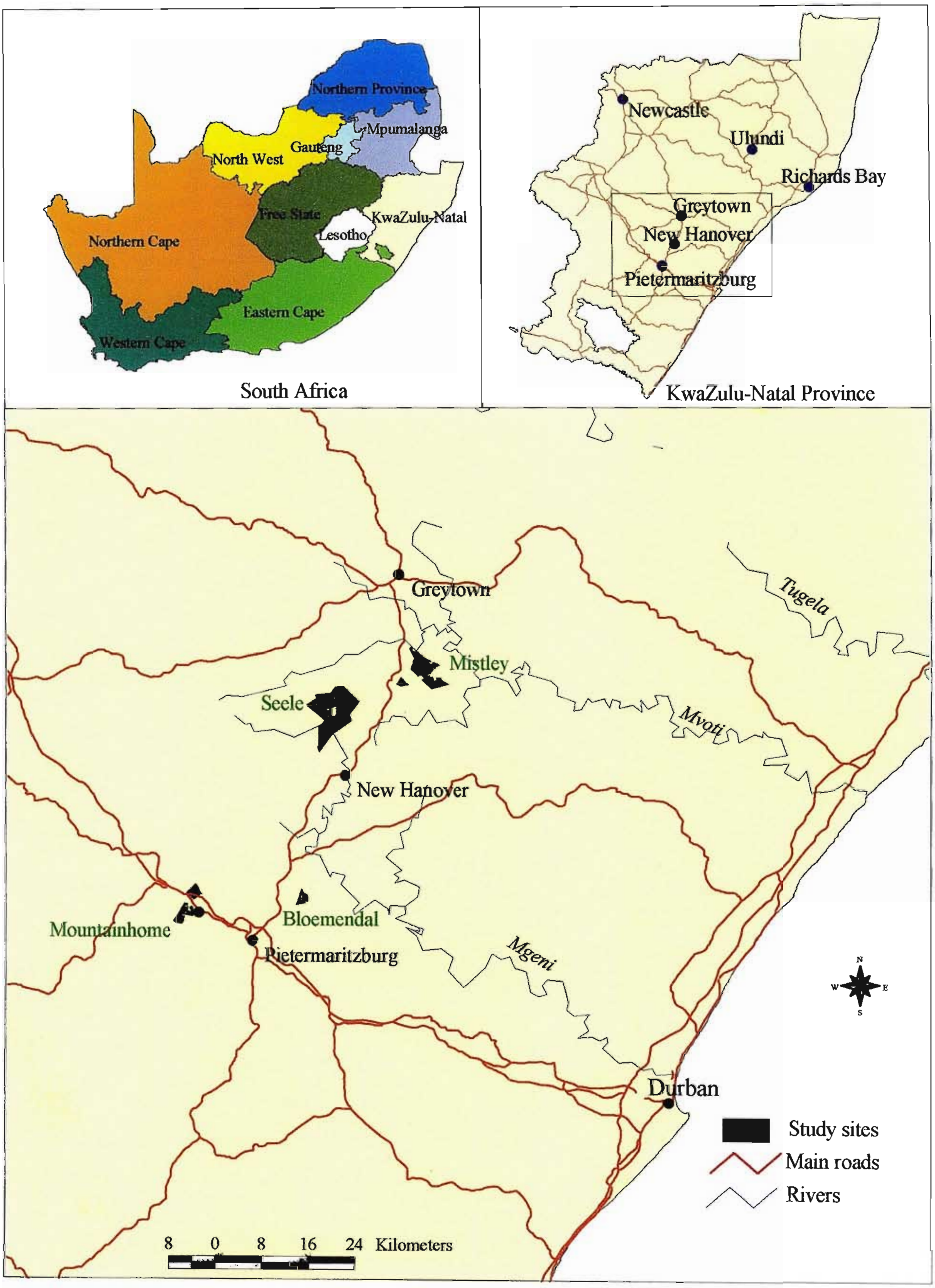

Figure 3.1 Map showing the locations of the study sites.

The sites selected had light understorey vegetation consisting of ferns, shrubs and various types of grasses. Sites with perennial understorey shrubs were deemed unsuitable. All plots appeared in reasonable health and visual estimation of canopy size was also helpful to encompass a range of LAIs.

The planting density of the sites was very high. The trees were 1.5 m apart with a row spacing of 3 m resulting in an initial stocking of 2222 trees per ha in Bloemendal, Seele and Mountain Home. In the case of Mistley the trees were grown from seed, which was line-sown, and the initial stocking was around 3000 trees per ha. Normally in line-sown plantations spacing and thinning are aimed at ensuring a final stocking of 1500 uniformly sized trees, per ha. The first thinning operation is done when the trees are 2 m tall to target stocking of 3000; when the trees reach 4 m tall the stocking should be reduced to 2000 trees per ha i.e., the second thinning; when the trees are 7 m tall the final thinning is done and the stocking is reduced to 1500 trees per ha (ICFR and SAWGU, 1993 cited by Smith and Dunlop, 2002). In addition, due to subsequent losses since planting the stocking rate or density decreased as the trees grew older.

Although the idea was to include sites of low, medium and high productivity there was no data available as an indicator of site quality or site index. In addition the variation in growth of stands in different compartments within one site was found to be great due to the different climatic conditions experienced over a long period of time and due to site differences. For example, in Bloemendal it was apparent that the growth in the four and six year old stands was superior to that of the eight and ten year old stands and would result in higher volumes at clear felling. This could be due to the low amount of rainfall that Bloemendal has received from 1992 to 1994 when the eight and ten year old stands were established. Therefore, in order to gain an estimate of site productivity, mean annual increment (MAI) and volume of each stand were initially estimated from the Diameter at Breast Height (DBH) and height measurements of the sample trees. In addition MAP, mean annual temperature (MAT) and soils data were taken into consideration to include stands of different levels of productivity. Thus the selection was based on stand and tree age rather than on site characteristics *per se*. The general description of the sites is presented in Table 3.1 and a more detailed description is available in Appendix 1.

Table 3.1 General description of the study sites

Study Site	Tree Age (yr)	Compartment No.	Initial stocking (Stems ha^{-1})	Final Stocking (Stems ha^{-1})	Compartment Area (ha)	MAI (m^3 ha^{-1} annum^{-1})	Volume (m^3 to 5cm tip)
Bloemendal	4	014	2222	1981	7.5	18	73
	6	012	2222	1517	10.5	17	103
	8	009	2222	1455	10.6	14	114
	10	013	2222	1348	8.1	11	112
Mistley	3	A01	3000	1950	19.9	28	94
	5	B16	3000	1084	40.3	13	88
	7	B27	3000	1373	27.1	19	104
	11	C01A	3000	1156	42.9	12	135
Seele	4	D27	2222	1296	13.9	29	121
	7	E03	2222	1790	16.7	26	186
Mountain Home	8	D03	2222	1650	14.1	20	160
	11	D01A	2222	1728	25.7	17	198

MAI: Mean Annual Increment

Due to the differences in location and physical setup of the sites each study site will be described separately in the remaining part of this chapter with its accompanying maps.

3.2 Bloemendal

3.2.1 Site Location and Description

The Bloemendal Experimental Station of the ICFR, is situated 10 km northeast of Pietermaritzburg at latitude 29°32' South, longitude 30°28' East and at an altitude of 850 m.a.s.l (Figure 3.1). Trees were sampled from compartments, which were located in a gently undulating landscape. Bloemendal is regarded as marginal for all commercial forestry crops except *Acacia mearnsii* due to the steep slopes, shallow soils and high air temperatures (Boden, 1991). Figure 3.2 shows the description of the sample plots in Bloemendal.

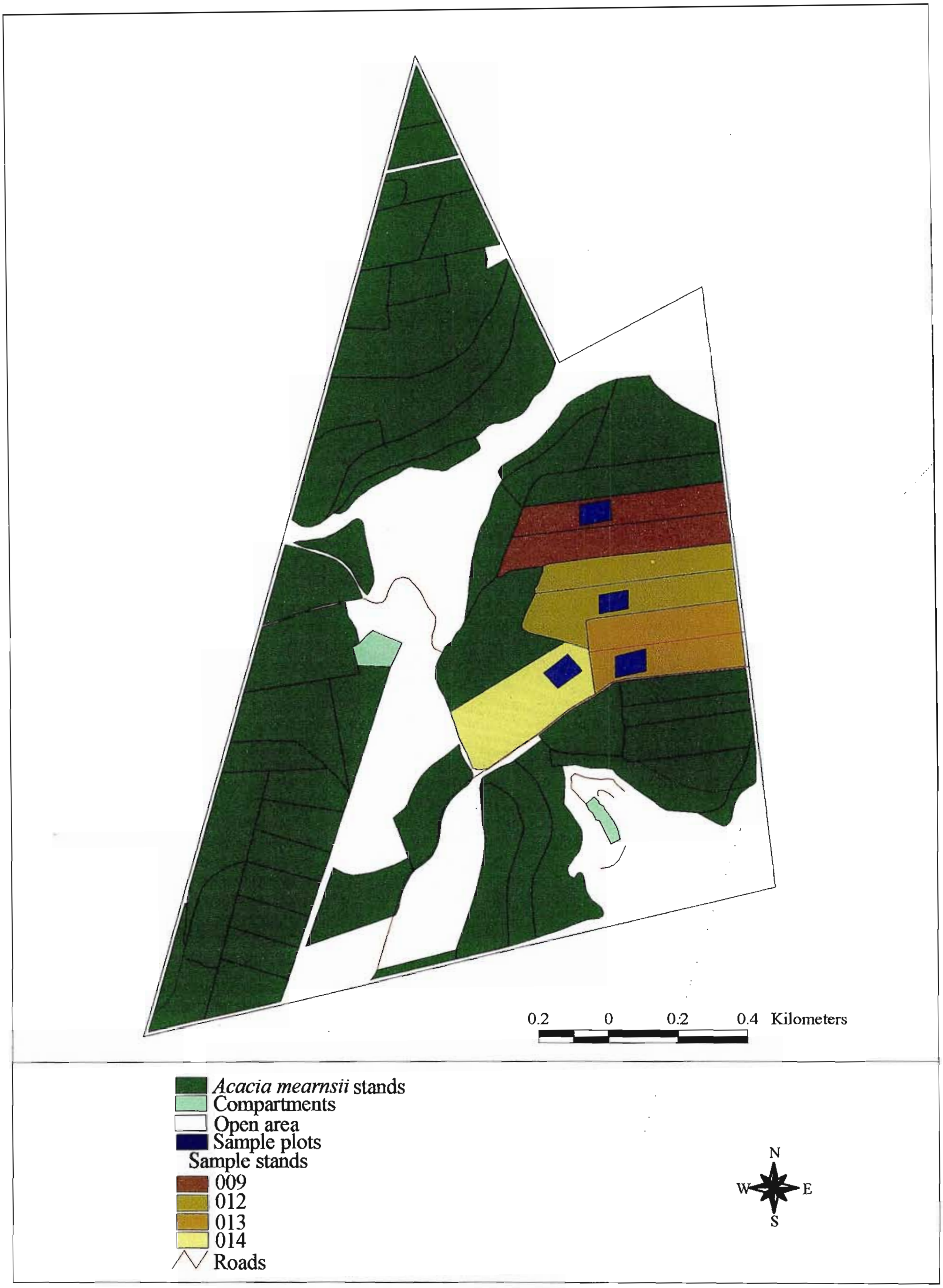

Figure 3.2 Sample stands of Bloemendal study site.

3.2.2 Physical Environment

a. Climate

Table 3.2 shows monthly mean maximum temperature, mean minimum temperature and mean monthly rainfall records over 20 or more years of Bloemendal. The climate of Bloemendal is warm temperate having an MAT of 17.3 °C. The lowest temperature occurs in June and February is the hottest month (Table 3.2). The study area occurs within the summer rainfall area of Southern Africa. The MAP reaches 792 mm (CCWR, 1989). The highest rainfall months are December to January, and the rainy season lasts from November to March, although rainfall can be quite variable seasonally and annually.

Table 3.2 Mean monthly climate data, Bloemendal

	Mean Maximum Temperature (°C)	Mean Minimum Temperature (°C)	Mean Monthly Rainfall (mm)
JANUARY	26.8	16.3	134.3
FEBRUARY	27.2	16.4	120.2
MARCH	26.4	15.3	95.5
APRIL	24.8	12.4	48.5
MAY	22.7	9.1	15.6
JUNE	20.6	5.9	5.1
JULY	20.8	5.9	7.6
AUGUST	22.2	7.8	18.9
SEPTEMBER	23.3	10.5	51.1
OCTOBER	23.9	12.2	81.7
NOVEMBER	24.8	13.7	98.7
DECEMBER	26.6	15.4	114.8

(Source: CCWR, 1989)

b. Geology and Soils

The geology of the area is relatively simple, consisting mainly of shales of the lower and middle Ecca (karoo series), injected extensively by dykes and sills of dolerite. A very limited area of Dwyka tillite is exposed on the southeast corner of the station. A considerable colluvial redistribution of weathered materials has taken place in the landscape and consequently in many cases the relationship between soil types and underlying weathered rock is unclear. Thus red soils, which are normally associated with dolerite, are found extensively overlying weathered shale that elsewhere on the station gives rise to grey-brown soils (MacVicar *et al.*, 1997). Most of the station is, therefore, characterized by fairly deep soils (i.e. more than one meter to saprolite or bedrock). Soils exhibiting evidence includes gleying and the occasional development of subsurface plinthite on the periphery of vleis (Fey and Schönau, 1982).

c. Topography

The topography of Bloemendal could be described as undulating to steep, with a smooth, predominantly convex hill form and rather restricted concave bases along drainage lines. The drainage pattern is such that although soils on the primary convex divides are shallow, relatively deep soils have developed through colluvial aggradations on secondary divides, owing mainly to the length and shallowness of slope angle of these divides in the direction normal to that of primary run-off.

d. Natural Vegetation

Bloemendal falls in the bioclimatic group 3 (Midlands misbelt) of Phillps (1973) and Acocks (1988) with characteristics of group 6 (Tall grass veld) and group 2 (coast hinterland). The climatic conditions in Bloemendal have resulted in a moderate to strong degree of weathering and an intermediate to high degree of leaching (Fey and Schönau, 1982).

3.3 Mistley

3.3.1 Site Location and Description

Mistley is situated 80 km northeast of Pietermaritzburg on the way to Greytown. The plantation is used for both timber and sugarcane cultivation. Many trials are conducted on Mistley and the farm also has a holding nursery. It is located at latitude 29°12' South and longitude 30°40' East and at an altitude of 847 m.a.s.l (See Figure 3.1). Figure 3.3 shows the locations of the sample stands in Mistley.

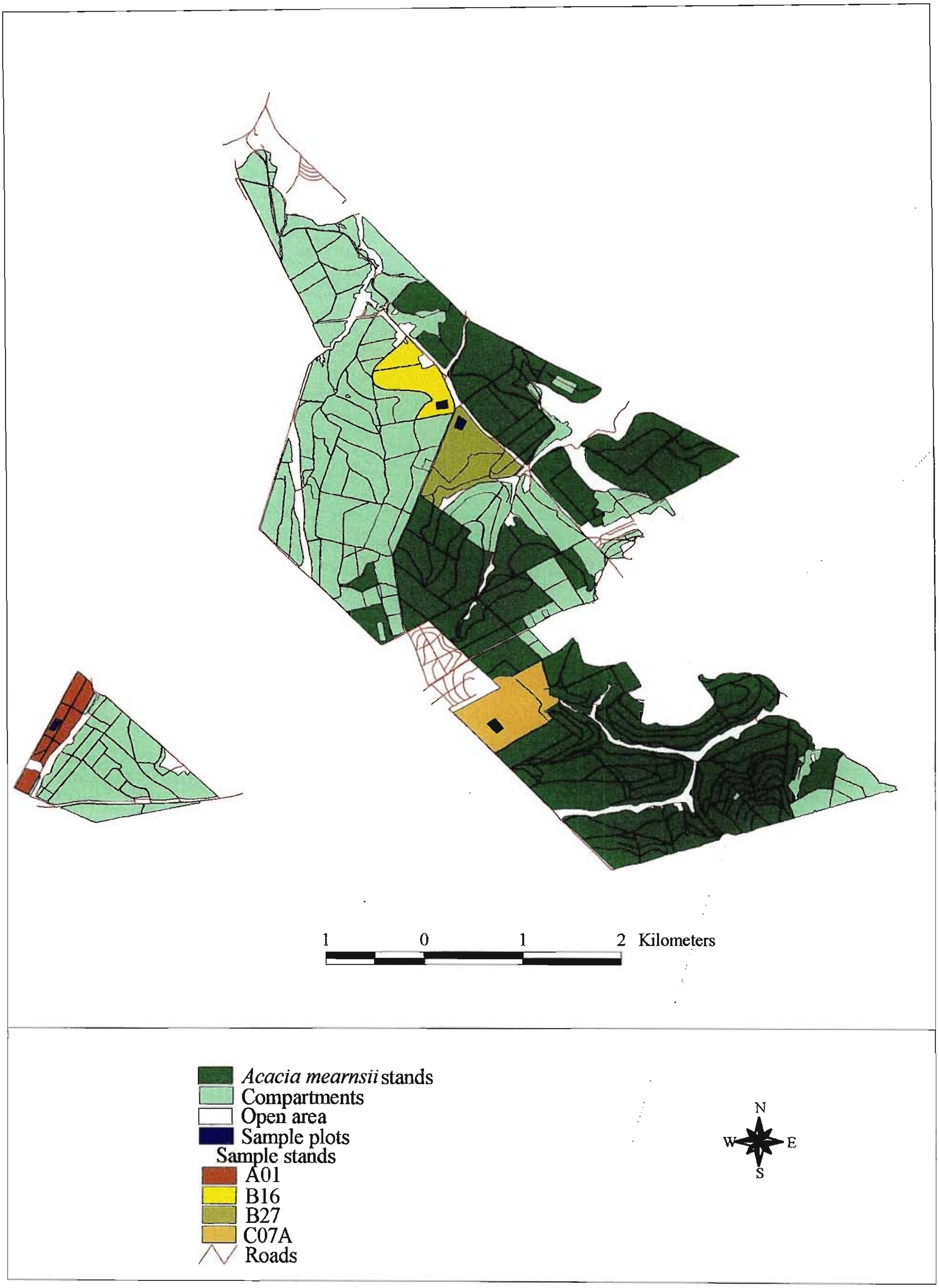

Figure 3.3 Sample stands of Mistley study site

3.3.2 Physical Environment

a. Climate

Generally, the KwaZulu-Natal region has hot summers and mild to cold winters. Rainfall varies between 700 mm and 1,200 mm per year. The MAP for Mistley reaches 836 mm though there is considerable variation within the plantation. MAT of the area reaches 18.2 °C. The mean monthly climate data over 20 or more years for Mistley is summarized in Table 3.3 below (CCWR, 1989).

Table 3.3 Mean monthly climate data, Mistley

	Mean Maximum Temperature (°C)	Mean Minimum Temperature (°C)	Mean Monthly Rainfall (mm)
JANUARY	27.6	16.9	114.9
FEBRUARY	27.9	16.9	93.9
MARCH	27.1	15.9	80.3
APRIL	25.5	12.9	40.6
MAY	23.6	9.2	12.8
JUNE	21.4	6.0	4.4
JULY	21.6	6.0	4.6
AUGUST	23.0	8.1	19.0
SEPTEMBER	24.2	10.9	32.5
OCTOBER	24.8	12.8	67.5
NOVEMBER	25.5	14.4	34.4
DECEMBER	27.4	16.0	91.7

(Source: CCWR, 1989)

b. Geology and Soils

Lithology is predominantly Natal group sandstone, with significant occurrences of shale. Dolerite outcrops are not uncommon. The geology and the soils of this site vary from one area to another. The most dominant lithology throughout the site is Southern Mudstone, Southern Shale and Sandstone. Soils are mostly characterized by fine to medium sandy clay loam, humic topsoils, underlain by yellow or red apedal subsoils. Dominant soil forms are Inanda, Magwa and Kranskop. Clay content in most areas varies between 25-35 % in topsoil horizons and attains values of between 45 and 60 % in subsoil horizons. Significant riparian areas occur with associated soil forms of Tukulu (Mondi, 2002).

c. Topography

Topography is mostly gentle to moderately steep in places. Areas towards the Tugela River have steep slopes. Watercourses are seldom incised.

d. Natural Vegetation

The natural vegetation of this area is predominantly Natal Mist Belt 'Ngongoni Veld (veld type 45 according to Acocks, 1988). This veld type is transitional from the Highland Sourveld to the 'Ngongoni veld proper. It is associated with the higher-lying areas, and changes to 'Ngongoni Veld (Acocks veld type 5) in the lower-lying areas and incised river valleys. These veld types form part of the Grassland Biome, and are associated with the Short Mistbelt vegetation type.

3.4 Seele

3.4.1 Site Location and Description

Seele is in the midlands of KwaZulu-Natal at latitude 29°16' South and longitude 30°33' East and at an altitude of 950 m.a.s.l (See figure 3.1). It was previously used for tea and sugarcane plantation before afforestation. Figure 3.4 shows the locations of the sample plots in the site.

3.4.2 Physical Environment

a. Climate

Generally, Seele has similar climatic conditions as Mistley with hot summer and mild to cold winters. Seele has MAT of 18 °C and MAP reaches 884 mm. The mean monthly climatic data over 20 or more years of the area is summarized in Table3.4.

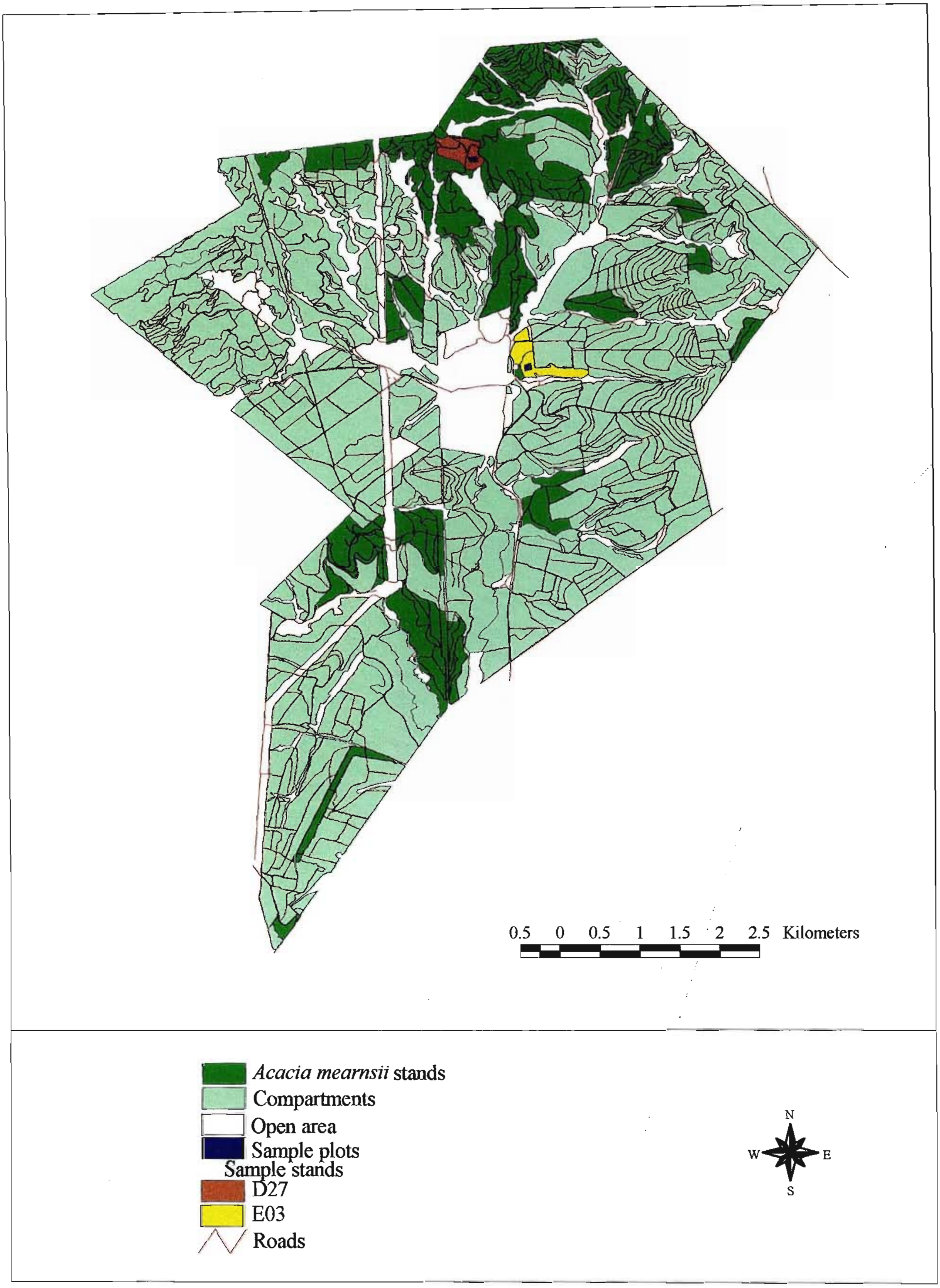

Figure 3.4 Sample stands of Seele study site.

Table 3.4 Mean monthly climate data, Seele

	Mean Maximum Temperature (°C)	Mean Minimum Temperature (°C)	Mean Monthly Rainfall (mm)
JANUARY	27.1	16.2	132.6
FEBRUARY	27.5	16.2	115.4
MARCH	25.0	15.1	97.7
APRIL	22.9	12.2	46.7
MAY	20.6	8.6	16.8
JUNE	20.9	5.3	4.8
JULY	21.6	5.3	5.9
AUGUST	22.4	7.4	15.4
SEPTEMBER	23.7	10.2	40.1
OCTOBER	24.5	12.0	79.1
NOVEMBER	25.3	13.7	103.9
DECEMBER	27.2	15.3	121.4

(Source: CCWR, 1989)

b. Geology and Soils

Soils are characterized by well-weathered fine sandy clay loam, humic topsoils, underlain by yellow or red apedal subsoils. High topsoil carbon contents are common. Good internal profile drainage occurs with favorable water holding capacities. Dominant soil forms are Sweetwater, Inanda, Kranskop and Magwa, while Hutton, Clovelly and Oakleaf forms are associated with the lower-lying areas and drier northern aspects. Clay content varies between 25-35 % in topsoil horizons and attains values of up to 55 % in deeper subsoils. Lithosols (rocky soils of the Mispah and Glenrosa forms) occur commonly on steep slopes and are especially prevalent in the drier, hotter areas towards the Tugela River. Hydromorphic soils of the Tukulu form tend to occur immediately adjacent to riparian areas (Mondi, 2002).

c. Topography

Topography of the area is mostly gentle to steep in places and most of the slopes are south facing.

d. Natural Vegetation

The natural vegetation of this area is predominantly Natal Mist Belt 'Ngongoni Veld (veld type 45 according to Acocks, 1988). This veld type is transitional from the Highland Sourveld to the 'Ngongoni veld proper. It is associated with the higher-lying areas, and changes to 'Ngongoni Veld (Acocks veld type 5) in the lower-lying areas and incised river valleys. These veld types form part of the Grassland Biome, and are associated with the Short Mistbelt vegetation type.

Woodland and thicket are common in river valleys. Dominant tree species are *Rapanea melanophloeos*, *Cryptocarya woodii* and *Syzygium gerrardii*. Shrubs and climbers also form an important part of the thicket canopy, mainly dominated by *Dalbergia obovata* and *Uvaria caffra*.

3.5 Mountain Home

3.5.1 Site Location and description

Mountain Home is situated in the vicinity of Hilton, 7 km northwest of Pietermaritzburg at latitude 29°33' South and longitude 30°16' East and at an altitude of 1214 m.a.s.l (Figure 3.1). The site was a farmland (grazing, dairy and crops) before Mondi Forests purchased the land and there are still remnants of stone stock control walls constructed by the early settlers. Natal Tanning Extract (NTE) Ltd. has afforested Mountain Home since 1926 and it was also used as an experimental farm for a short period. Figure 3.5 shows the locations of the sample stands in Mountain Home.

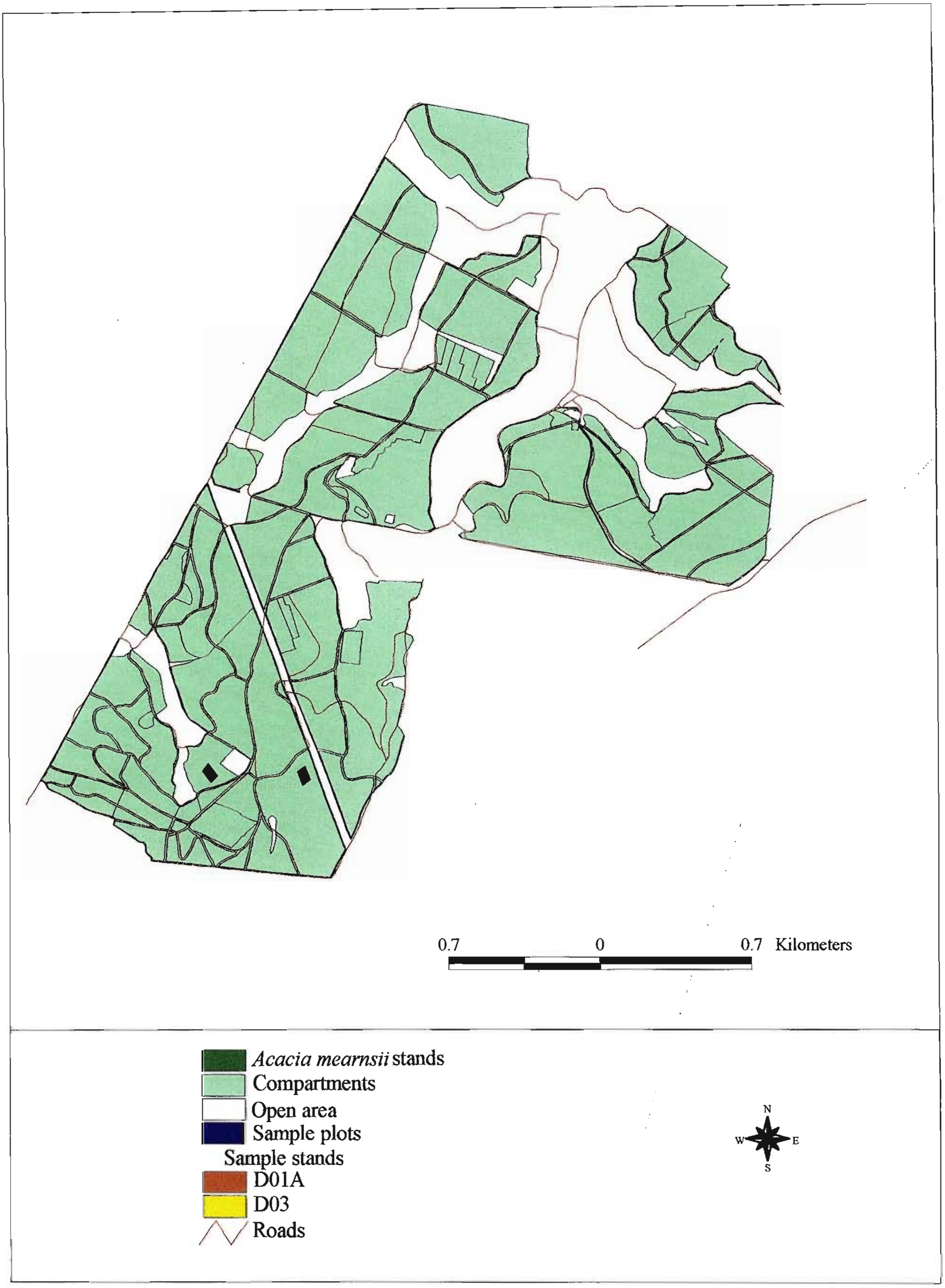

Figure 3.5 Sample stands of Mountainhome study site.

3.5.2 Physical Environment

a. Climate

In Mountain Home the MAP reaches 1111 mm and the MAT was recorded as 16 °C. The mean monthly climatic data over 20 or more years of the area is presented in Table 3.5.

Table 3.5 Mean monthly climate data, Mountain Home

	Mean Maximum Temperature (°C)	Mean Minimum Temperature (°C)	Mean Monthly Rainfall (mm)
JANUARY	24.7	14.3	162.3
FEBRUARY	24.9	14.4	137.7
MARCH	24.1	13.3	126.3
APRIL	22.5	10.5	57.5
MAY	20.5	7.5	21.1
JUNE	18.4	4.6	6.1
JULY	18.6	4.6	8.1
AUGUST	20.1	6.4	20.6
SEPTEMBER	21.5	8.7	49.8
OCTOBER	22.0	10.2	94.8
NOVEMBER	22.7	11.8	133.7
DECEMBER	24.4	13.4	154.7

(Source: CCWR, 1989)

b. Soils and Geology

The soils on this site are characterized by fine sandy clay, humic topsoils, underlain by yellow or red apedal subsoils. Dominant soil forms are Inanda and Magwa, with Hutton being the subdominant soil form. Clay content varies between 34 and 45 % in topsoil horizons and attains values of up to 60 % in deeper subsoils. Dolerite dykes and sills occur commonly in the landscape with associated "red" soils of the Hutton and Inanda forms. Narrow riparian areas have hydromorphic soils of the Tukulu and Katspruit forms. The Mispah soil form is also present in this area and also shallow soils on shales (Mondi, 2002).

c. Topography

The topography of the area is almost flat with some undulating places around the riverbanks. In some of the plots the bedrocks are exposed resulting in big stones among the trees.

d. Natural Vegetation

The natural vegetation of these areas varies between Southern Tall Grassveld (Acocks Veld type 65) and Natal Mist Belt 'Ngongoni Veld' (Veld type 44). This area forms part of the Moist Upland Grassland vegetation type of the Grassland Biome.

Woodland and thicket are more common as sheltered sites and rocky outcrops, or open savanna areas (dominated by *Acacia sieberana*) in the drier areas. Dominant tree species are *Maytenus heterophylla, Zanthozylem capense, Ziziphus mucronata, Rhus rehmanniana* and *Acacia sieberana.* In fire-protected areas, the incidence of forest pioneers such as *Rapanea melanophloeos,* and Fynbos species such as *Cliffortia* spp., are on the increase (Mondi, 2002).

Chapter 4: Materials and Methods

4.1 Introduction

As it has been described in chapter one that the aim of this project is to develop an acceptable framework for estimating the LAI of *Acacia mearnsii* using Landsat ETM+ satellite imagery. But the use of remotely sensed data to estimate forest attributes or biophysical factors demands that there should be some methods of calibrating the sensors in use or checking the accuracy of the obtained data. Thus destructive sampling from direct field-based LAI measurements and LAI-2000 from indirect field-based LAI measurements were carried out in this study. Therefore, this chapter begins by briefly describing the direct and indirect field-based methods of estimating LAI. A description of how the satellite images were processed and the methods used in calculating the different VIs then follows. The chapter concludes by a description of the statistical analyses used.

4.2 Field Estimation of Leaf Area Index

4.2.1 Direct Field-based LAI Estimation (Destructive Sampling)

The sampling procedure was based on that described by Cherry *et al.* (1998), Deblonde *et al.* (1994) and Snowdon *et al.* (2001). Tree stands having four different ages from each of the four study sites were selected to represent the variation in LA present in the different sites. In Bloemendal four, six, eight and ten year old stands were selected; in Mistley the stands selected were three, five, seven and eleven year old. Four and seven year old stands were selected in Seele and eight and eleven year old in Mountain Home. Field plots, 17 by 19 m having an area of 323 m^2, were demarcated within each of the stands/ compartments on near-level terrain to minimize topographic effects. DBH (1.3m above ground) was measured in cm for all the trees in these plots. Based on their DBH distribution, four representative trees were selected from each of the demarcated plots. Each tree was felled as close to ground level as possible with a chainsaw. Tree height and height to the first limb carrying live foliage were measured and the difference, crown length, calculated. The crown was divided into upper (u), middle (m) and lower (l) zones of equal length and branches were allocated to crown sections based on the origins at the stem. This is represented diagrammatically in Figure 4.1.

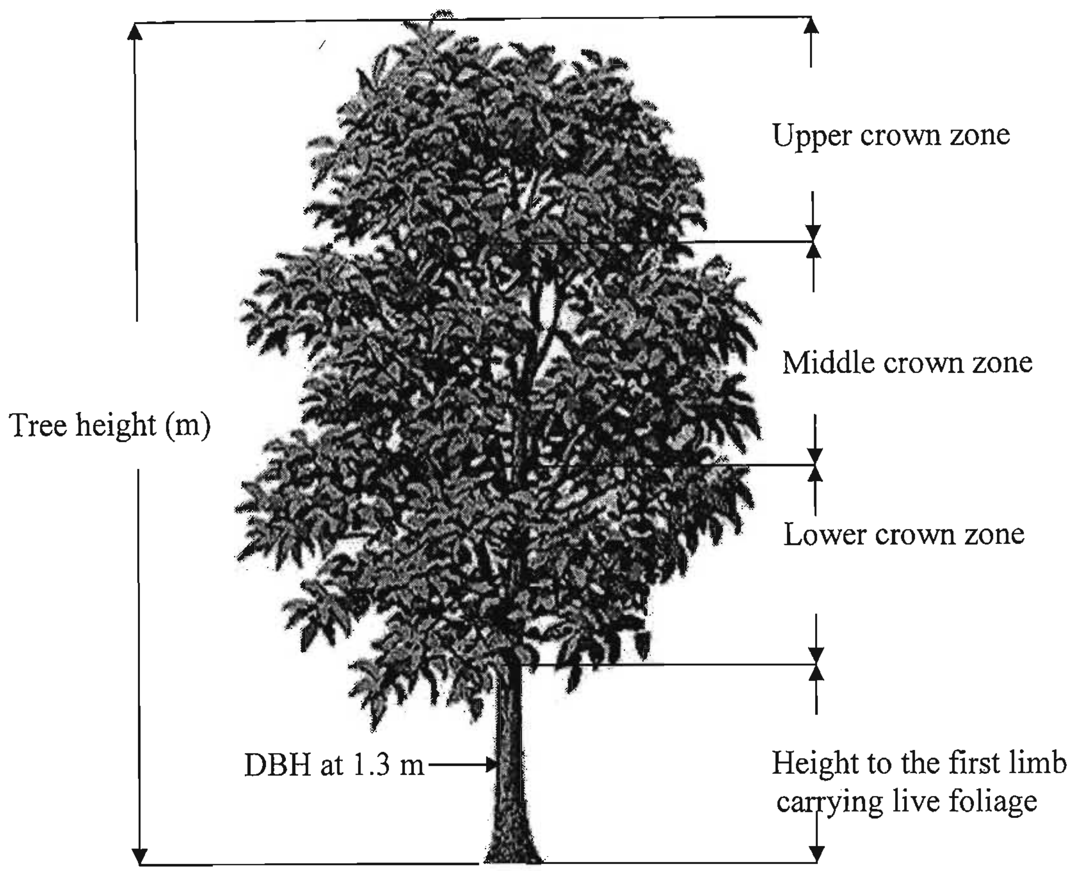

Figure 4.1. Diagrammatic representation of a sample tree and the parameters measured.

The major biomass components of the felled trees were isolated as stem-bark; stem-wood to a diameter of 5 cm, dead branches, live branches and leaves were stripped by hand. All the components were weighed fresh in the field using a 30 kg spring balance to an accuracy of ± 1 g. Three sub-samples of each component were collected and their fresh weight determined using a more precise laboratory balance. Sub-samples were then oven dried to constant weight at 65 °C. Weighing of the dried sub-samples was done as soon as possible after removing them from the oven to prevent absorption of moisture. For each sub-sample, a ratio of oven-dry-to-fresh weight was calculated and an average ratio was calculated. An estimate of the dry weight of each component was obtained by multiplying the total fresh weight of the component by the corresponding oven-dry-to-fresh-weight ratio. A step-by-step procedure of the destructive sampling is presented in Appendix 2.

4.2.1.1 Leaf Area Determination

A sub-sample of leaves was used for the determination of SLA because SLA was required to relate foliage dry mass to a LA. This can be obtained by the equation:

$$SLA\ (mm^2g^{-1}) = LA\ (mm^2)/\ Leaf\ dry\ matter\ (g) \qquad [Eq.\ 4.1]$$

Ten leaves were selected randomly from each of the three zones of the crown. The leaves were removed from the branches, labeled, and, to ensure they remained flat, they were transported to the laboratory pressed in books and plant presses. Leaves were scanned using LI-3100 Leaf Area Meter to determine the LA and oven-dried to constant weight at 65 °C. The leaves were cooled in desiccators and weighed to obtain their dry mass. The leaf area meter used was calibrated in 0.1 mm^2 to correct the LA of each sample. SLA (the one-sided area of the leaf divided by the dry weight of the leaf) was calculated on a projected LA or single-sided basis. LA for the different parts of the canopy was then calculated separately as the product of total leaf dry weight and SLA. The LAs of the upper, middle and lower parts of the canopy were then summed up for individual trees to give tree LA.

4.2.1.2 Scaling Up

The aboveground oven-dry-weight of trees can be measured directly by felling them, oven-drying all components and then weighing them. However, it is not realistic to do this for all inventories. Instead, a practical solution is to develop regression equations based on data from felled trees where this is possible. Such functions use some easily measurable dimensions such as stem diameter, size of live crown and sometimes height. LA and the DBH have a direct relationship, i.e., the increase in LA leads to an increase in DBH. This relationship has been used in other studies, for instance Battaglia *et al.* (1998).

Many researchers in different parts of the world have also established allometric relationships for different forest species. The use of such general relationships may, however, lead to significant errors due to the influence of different abiotic factors (Gower *et al.*, 1999). To obtain more accurate relationships, it is generally advisable to estimate these in the specific sites under study. Thus, regression analysis was used to develop relationships between DBH for the harvested trees and LA in each study site. From these models LA of the plot trees was calculated by expressing the DBH as LA for each tree in the plot measured. Finally, LAI was computed as the sum of the tree LAs for each plot per the ground area these trees covered.

4.2.2 Indirect Field-based PAI Measurement (LAI-2000)

A LAI-2000 was used to measure forest PAI. The operation instructions for the LAI instrument were followed carefully to make sure that the measured LAIs were within 10 % of the mean values with a 0.95 confidence level (LI-COR, 1990). Since the trees were tall the remote mode method was used. Thus two control units each with one optical sensor to log the above and below readings were utilized.

Readings using the LAI-2000 were taken under the canopy in the plots that were sampled for foliar biomass. Measurements were made by positioning the optical sensor and pressing a button, data were automatically logged into the control unit for storage and LAI calculations. Three sets of twelve readings (termed "B" readings) were taken under the canopy in each plot, each set being taken at random points. These multiple below canopy readings and the fish-eye field-of-view assure that LAI calculations are based on a large sample of foliage canopy. All readings were taken with the instrument pointing in the direction away from the sun. A separate synchronized instrument was located in the center of a clearing of at least 40 m in diameter, the minimum area necessary at these sites to ensure an uninterrupted view of open sky conditions. The sensor was taking readings every 15 seconds representing the above-canopy readings (termed "A" readings). During the data processing stage, below-canopy readings were compared with the above canopy readings closest in time.

As the LAI-2000 sensor head measures diffuse radiation, direct sunlight on the sensor or sunlit portions of the canopy causes the leaves to appear brighter, and thus, the "B" reading will be increased, resulting in an underestimation of PAI. A sunlit canopy was avoided by taking measurements just after sunrise and just before sunset when the solar elevation is low (below 45°), as well as days of uniform and dense cloud cover whenever possible.

A 45° view lens was used to restrict the view of the sensor such that the instrument did not see a 315° arc. Lang and Xiang (1986) showed that averaging the logarithms of transmittances (rather than a linear average) obtained along a transect in heterogeneous canopies overcomes the errors due to gaps. At any point where there are significant gaps in the canopy, the sensor might "see" these in one direction while simultaneously "seeing" full canopy in another direction for the same sensing ring. By restricting the view of the sensor using 45° lens cap, this problem was alleviated.

The outermost ring (zenith angle >61°) was removed from the calculations of PAI to prevent measurements in neighboring plots or edge tree rows. This was easily accomplished through the PCA 2000-90 Support Software supplied with the device. Both Chason *et al.* (1991) and Grantz *et al.* (1993) found that the outermost ring gave greater transmittance, which resulted in lower PAI values than produced by destructive sampling.

4.3 Image Processing

4.3.1 Locating the Study Sites

Digital coverages (vector files) of the study sites were available from the SAWGU and Mondi Forests and to check the accuracy of the map point locations were captured using a GeoExplorer Global Positioning System (GPS) (Tremble, 1994). Once the point locations were captured they were entered into an ArcGIS 8.1 (ESRI, 2000) to overlay them with the polygon features of the compartments in the digital coverage. Then the exact positions of the study plots were ascertained. However, the vector files were in shape file format and were in different projections. In order to make them compatible with the satellite images they were imported into Arc Coverage format and reprojected to Transverse Mercator projection, Clarke 1880 Cape Datum and a central meridian of lo 31° in ERDAS Imagine 8.4 (ERDAS Imagine Inc., 1999). After checking their accuracy and reprojecting them these digital coverages were used to clip (extract) the satellite data of the study sites.

4.3.2 Extracting Reflectance Data of Sample Plots

A common problem encountered in the analysis of satellite imagery is that ground survey plots tend to be much smaller than the ground resolution of the imagery, and as a result the data are not representative of the full area that contributes towards the reflectance recorded in each pixel (Curran and Hay, 1986). This can be a major source of error, especially considering blurring effects from neighboring pixels and the fact that it is generally impossible to locate ground survey plots that are smaller than ground resolution of the imagery on a satellite image to pixel accuracy (Curran and Williamson, 1985). Because of this Justice and Townshend (1981) cited by Puhr and Donoghue (2000) suggest that ground survey plots at least four times the ground resolution of the sensor are needed to adequately interpret the reflectance characteristics of a surface. Thus the mean, maximum, minimum and standard deviation of the digital number (DN) of a 3x3 window around the plot location was used for each stand in each VI calculated. The use of a 3x3 mean values, instead of the values of the exact pixel believed to correspond to the survey plot, should help further reduce potential errors arising from difficulties of finding the exact location of a survey plot on the ETM+ satellite imagery.

4.3.3 Transformation of Remotely Sensed Data

4.3.3.1 Image Data

The images used in this study were two Landsat ETM+ quarter scenes of path 168 and row 80. The first image was obtained on October 05, 2001 (Figure 4.2) and the second image obtained on March 30, 2002 (Figure 4.3). These images were selected because they are the closet passes to the field data collection dates, i.e., the October image was used to estimate VIs of Bloemendal study site while the March image was used to estimate VIs of Mistley, Seele and Mountain Home study sites. Both the images were cloud free and were in Transverse Mercator projection and Clarke 1880 Cape Datum. The size of each quarter scene was 3822 by 3582 pixels. The images were radiometrically and geometrically corrected by South African Satellite Applications Center (SAC). Details of the scene parameters are presented in Appendix 3.

All image processing was done using ERDAS Imagine 8.4. This consisted of ortho-rectifying the image, registering the bands, sub-setting the fields of interest and calculating various VIs. The ortho-rectification process was carried out by SAC using a 10 m digital elevation model (DEM).

The Landsat ETM+ bands used in this project were red, near infrared and middle infrared. As it has been explained in Chapter two the red and near infrared bands are the most important for vegetation discrimination and computation of VIs. These red, near infrared and middle infrared bands were separated and saved as binary bytes of approximately 3822 x 3582 pixels each and they were allocated to numerical bands and colors in ERDAS Imagine 8.4. The relationships between image data and plot-level forest inventory were obtained by image sub-setting. Here the different compartments were cleaned and a topology was built as polygon features. Then they were changed from vector to raster format and were used to mask the original orthorectified image. In addition, the image interpretation was supplemented by image enhancement and unsupervised classification using a maximum likelihood decision rule.

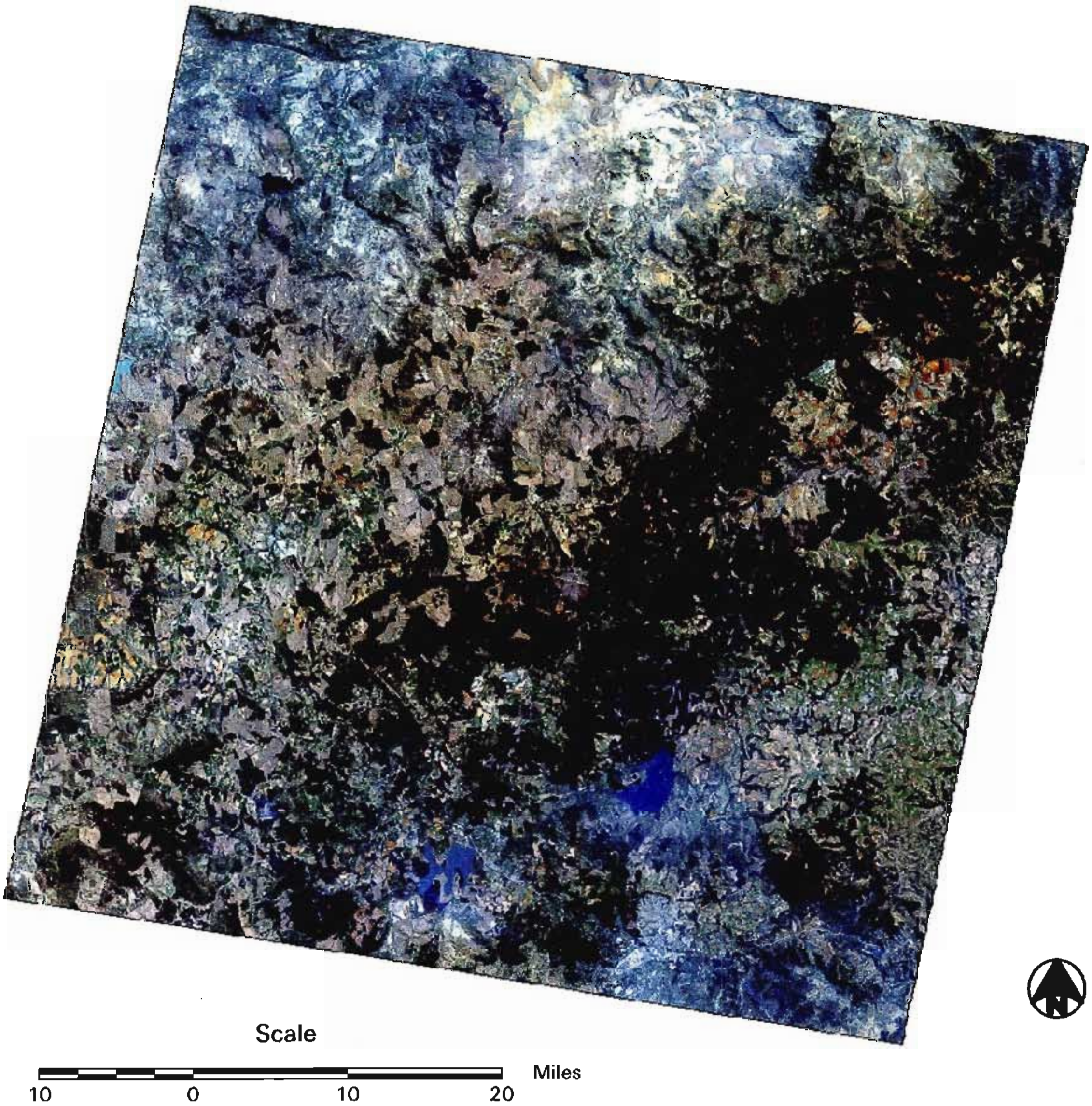

KwaZulu-Natal Midlands Subscene
Bands 3, 2, 1 Composite
Subscene Size: 3822 x 3582; Pixel Size: 30 x30 m
Transverse Mercator, Clarke 1880, Cape Datum

Figure 4.2 Landsat ETM+ Subscene, 05 October 2001.

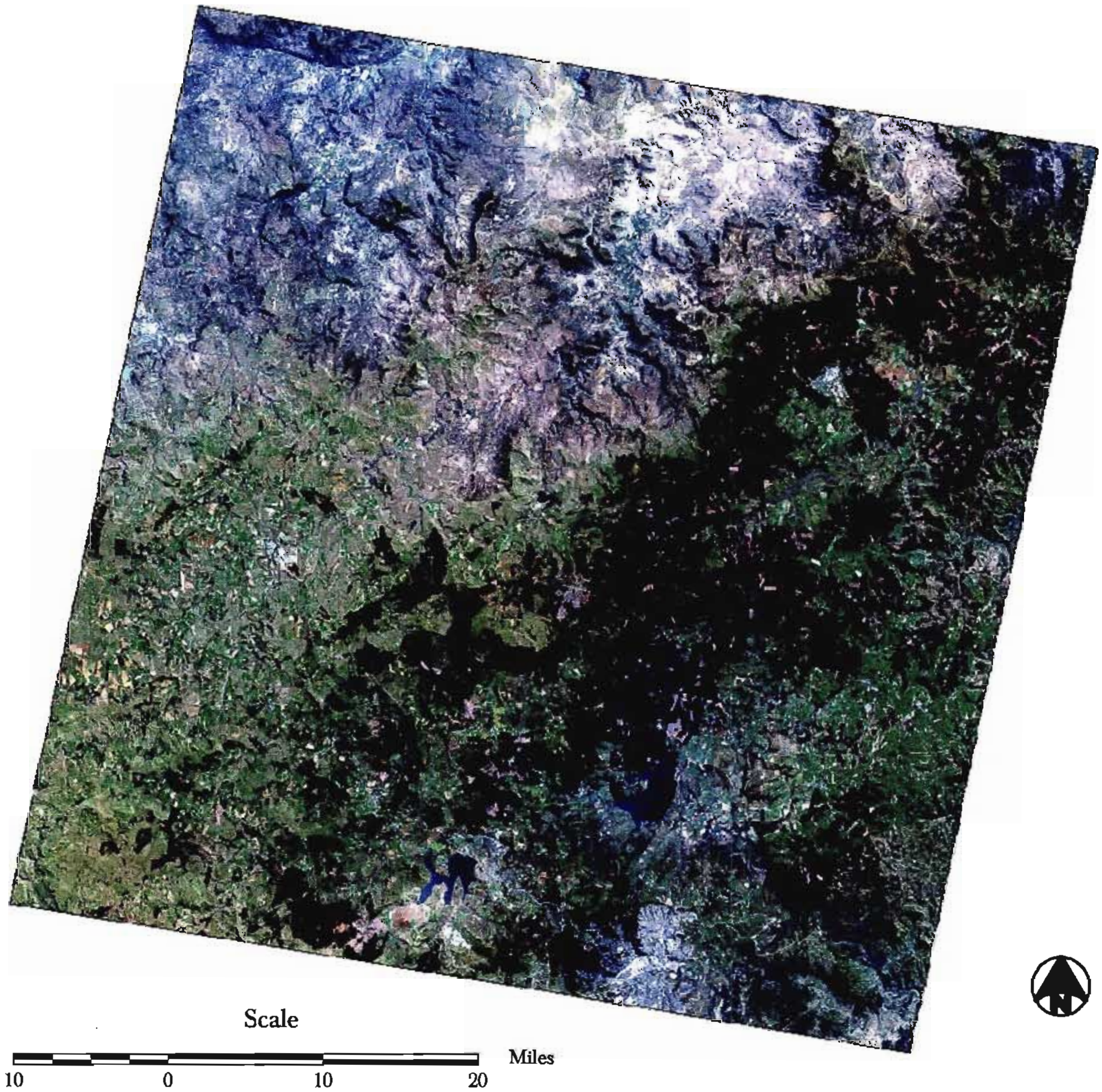

KwaZulu-Natal Midlands Subscene
Bands 3, 2, 1 Composite
Subscene Size: 3822 x 3582; Pixel Size: 30 x 30 m
Path 168, Row 80
Transverse Mercator, Clarke 1880, Cape Datum

Figure 4.3 Landsat ETM+ Subscene, 30 March 2002.

4.3.3.2 Calculating the Various Vegetation Indices

The data processing procedures for vegetation transformations were performed using models from the model maker in ERDAS Imagine 8.4. The four VIs chosen for the determination of LAI were NDVI, RVI, TVI and VI3. ERDAS Imagine 8.4 provides options for choosing one of the models built in to the package or building a new model. For this study a built in model was found from the examples in the model librarian for NDVI (see Figure 4.4) and new models were created in model maker using the available functions and tools for RVI, TVI and VI3. The models were run using the appropriate images as inputs and the output thematic/ spatial maps depicting VI values throughout the compartments were computed.

4.3.3.3 LAI Estimation

To use remotely sensed data to estimate LAI, there needs to be a sound model to describe the relationship between these remotely sensed data (VIs) and LAI. Ideally, workers would like to use deterministic (e.g. Chance, 1981) or stochastic models (e.g. Goel and Thompson, 1984). However, due to the presence of many unknown or immeasurable variables and a high degree of experimental error, it has often only proved possible to use empirical models. These models, which are usually regression-based calibration relationships between remotely sensed radiance indices and LAI, have been shown to have validity for a wide range of scenes and sensors (Ajai *et al.*, 1983; Tucker, 1979). In this study, regression-based calibration relationships between remotely sensed NDVI and both actual LAI and PAI values from the field have been developed. A summary of the overall methods used in this study is presented in Figure 4.5.

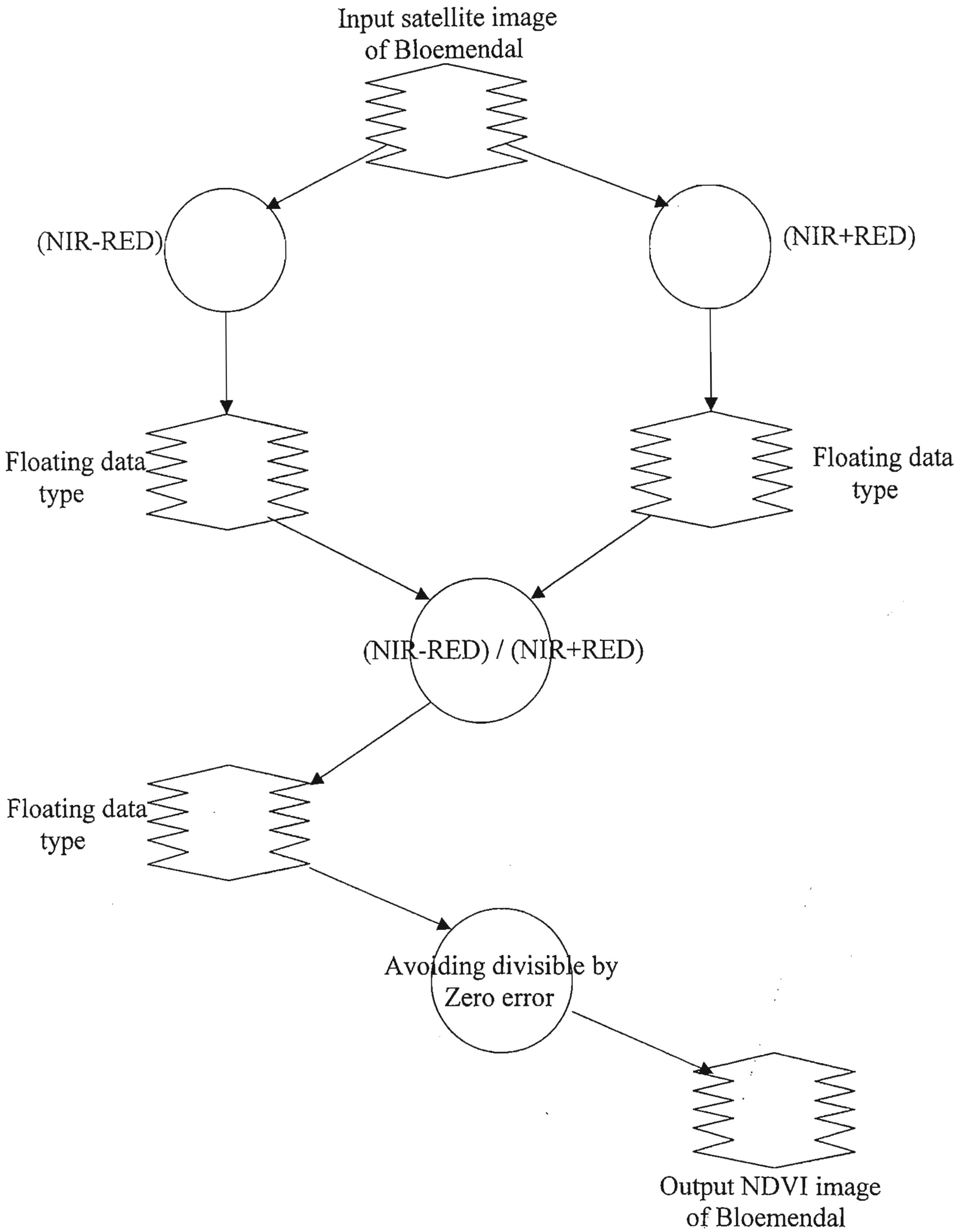

Figure 4.4 Spatial model diagram showing computation of NDVI of Bloemendal study site

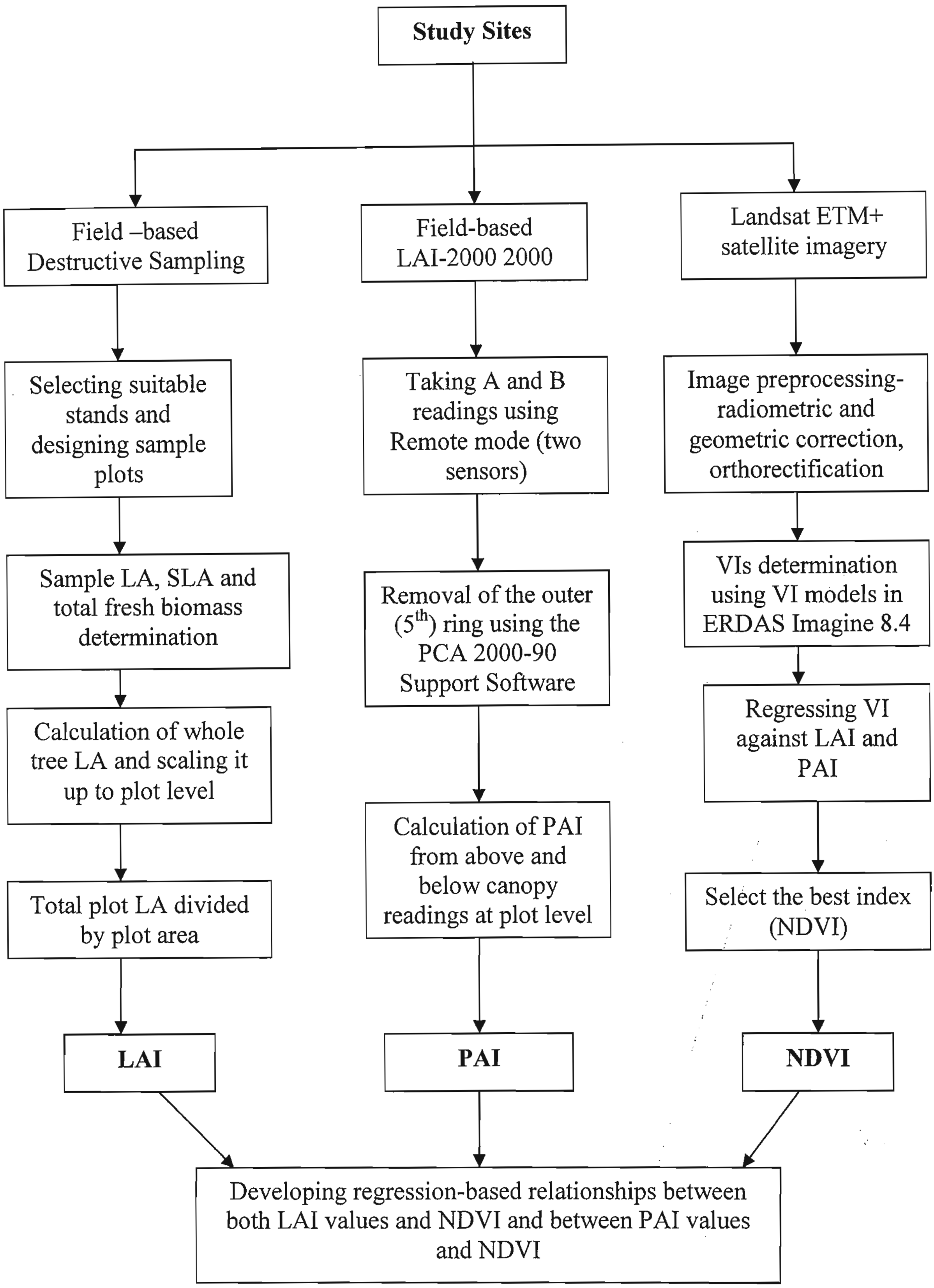

Figure 4.5 Summary flow chart showing the different methods of determining LAI.

4.4 Statistical Analyses

The utility of Landsat ETM+ data for estimating LAI of *Acacia mearnsii* was ascertained using two methods. In the first method, correlation analysis was performed between LAI, PAI and the various VIs to investigate the direction and strength of their relationship by observing the correlation coefficient (r). The correlation coefficients were also tested for their significance at 0.01 and 0.05 levels by comparing them with their tabulated critical values. For the second method of determining the utility of Landsat ETM+ data for determining LAI, different kinds of models (i.e. linear, logarithmic, power and exponential) were investigated using regression procedures, where the VIs were taken as independent variables. Here the coefficient of determination (R^2), overall significance of the model, level of significance of the constant and the independent variable, standard error obtained from the analysis of variance (ANOVA) of regression and root mean square error (RMSE) were used to indicate how well the regression line fitted the data. Similarly the relationships between SLA and the various VIs derived from satellite imagery were investigated using correlation and regression analyses. The relationships between tree LA and DBH were also investigated using regression analyses to arrive at the best predictive equation for each site. All statistical analyses were performed using Genstat 4.2 statistical package (Genstat, 2000).

ANOVAs were performed to test for any significant differences in SLA and LA measurements between both age groups and sites, and any significant differences in LAI and PAI values between age groups only.

Chapter 5: Results and Discussion

5.1 Introduction

In the previous chapters a brief introduction of the study, its literature background, description of the sites where the study was carried out and the materials and methods used in the project were discussed in detail. This chapter presents the results obtained from the study and are discussed simultaneously.

5.2 Estimation of LAI by Destructive Sampling

As it has been discussed in the previous chapter, to obtain the LAI values using destructive sampling, the LA values had to be calculated from SLA and total dry leaf mass of selected sample trees first and then the values scaled up to determine LA of the stand in focus. Thus the results are presented in sequence as follows:

5.2.1 Specific Leaf Area

The SLA values of all sample trees in this study are presented in Appendix 4a. Table 5.1 shows a summary of the mean SLA values. The measured SLA values ranged from 5.0 to 13.0 m^2kg^{-1} (Appendix 4a).

Tables 5.1 Mean SLA of sample plots estimated by destructive sampling.

Study Site	Tree Age (yr)	Compartment No.	Mean SLA ($m^2 kg^{-1}$)
Bloemendal	4	014	8.21
	6	012	7.40
	8	009	7.82
	10	013	7.83
Mistley	3	A01	8.85
	5	B16	8.12
	7	B27	8.16
	11	C01A	8.10
Seele	4	D27	8.36
	7	E03	8.68
Mountain Home	8	D03	8.56
	11	D01A	9.28
		Overall Mean SLA	8.28

The overall mean SLA obtained was 8.28 m^2kg^{-1}. The mean SLA of *Acacia mearnsii* was also calculated by Dicks (2001) in South Africa but it was only 5.80 m^2kg^{-1}. This could be due to the very small sample size taken, loss of some leaflets caused by bagworm infestation and that the main petioles of the leaves were removed from the analysis, which had resulted in decreased mass and area of the sample leaves.

The mean SLA values were found to be 7.81, 8.31, and 8.72 m^2kg^{-1} for Bloemendal, Mistley and Seele/Mountain Home, respectively. The statistical means of SLA, LA and LAI used to assess whether their differences were statistically significant between the different study sites and age groups are presented in Appendix 4b. The ANOVA showed that there was a significant difference between the mean SLA values of the different sites ($\rho<0.05$) (Table 5.2). For analysis purpose, the sample stands were grouped into four age groups; these were 3-4, 5-6, 7-8 and 10-11 year old and are referred to as age group one to four, respectively. The mean SLA values for the age groups one to four were found to be 8.47, 8.06, 8.18 and 8.40 m^2kg^{-1}, respectively and statistically the differences were insignificant (Table 5.2). This agrees with the results obtained by Hunt (1999), who reported that the variation of SLA was small for *Eucalyptus nitens* and *Acacia dealbata* and differences between ages within each species (across and within crown zones) were not significant. Within each of the sites, SLA seemed to decrease as tree age increased within the same site but it was not significant statistically.

In this study it was noticed that the leaf structure of *Acacia mearnsii* was quite different between young, juvenile and older leaves found on the lower parts the stems. The younger leaves were softer, lighter in color, while the older leaves were darker in color and smaller in size than the younger leaves. As a result the SLA values were variable for the leaves taken from the different crown zones. SLA values increased from the upper to the lower zones of the crown in most of the sampled trees. Differences between mean SLA values of the different crown zones were found to statistically significant (Table 5.2). Similar results were reported by Ellsworth and Reich (1993) cited by Lymburner *et al.* (2000) and Hunt (1999) for *Eucalyptus nitens* and *Acacia dealbata.* Hunt (1999) showed that SLA increased with crown depth (i.e. from upper crown foliage) for trees of both species and this has been related more to leaf age than to morphological plasticity.

Table 5.2 Summary statistics of ANOVA, SLA

	n	Parameter tested (Differences of mean values)	ρ value	LSD
Over all sites	144	SLA between sites	<0.001*	0.459
		Bloemendal vs Mistley	<0.036*	
		Bloemendal vs Seele/Mountain Home	<0.001*	
		Mistley vs Seele/Mountain Home	0.077	
	144	SLA between age groups	0.432	0.554
	144	SLA between crown zones	<0.001*	0.426
		Upper vs middle	0.006*	
		Upper vs lower	<0.001*	
		Middle vs lower	0.001*	
Within sites	48	Bloemendal- SLA between age groups	0.127	0.663
		SLA between crown zones	<0.001*	0.418
		Upper vs middle	0.049*	
		Upper vs lower	<0.001*	
		Middle vs lower	0.017*	
	48	Mistley - SLA between age groups	0.493	1.140
		SLA between crown zones	.0018*	0.918
		Upper vs middle	0.082	
		Upper vs lower	0.005*	
		Middle vs lower	0.251	
	48	Seele/Mountain Home		
		- SLA between age groups	0.221	0.918
		SLA between crown zones	<0.001*	0.058
		Upper vs middle	0.141	
		Upper vs lower	<0.001*	
		Middle vs lower	0.001*	

* The mean difference is significant at $\rho < 0.05$.

LSD: Least significant difference

SLA indicates leaf thickness; in addition it has also been related to leaf structure, growth and net photosynthesis (Barden, 1977). SLA can also be used in conjunction with LA to estimate leaf mass for nutrient balance calculations and growth estimates. Rather than point data of SLA, a spatial SLA dataset could be incorporated into ecological and biogeochemical models in a similar fashion to LAI dataset, potentially allowing the inclusion of parameters such as life span, litter fall rate, leaf carbon to nitrogen ratio, and canopy nitrogen content. The inclusion of SLA and associated parameters into future ecological models would facilitate parameterization of more plant ecophysiological constraints. Thus, SLA is one of the main plant parameters that it is needed by 3-PGS model for estimating growth and water use of *Acacia mearnsii*. SLA is included in 3-PGS as a function of time (i.e., SLA decreasing with time). In this study the results showed that a constant value is possible for *Acacia mearnsii*. SLA is also needed to calculate LAI by destructive sampling.

Recently researchers have attempted to estimate SLA from remotely sensed data in a similar manner to LAI. For instance, Lymburner *et al*., (2000) tried to estimate canopy-average surface-SLA using Landsat TM data and the results were promising. Lymburner *et al*. (2000) reported a strong correlation between SLA and NDVI (R^2=0.83), SLA and RVI (R^2=0.91) and SLA and soil and atmosphere resistant vegetation index (SARVI2) (R^2=0.88) and suggested that these VIs could be used to estimate canopy average SLA. All the leaves used by Lymburner *et al*. (2000) to estimate species SLA were sun leaves chosen from the top part of the canopy. This is of particular importance with SLA, which has been shown to vary with depth in the canopy in both this study and the study conducted by Lymburner *et al*. (2000).

An attempt was made to assess the relationships between Plot SLA from destructive sampling and the VIs derived from remotely sensed data. The results showed that SLA was strongly correlated with NDVI (r=0.71, ρ<0.01) and RVI (r=0.76, ρ<0.01) and moderately correlated with TVI (r=0.66, ρ<0.05), see Table 5.3.

Table 5.3 Correlation Matrix (VIs and SLA values)

	SLA	NDVI	RVI	TVI	VI3
SLA	1.000				
NDVI	0.714**	1.000			
RVI	0.762**	0.588**	1.000		
TVI	0.657*	0.535*	0.788**	1.000	
VI3	-0.205	-0.264	-0.305	- 0.128	1.000

** Correlation is significant at ρ<0.01.

* Correlation is significant at ρ<0.05.

Further regression analysis indicated that 58.8 % of the variation in the relationship between Plot SLA and RVI and 51 % between Plot SLA and NDVI could be explained by regression. The regression relationship between SLA and TVI and VI3 were found to be very weak. Therefore, it is possible to obtain a preliminary or rough estimate of SLA of *Acacia mearnsii* in KwaZulu-Natal midlands using NDVI or RVI derived from Landsat ETM+ imagery. Equations that can be used to predict SLA from RVI and NDVI values are presented in Table 5.4 below.

Table 5.4 Equations for predicting SLA from VIs

Vegetation index	Equations	R^2	Significance	n
RVI	SLA=0.7915*RVI+5.1164	0.58	0.009	12
NDVI	SLA=8.3651*NDVI+3.3434	0.51	0.004	12

n represents number of sample stands.

5.2.2 Leaf Area

The relationship between LA and DBH was described for each study site by an allometric relationship. The weighted non-linear regression (exponential) in the case of Bloemendal and Mistley and the linear regression analysis in Seele/Mountain Home of tree LA and DBH provided a unique equation for each site (Table 5.5). In these equations x and y represent DBH and tree LA, respectively.

Table 5.5 Equations describing the relationship between DBH and tree LA.

Study Site	Regression Equations	R^2	Significance	n
Bloemendal	$y= 2855.28e^{0.17x}$	0.61	<0.001	16
Mistley	$y= 4578.71e^{0.12x}$	0.77	<0.001	16
Seele/Mountain Home	$y= 3503.49x-20479.92$	0.71	<0.001	16

n represents number of sample stands.

The relationship between DBH and LA is also shown diagrammatically in Figures 5.1(a-c) below.

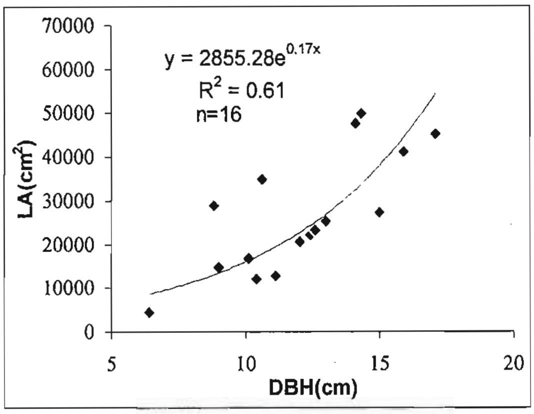

a. Bloemendal

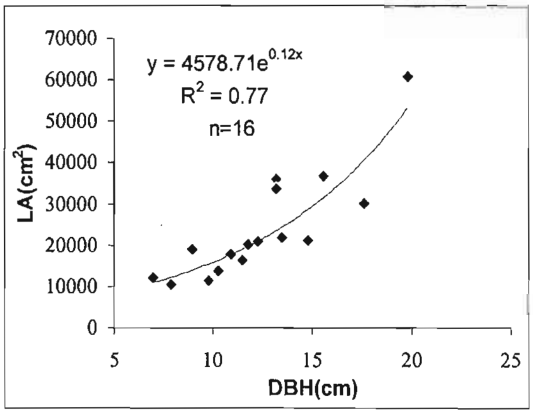

b. Mistley

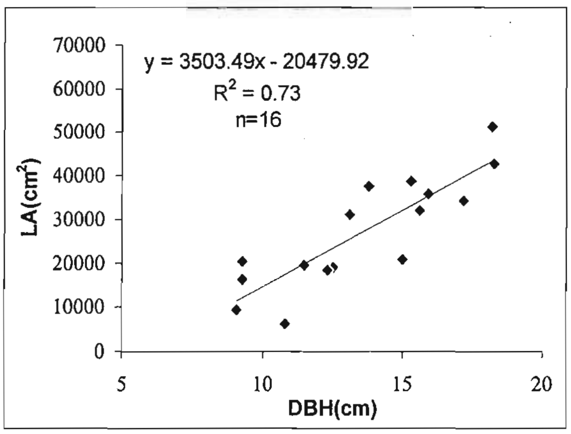

c. Seele/Mountain Home

Figure 5.1 Regression equations showing the relationship between DBH and LA for each of the study sites.

The LA data of the sample trees used to derive the relationships between DBH and LA are presented in Appendix 4c. The above equations were used to calculate the LA of all the trees found in the sample plots and the individual tree LAs were summed up to obtain the total LA for the sample plots (Table 5.6).

Table 5.6 Total LA of the sample plots obtained by destructive sampling.

Study Site	Tree Age (years)	Compartment No.	Total Plot LA (m^2)
Bloemendal	4	014	1017.45
	6	012	1021.43
	8	009	1112.16
	10	013	1109.63
Mistley	3	A01	1075.31
	5	B16	1032.28
	7	B27	1018.61
	11	C01A	1195.93
Seele	4	D27	1221.95
	7	E03	1491.34
Mountain Home	8	D03	1588.13
	11	D01A	1839.02

The mean tree LA values for Bloemendal, Mistley and Seele/Mountain Home were found to be 27.9, 23.96 and 27.08 m^2, respectively (Appendix 4b). ANOVA showed that the differences between the mean tree LA values of the different sites were significant ($\rho<0.05$). The mean tree LA values for age groups one to four were found to be 49.4, 42.9, 48.0 and 67.9 m^2. The differences between the mean tree LA values of the different age groups were statistically insignificant (Table 5.7).

The total plot LA ranged from 1017.45 m^2 for the four year old stand in Bloemendal to 1839.02 m^2 for the eleven year old stand in Mountain Home. The mean plot LA was found to be 1065.66, 1080.53 and 1535.11 m^2 for Bloemendal, Mistley and Seele/Mountain Home, respectively. The ANOVA test showed that the difference between the mean plot LA of the different sites was significant ($\rho<0.05$) (Table 5.7).

Table 5.7 Summary statistics of ANOVA, LA

	n	Parameter tested (Differences of mean values)	ρ value	LSD
Over all sites	48	Tree LA between sites	<0.001*	16.47
		Bloemendal vs Mistley	<0.001*	
		Bloemendal vs Seele/Mountain Home	<0.001*	
		Mistley vs Seele/Mountain Home	0.152	
	48	Tree LA between age groups	0.175	27.68
	12	Total plot LA between sites	0.003*	251.80
		Bloemendal vs Mistley	0.893	
		Bloemendal vs Seele/Mountain Home	0.002*	
		Mistley vs Seele/Mountain Home	0.003*	
	12	Total plot LA between age groups	0.699	545.00

* The mean difference is significant at $\rho < 0.05$.

LSD: Least significant difference

The mean plot LA values were found to be 1105.90, 1181.68, 1239.63 and 1381.52 m^2 for age group one to four, respectively. There were no significant differences between mean LAs of the different age groups even though mean LA increased from age group one to four (Table 5.7). Veldtman *et al.* (1995) also reported that there was no significant difference between mean LAs for the three age groups of *Acacia mearnsii* that he had studied. The reason for no significant difference in overall LA between age groups would suggest that overall LA is maintained at a constant level through a balance of leaf numbers to LA. There was also no significant difference in LA values between age groups within each of the study sites.

5.2.3 Calculation of LAI values

In destructive sampling LAI was obtained by dividing the total LA of trees in the sample plot by the plot area. The LAI values derived from destructive sampling are shown in Table 5.8. The LAI values ranged from 3.15 to 5.69 with a mean value of 3.80. These results fall within the range of the LAI values of *Acacia mearnsii* estimated by Veldtman *et al.* (1995) where the LAI values for three age groups, 1-3, 6-7, and 8-13 year old, were found to be 3.23 ± 2.25, 4.37 ± 2.51 and 3.82 ± 2.62, respectively through methods of destructive sampling which was carried out in Bloemendal, Mistley and Harden Heights, KwaZulu-Natal, South Africa.

Tables 5.8 LAI estimates calculated from destructive sampling

Study Site	Tree Age (yr)	Compartment No.	Total Plot LA (m^2)	Plot Area (m^2)	LAI
Bloemendal	4	014	1017.45	323	3.15
	6	012	1021.43	323	3.16
	8	009	1112.16	323	3.44
	10	013	1109.63	323	3.44
Mistley	3	A01	1075.31	323	3.33
	5	B16	1032.28	323	3.20
	7	B27	1018.61	323	3.15
	11	C01A	1195.93	323	3.70
Seele	4	D27	1221.95	323	3.78
	7	E03	1491.34	323	4.62
Mountain Home	8	D03	1588.13	323	4.92
	11	D01A	1839.02	323	5.69
				Mean LAI	3.80

The mean LAI values for Bloemendal, Mistley and Seele/Mountain Home were found to be 3.30, 3.35 and 4.75, respectively. While the mean LAI values for age groups one to four were found to be 3.42, 3.66, 3.84 and 4.28, respectively (Appendix 4b). Significant differences were observed between mean LAI values of the different sites ($\rho<0.05$) (Table 5.9). Although it was expected to observe an increase in LAI as stands develop and reach steady state or equilibrium for older stands, there were no significant differences in estimated LAI values between the different age groups. The reason for this could be the decrease in stocking of the stands, as the trees grew older. *Acacia mearnsii* stands have higher stocking (trees ha^{-1}) at young ages and this decreases with age because thinning is always done to remove diseased trees. This can be seen from the figures of final stocking in Table 3.1.

Table 5.9 Summary statistics of ANOVA, LAI

	n	Parameter tested (Differences of mean values)	ρ value	LSD
Over all sites	12	LAI between sites	0.003*	0.692
		Bloemendal vs Mistley	0.893	
		Bloemendal vs Seele/Mountain Home	0.002*	
		Mistley vs Seele/Mountain Home	0.003*	
	12	LAI between age groups	0.700	1.688

* The mean difference is significant at $\rho < 0.05$.

LSD: Least significant difference

In general, mean SLA and LA showed significant differences between different sites, while neither of them varied significantly with age both within sites and between sites. LAI values were also observed varying significantly between sites but their variation was insignificant between age groups.

5.3 Estimation of PAI by LAI-2000

The mean values of PAI measured using LAI-2000 for all the twelve stands in the four sites are presented in Table 5.10. Full details are presented in Appendix 5. The lowest value recorded was 2.61 and the highest was 4.62 with an overall mean PAI was 3.35 (Table 5.10).

Table 5.10 Plant Area Index (PAI) and its standard error (STDERR) of the sample plots.

Study Site	Tree Age (years)	Compartment No.	Mean PAI	Mean STDERR
Bloemendal	4	014	3.35	0.026
	6	012	2.62	0.023
	8	009	2.79	0.013
	10	013	2.61	0.025
Mistley	3	A01	3.27	0.031
	5	B16	3.20	0.031
	7	B27	3.31	0.029
	11	C01A	3.09	0.026
Seele	4	D27	3.55	0.022
	7	E03	3.79	0.038
Mountain Home	8	D03	3.96	0.081
	11	D01A	4.62	0.064
		Mean	3.35	0.034

STDERR= Standard errors of the contact frequencies

The mean PAI values for Bloemendal, Mistley and Seele/Mountain Home were found to be 2.84, 3.22 and 3.98, respectively; while the mean PAI values for age groups one to four were 3.39, 3.20, 3.35 and 3.44, respectively (Appendix 4b). Statistical analyses showed that the differences in mean PAI values of all the stands were found to be significant between sites but varied insignificantly between age groups (Table 5.11).

Table 5.11 Summary statistics of ANOVA, PAI

	n	Parameter tested (Differences of mean values)	ρ value	LSD
Over all sites	36	PAI between sites	<0.001*	0.263
		Bloemendal vs Mistley	0.006*	
		Bloemendal vs Seele/Mountain Home	<0.001*	
		Mistley vs Seele/Mountain Home	<0.001*	
	36	PAI between age groups	0.849	0.580

* The mean difference is significant at ρ < 0.05.

LSD: Least significant difference

The PAI values recorded for stands of the same age group but from different study sites were found to be slightly different even though it was not significant statistically. For instance, the PAI value of the four year old stand in Bloemendal was 3.35 whereas the PAI value of the four year old in Seele was found to be 3.55. This could be mainly attributed to the difference in stand density and site quality. Since the crowns were of different shape for the different sites and age groups, the estimation procedure of LAI-2000 may be affected by crown shape to a sufficient degree to yield different biases for different compartments. The mean standard deviation of the LAI estimates ranged from 0.023-0.081 and is controlled by the spatial heterogeneity present within the overstorey of a stand.

As it has been discussed in chapter two, forest canopies do not conform to the assumptions used in calculating PAI from LAI-2000 measurements because branches and leaves are clumped and are not optically black, leading to an underestimation of LAI. To see whether the LAI-2000 has underestimated PAI in this study the ratio of LAI to PAI was calculated and the results are presented in Table 5.12.

The LAI-2000 underestimated the actual LAI values for all the stands except for the four year old stand in Bloemendal and the seven year old stand in Mistley. But the magnitude of underestimation is better for this study compared to previous studies because the mean rate of underestimation was found to be only 17 % with a maximum of 32 %. It has also been observed in previous studies (e.g. Chason *et al.*, 1991; Chen, 1996; Chen *et al.*, 1991; Fassnacht *et al.*, 1994; Smith *et al.*, 1993; Stenberg *et al.*, 1994) that PAI assessed with the LAI-2000 was consistently less than actual LAI. PAI was underestimated by 43 % in Scots pine (*Pinus sylvestris* L.) stands (Stenberg *et al.*, 1994) and by 62 % in Douglas-fir stands (Smith *et al.*, 1993). It has been suggested that underestimation of LAI at high LAs due to clumping of the foliage. Apart from the LAI values obtained by destructive sampling the LAI-2000 underestimated PAI derived from hemispherical photographs by 15% (Wang *et al.*, 1992). Therefore, it is necessary to calibrate the LAI-2000 so that measured PAI can be used to predict actual LAI (Cherry *et al.*, 1996).

Table 5.12 The ratio of LAI to PAI values of the sample plots.

Study Site	Tree Age (years)	Compartment No.	Mean PAI	Mean LAI	LAI/ PAI
Bloemendal	4	014	3.35	3.15	0.94
	6	012	2.62	3.16	1.21
	8	009	2.79	3.44	1.23
	10	013	2.61	3.44	1.32
Mistley	3	A01	3.27	3.33	1.02
	5	B16	3.20	3.20	1.00
	7	B27	3.31	3.15	0.95
	11	C01A	3.09	3.70	1.20
Seele	4	D27	3.55	3.78	1.06
	7	E03	3.79	4.62	1.22
Mountain Home	8	D03	3.96	4.92	1.24
	11	D01A	4.62	5.69	1.23
		Overall Mean	3.35	3.80	1.13

On the other hand, Gower and Norman (1991) caution that the LAI-2000 could overestimate LAI in deciduous canopies with numerous low dead branches and suggest that measurements be made at the base of the live crown if this situation exists. Overestimation can occur at lower values of LA than were measured in this study, or when the bias due to clumping is removed because of the effects of branch and stem area index on the estimation of LAI (Chen *et al.*, 1991; Deblonde *et al.*, 1994; Sampson and Allen, 1995).

Constant factors like shoot or branch leaf area indices were used to correct PAI to actual LAI by Gower and Norman (1991) and Smith *et al.* (1993), taking into account underestimation of actual LA due to clumping effects. Clumping effects result from a violation of one of the major assumptions for calculating PAI on the basis of radiation measurements. It is assumed that the foliage is randomly distributed within the canopy. In reality, foliage is clumped on different morphological hierarchies such as shoots, branches, or trees. Clumping effects lead to an increase in the amount of transmitted radiation and, consequently, can result in an underestimation of actual LAI as calculated by PAI.

The simplest way to derive coefficients to convert PAI to actual LAI is by comparing LAI-2000 output with LAI values derived from destructive sampling. Thus for this study correlation and regression analyses were used to assess the relationship of LAI values obtained from destructive sampling with PAI values measured by LAI-2000. The LAI and PAI were found to be highly correlated ($r=0.86$, $\rho<0.01$). Further regression analysis showed that 74% of the variation in the relationship between LAI and PAI could be explained by regression (Figure 5.2).

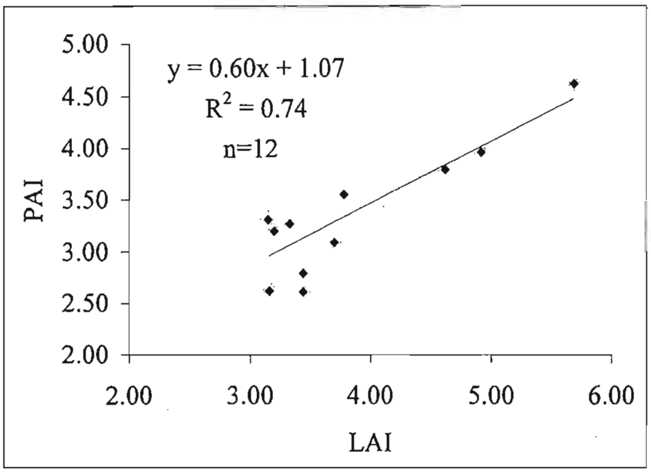

Figure 5.2. Calibration curve for LAI obtained by destructive sampling and PAI measured using LAI-2000.

Although the relationship between LAI and PAI was found to be satisfactory for *Acacia mearnsii* ($R^2=0.74$), it would not be possible to obtain better result because of the lack of uniformity and continuality of the canopy structure of the species. Uniformity and stocking in commercial forest plantations are affected by early silvicultural practices (Smith, 2002a). In addition, the loss of trees with age creates gabs in the stands.

5.4 Remotely Sensed Vegetation Indices

In estimating LAI from remotely sensed data the first step was transforming the imagery into VIs. The VIs calculated in this study were NDVI, RVI, TVI and VI3; the mean values of which for all the small plots are presented in Table 5.13.

Table 5.13 Mean values of VIs calculated from Landsat ETM+ satellite imagery.

Study Site	Tree Age (years)	Compartment No.	Mean NDVI	Mean RVI	Mean TVI	Mean VI3
Bloemendal	4	014	0.54	3.11	0.84	223
	6	012	0.59	3.21	0.82	190
	8	009	0.54	3.71	0.83	202
	10	013	0.54	3.84	0.82	193
Mistley	3	A01	0.60	4.50	1.06	204
	5	B16	0.56	4.05	1.04	174
	7	B27	0.56	3.91	1.03	209
	11	C01A	0.61	3.87	1.05	212
Seele	4	D27	0.60	4.44	1.04	228
	7	E03	0.62	4.57	1.05	182
Mountain Home	8	D03	0.59	4.32	1.02	163
	11	D01A	0.69	4.45	1.01	180

The mean NDVI values ranged from 0.54 to 0.69; the RVI values from 3.11 to 4.57; the TVI values from 0.82 to 1.05, while the VI3 values ranged from 163 to 228. The values of VI3 are spectral values (0-255) whereas the others are expressed in the form of real numbers, i.e. there are two possible ways of expressing VIs values. NDVI, RVI and TVI are the results of near infrared and red bands while VI3 is slightly different from them because it is calculated from the near infrared and middle infrared bands of the Landsat ETM+ imagery.

5.5 Relationships between LAI, PAI and VIs

Data analysis was orientated towards evaluating the VIs obtained by the processing of the Landsat ETM+ imagery compared with the LAI values obtained directly (destructive method) and indirectly (LAI-2000) from the sample plots. The results of the correlation analysis performed between LAI, PAI values and the various VIs to investigate the direction and strength of their relationships by determining the correlation coefficient (r) are shown in Table 5.14.

Table 5.14 Correlation Matrix (VIs, Actual LAI and PAI values)

	LAI	PAI	NDVI	RVI	TVI	VI3
LAI	1.000					
PAI	0.858**	1.000				
NDVI	0.789**	0.747**	1.000			
RVI	0.609*	0.626*	0.588*	1.000		
TVI	0.366	0.582*	0.535	0.788**	1.000	
VI3	-0.5251	-0.307	-0.264	-0.305	-0.128	1.000

** Correlation is significant at $\rho<0.01$.

* Correlation is significant at $\rho<0.05$.

The correlation coefficient obtained for LAI and PAI ($r=0.86$, $\rho<0.01$) indicates that there was a strong relationship between LAI and PAI. LAI was also strongly correlated with NDVI ($r=0.79$, $\rho<0.01$). Moderate correlation was also observed between LAI and RVI ($r=0.61$, $\rho<0.05$). LAI was observed to have no significant correlation with TVI ($r=0.37$) and VI3 ($r=-0.53$).

The PAI values were strongly correlated with NDVI ($r=0.75$, $\rho<0.01$) and moderately correlated with RVI ($r=0.63$, $\rho<0.05$) and TVI ($r= 0.58$, $\rho<0.05$). No significant correlation was observed between PAI and VI3 ($R=0.31$).

Between the various VIs themselves, the strongest correlation observed was between RVI and TVI ($r=0.79$, $\rho<0.01$). NDVI and RVI are moderately correlated ($r=0.59$, $\rho<0.05$). The correlation between NDVI and TVI was found to be insignificant ($r=0.54$). VI3 was observed to have no significant correlation with NDVI, RVI and TVI.

In general, the best correlation was found between actual LAI and PAI. All the VIs were positively correlated with LAI and PAI except VI3. Such results were expected because all the indices used were ratio VIs in which the value of near infrared and red bands were utilized.

In addition to correlations, regression analyses were performed to investigate the relationships between LAI, PAI values and the various VIs. The various VI values obtained from the sample plots were plotted against field LAI values. Various regression models (linear, logarithmic, power or exponential) were fitted to determine the relationship between LAI and the various VIs. Here the various VIs were taken as independent variables and LAI as a dependent variable. The regression equations developed to investigate the relationships are shown in Table 5.15. Actual LAI values were found to have significant relationship only with NDVI and RVI.

Table 5.15 Regressions of actual LAI and VIs.

Independent Variable (VI)	Equations	Significance	R^2	n
NDVI	$LAI = 15.13 * NDVI - 5.08$	0.002*	0.62	12
RVI	$LAI = 1.33 * e^{0.26*RVI}$	0.027*	0.40	12
TVI	$LAI = 2.92 * TVI + 0.98$	0.242	0.13	12
VI3	$LAI = -0.02 * VI3 + 8.09$	0.082	0.27	12

n represents number of sample stands.

Figures 5.3 (a-d) show the relationships that have been determined between LAI and the various VIs. From the four VIs utilized, NDVI showed better relationship with LAI (R^2=0.62).

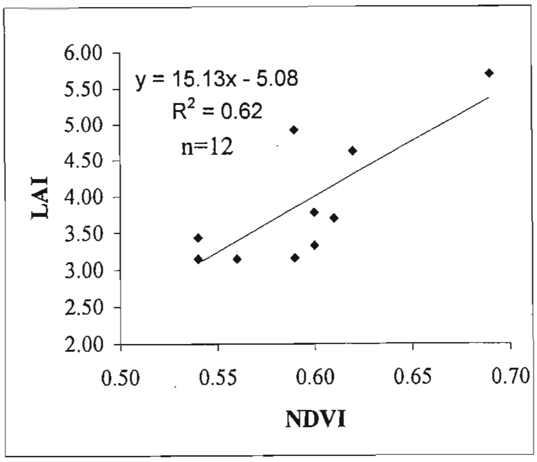

a.

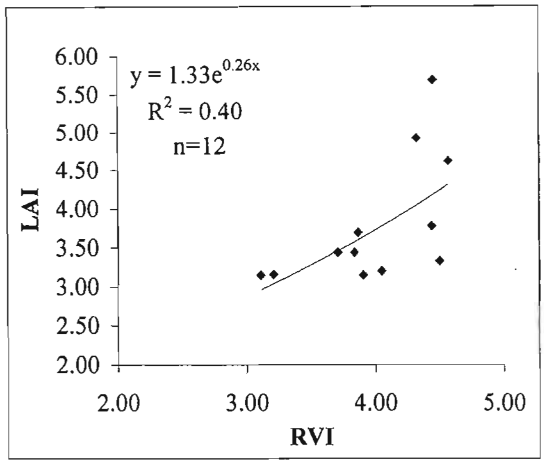

b.

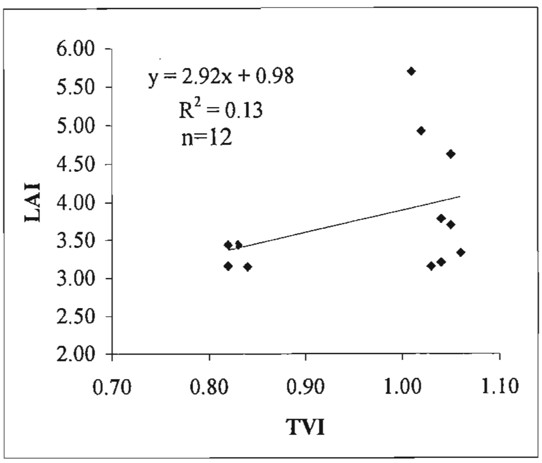

c.

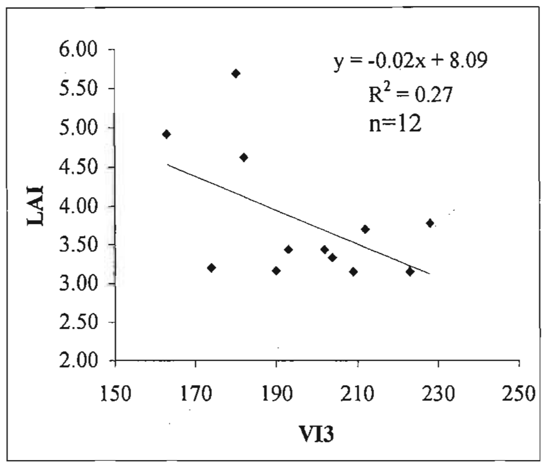

d.

Figures 5.3 Relationships between Actual LAI and VIs: (a) LAI and NDVI, (b) LAI and RVI, (c) LAI and TVI, and (d) LAI and VI3.

The relationship between PAI and the various VIs was also investigated in the same manner as for the actual LAI and the results are shown in Table 5.16 and Figures 5.4 (a-d).

Table 5.16 Regressions of PAI and VIs.

Variable (VI)	Equations	Significance	R^2	n
NDVI	$PVI = 10.00 * NDVI - 2.52$	0.005*	0.56	12
RVI	$PAI = 1.37 * e^{0.22*RVI}$	0.029*	0.41	12
TVI	$PAI = 3.43 * TVI^{0.96}$	0.025	0.41	12
VI3	$PAI = -1.87* Ln(VI3) + 13.22$	0.297	0.11	12

The results demonstrated that PAI exhibits a relatively better relationship with NDVI (R^2=0.56) but the relationships of PAI with the other VIs were not satisfactory.

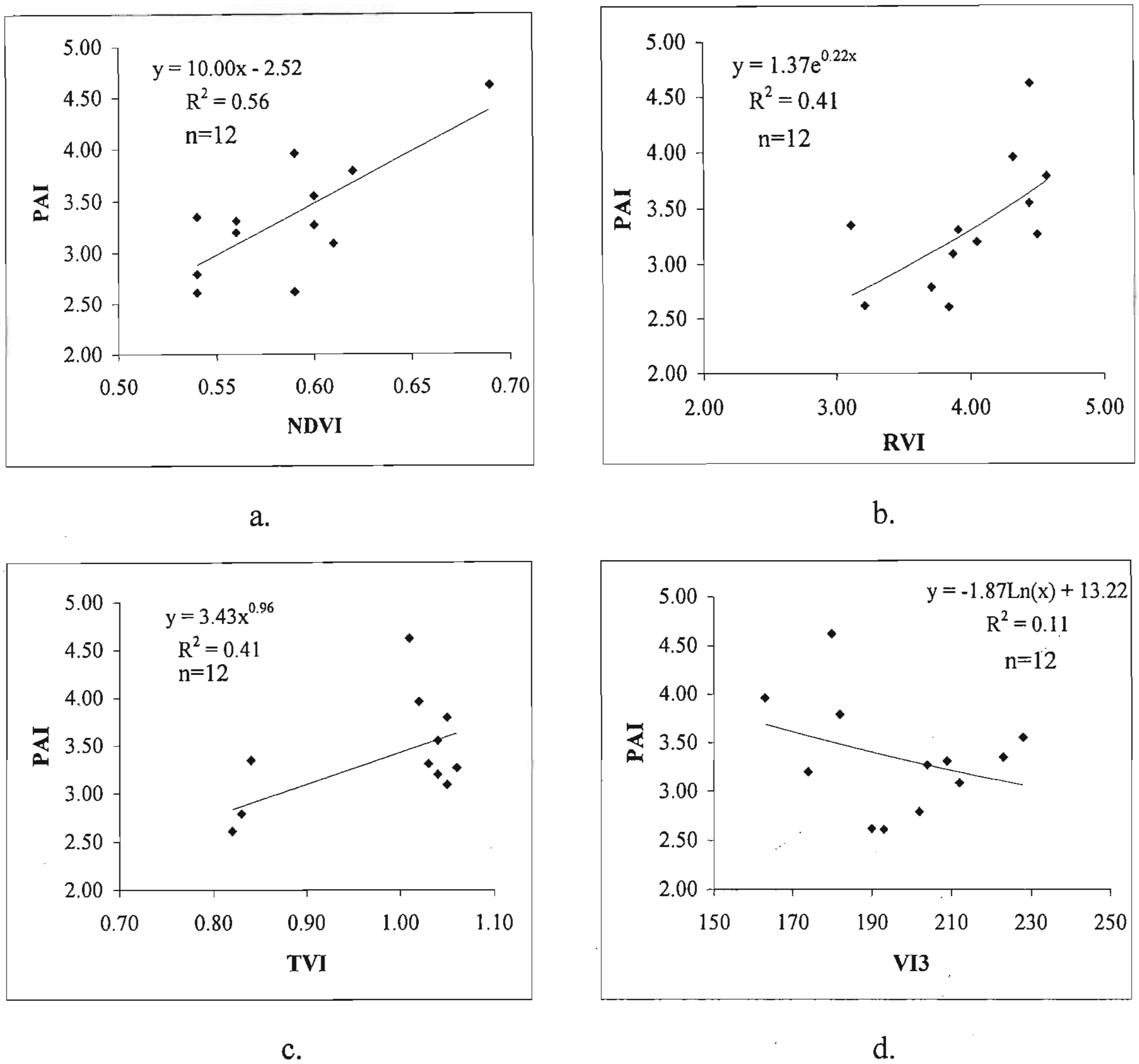

Figure 5.4 Relationships between PAI and VIs: (a) PAI and NDVI, (b) PAI and RVI, (c) PAI and TVI, and (d) PAI and VI3.

The performance of VIs in relation to biophysical characteristics and especially LAI has been varied. Running *et al.* (1986) reported both NDVI (R^2=0.55) and SR (R^2=0.76) to be useful for estimating the LAI of 18 conifer forests along a west-to-east transect in Oregon with the Airborne Thematic Mapper Simulator (TMS). Working in the same area Peterson *et al.* (1987) improved a linear TMS SR-LAI relationship (R^2= 0.83) by using a log-linear transformation (R^2=0.91). Similarly, Spanner *et al.* (1994) found that a logarithmic regression between SR and LAI explained 97% of the variation in LAI of stands included in the Oregon Transect Ecosystem Research project. Coops *et al.* (1997) also observed that linear relationships were shown to be appropriate to relate both NDVI and SR transformations to the LAI data with R^2 values of 0.71 and 0.53, respectively.

Herwitz *et al.* (1990), in contrast, reported that neither SR nor NDVI (R^2=0.10) were significantly related to the LA of white pine (*Pinus strobes* L.) and red pine (*Pinus resinosa* Ait) plantations in Central Massachusetts. Curran *et al.* (1992) showed that the correlation between NDVI and LAI varied with season (R^2= 0.35, 0.75, 0.86 for February, September, and March; n=16) for control and fertilized slash pine (*P.elliottii* Engelm.) sites in Florida. Danson and Plummer (1995) have also tested hypotheses on the relation between forest LAI, high spectral resolution reflectance data and red-edge position (REP). Linear correlations with reflectance were weak in the red and near infrared regions and there was no significant relation with the NDVI above an LAI of 6.

Boyd *et al.* (1999) reported that for a boreal forest canopy, the relationship between VI3 and LAI (R^2=0.62) was observed to be much stronger than that between NDVI and LAI (R^2=0.28). In addition, Boyd *et al.* (2000) investigated that the LAI estimated using VI3 accounted for about 76% of the variation in the field estimates of LAI, compared with about 46% when using the NDVI. They concluded that the inclusion of information provided by middle infrared reflectance enhanced the accuracy of LAI estimates and its subsequent use should be considered. But in this study the VI3 was found to have the weakest correlation with LAI and PAI values and this was suspected to be due to the differences in leaf moisture content at the time of image acquisition and sampling.

Curran and Williamson (1987) reported that three refinements to this methodology might offer significant improvements in the accuracy of LAI estimation. These are the suppression of environmental influences on the satellite data and allowance for both asymptotic relationship between VIs and LAI and error in measured LAI. There are many environmental factors that disturb the relationships between a vegetation index and LAI. In this study the most important environmental factors likely to be are the variation in soil background in space and the geometrical arrangement of the sun, canopy and sensor.

It is evident from the above that the use of the VIs for estimating LAI shows great variation in results from species to species and from place to place. No work has been reported on the utilization of Landsat ETM+ for the estimation of LAI of *Acacia mearnsii*. In addition, it has been observed that the results obtained in this study were not far from the previous studies. It is difficult to obtain an "excellent" relationship between LAI and VIs determined from satellite imagery. This is attributed to the various environmental factors that remain uncontrolled during image acquisition and LAI estimation by destructive sampling.

Therefore, from the results obtained so far, NDVI as a measure of LAI seems to be more robust than the other VIs. The NDVI is less sensitive to variations in location, viewing angle, and lighting conditions when compared with the near infrared satellite channels. Thus for the estimation of LAI at stand level in this study, NDVI was chosen simply as a result of its higher significant correlation with actual LAI ($r=0.79$, $\rho<0.01$) obtained by destructive sampling and PAI measured by LAI-2000 ($r=0.75$, $\rho<0.01$) and its reasonable regression relationship with NDVI ($R^2=0.62$).

Finally, from the results obtained by regression analyses, which were performed to investigate the predictive power of the VIs to estimate LAI from Landsat ETM+ satellite imagery (Table 5.15 and Figures 5.3a-d), the predictive equation that was found to be significant was:

$$LAI = 15.13 * NDVI - 5.08 \qquad [Eq.5.1]$$

This equation can be used to predict LAI from NDVI values transformed from Landsat ETM+ satellite imagery for *Acacia mearnsii* forest plantations in KwaZulu-Natal midlands. This regression-based relationship could also be used to derive thematic maps of LAI of the sample stands. This can be done in ERDAS Imagine 8.4 "model maker", thus the graphic model creator allows the user to place images, functions, tables and links using the tool palette. Thus to come up with thematic maps of LAI from remotely sensed data, the coefficients of this linear regression model could entered into model maker using the

NDVI images as an input and the final products will be thematic maps of LAI derived from NDVI.

The overall analyses observed so far showed that there is a potential of estimating LAI of *Acacia meansii* from Landsat ETM+ satellite imagery. LAI currently may be derived from remotely sensed data with limited accuracy. But there is a need for increased accuracy in the estimation of LAI through integration to the relationship between actual LAI and VIs. Wulder *et al.* (1998) reported that the inclusion of texture, which acts as a surrogate for forest structure, to the relationship between LAI and NDVI increased the accuracy of modeled LAI estimates.

Peddle and Johnson (2000) and Peddle *et al.* (2001) investigated that spectral mixture analysis (SMA)[1] has been shown to prove improved estimation of biophysical structural variables such as LAI, net primary productivity and biomass compared to NDVI in areas of flat and mountainous boreal forest terrain in Minnesota, USA. The basis for these improvements over the traditional vegetation index based approaches has been the ability to quantify and separate explicitly the fraction of shadow, background, and canopy components at sub-pixel scales. These components together comprise the overall pixel level signal received at an airborne or satellite remote sensing platform (Curran and Williamson, 1987). Results indicated that SMA provide significantly better results than any VIs, with improvements in the order of 20 % compared to the best vegetation index (NDVI) results. As *Acacia mearnsii* stands lack uniformity and suffer from gaps it could be possible to improve the results obtained in this study by performing sub pixel level analyses of LAI from Landsat ETM+ satellite imagery.

Concerns about the effects of site quality, management practices and stand structure on canopy architecture (Sampson and Allen, 1995) may not apply to the use of calibration curves relating LAI obtained from destructive sampling, PAI and satellite driven LAI, though clearly caution is required if measuring LAI in stands subject to silvicultural

[1] Spectral mixture analysis involves the systematic decomposition of spectral data to determine the percent area within a pixel, which may be attributed to individual scene components such as sunlit canopy, sunlit background and shadow.

interventions such as thinning or pruning that will affect the structure of canopies and frequency of canopy gaps. In the case of *Acacia mearnsii* stands continuous thinning to remove diseased trees takes place that LAI estimation was found to have limited accuracy.

In summary, many important limitations restrict the global (temporal and spatial) extensions of VIs for estimating LAI and other biophysical parameters. These include:

1. External effects caused by atmosphere, clouds and view-sun geometries;
2. Ground contamination (soil background, litter, senesced vegetation); and
3. The structural and optical properties of the vegetation canopy itself. This highlights the need for a more complete biophysical understanding of VIs, which will be crucial for their validation as well as for providing estimates of their accuracy and uncertainty.

Chapter 6: Conclusions and Recommendations

6.1 Conclusions

Satellite remote sensing techniques can provide resource managers with an efficient and economical means of acquiring timely data for the development and management of natural resources. In comparison with traditional methods, these techniques have the inherent properties of being able to provide synoptic observations with high observational density over relatively large areas. Remote sensing minimizes the logistical and practical difficulties of fieldwork in inaccessible areas. It has many applications in forestry. Various studies have been carried out to ascertain the potential of estimating forest LAI of coniferous and deciduous hardwoods from remotely sensed imagery, but less attention has concentrated on the estimation of LAI of *Acacia* stands. Several VIs closely reflect the LAI of specific plants but no single index is effective for all crops/ plants in all-atmospheric conditions. Thus, a species-specific evaluation on the utility of Landsat ETM+ imagery for the estimation of LAI was needed.

This study is a first step towards the remote estimation of LAI of commercial plantations of *Acacia mearnsii* in South Africa. While it provides some insights into the utility of Landsat ETM+ data for this purpose and meets all the planned objectives, it is clear that more research is required to improve the level of accuracy. The sample size in this study was small (twelve stands), which should be kept in mind when interpreting the empirical relationships. This means that the full range of variation occurring under natural conditions might not be represented, however, the relationships are useful across the range of sites tested.

Although the estimation of LAI of *Acacia mearnsii* by destructive sampling was very tedious, it provided good results for ground checking. In addition to the estimation of actual LAI values, total biomass sampling was carried out to determine dry biomass of the various components of the sample trees (see Appendix 6). There was a surprising lack of physiological data for this species. As a consequence when Dicks (2001) was undertaking a preliminary parameterization of 3-PG, some of the required variables were unknown and had to be estimated from default values from data applicable to other forest species. The large amount of biomass data determined in this study for a wide range of age groups from four study sites could be used to parameterize 3-PG and 3-PGS models.

SLA is an important plant attribute. Other than being one of the main parameters in estimating LA and LAI by destructive sampling, SLA could be incorporated into ecological and biogeochemical models in a similar fashion to LAI. Thus it is crucial to investigate how SLA values of *Acacia mearnsii* vary within one tree in the different crown zones and from one site to another. The field-based results of this study indicate that SLA values increased from the upper to the lower zones of the crown in most of the sampled trees. The mean SLA values varied significantly between sites but no significant difference was observed between the mean SLA values of the different age groups. In addition good relationships were found between RVI and NDVI from remotely sensed data and the SLA values from destructive sampling. This enabled the construction of site-specific empirical models that would be useful for preliminary estimation of SLA from Landsat ETM+ imagery.

Leaves are the primary sites of energy and mass exchange within the forest environment (Pierce and Running, 1988). Knowing actual LA and LAI in plantations is important in studies of forest productivity and modeling canopy structure (Borghetti and Vandramin, 1986) and estimating aboveground biomass (van Laar, 1984) cited by Veldtman *et al.*, (1995). In this study LA and LAI were analyzed by destructive sampling for the entire sample stands. Results showed that neither LA nor LAI of *Acacia mearnsii* varied significantly between age groups. This implies that overall leaf area is maintained at a constant level through a balance of leaf numbers to LA.

Obtaining actual LAI values for each site or plantation would entail destructive sampling, which would not be easy and serve the needs of resource managers. Thus, various indirect methods of estimating LAI have been used and regressed with various factors to try and obtain actual LAI values. Results showed that PAI values measured by LAI-2000 were significantly correlated with actual LAI obtained using destructive sampling. The relationship was reasonably strong enough such that this regression equation can be used to calibrate the analyzer, hence providing easier, more reliable measurements.

The VIs derived from red, near infrared and middle infrared bands of Landsat ETM+ satellite imagery were used to estimate the LAI of the four study sites. The relationship between NDVI and LAI values obtained by destructive sampling was found to be better than the relationship between actual LAI and the other VIs utilized in this study. This shows that NDVI could be used to estimate LAI of *Acacia mearnsii* forest plantations from Landsat ETM+ satellite imagery with a reasonable degree of accuracy. Thus a predictive empirical model was developed based on the relationship between NDVI and actual LAI values, which can be utilized to obtain point and spatial LAI estimate of *Acacia mearnsii* stands in KwaZulu-Natal midlands of South Africa.

The extent to which LAI obtained from remotely sensed imagery can be used to model ecological processes in forest plantations is only limited by the availability of supporting data. If appropriate data exist, the LAI estimates may be used to produce thematic maps of, for example, rates of photosynthesis, transpiration, respiration and nutrient uptake. Such thematic maps could then be combined with other spatial data in a GIS for management purposes. Above all, the spatial LAI or thematic maps are needed in the estimation of water use of plants or forest stands using process-based models (e.g., 3-PGS).

In general, this study has provided "reasonable" input data to parameterize and validate 3-PG and 3-PGS models for *Acacia mearnsii.* In the long term this could contribute to the fulfillment of the Water Act, which makes provisions for the classification of various crops and land use practices as stream flow reduction activities, which are then subject to controls to ensure equity in water allocation. Apart from estimating water use 3-PG and 3-PGS models enable the spatial estimation of vegetation/ forest productivity. The prediction of forest growth variables at specific stand ages and their capability to be extrapolated across the landscape using GIS could be used in forest management and planning.

6.2 Recommendations

Based on the work conducted in this study, several recommendations can be made with respect to future research:

- Estimates of LAI should represent samples across the full range that can be expected within a geographical region in order to gain a better understanding of the true form of VI-LAI relationships and better estimation accuracy of LAI from satellite imagery. Larger data sets should be obtained to more effectively explore the benefit of remotely sensed VIs and LAI estimated from VIs. This study only included trees from four sites including twelve stands. The sample size was small.

- Possible seasonal dependence of the regressions should be explored. Consequently, caution should be exercised in extrapolating results of this study temporally beyond the time period of sampling. Also the extrapolation could not be extended beyond KwaZulu-Natal midlands.

- The validity in extending this technique of LAI estimation to other species/ regions and for biomass and volume assessment should be considered. In addition, comparison of the accuracy and cost effectiveness of remotely sensed imagery with ground mensuration techniques should be carried out.

- Some useful relationships have been observed between actual LAI and VIs derived from remotely sensed data, particularly NDVI. However, the general validity of the relationships is limited may be due to some uncontrolled environmental factors. Follow-up studies are necessary, involving some parameters not thoroughly investigated in this study, such as the effect of soil background and understorey vegetation.

- Spectral mixture analysis has been shown to provide improved estimation of biophysical structural variables compared to NDVI in a montane forest environment (Peddle and Johnson, 2000). The basis for these improvements over more traditional VI-based approaches has been the ability to quantify and separate explicitly the fraction of shadow, background, and canopy components at sub-pixel scales. Thus, it is advisable to try to utilize the spectral mixture analysis for better results. It is clear that there is a potential of quantifying the impacts of forestry on water resources if small improvements could be introduced in the estimation technique like spectral mixture analysis.

- Although the use of Landsat ETM+ satellite imagery enabled the estimation of LAI of *Acacia mearnsii* with a reasonable degree of accuracy, further investigation on the use of relatively higher resolution satellite imagery is recommended and can improve the level of accuracy of the LAI estimates.

- Further work on the verification of the empirical models developed in this study to estimate SLA and LAI from NDVI and RVI is also required.

- Although the results presented would allow paramerization of process based models (e.g., 3-PGS) it is suggested that more research should be done in the area of LAI estimation from remotely sensed data to improve accuracy of process-based models for *Acacia mearnsii.*

REFERENCES

Acocks, J.P.H. 1988. Veld Types of South Africa. Memoirs of the Botanical Survey of South Africa, No 40, Botanical Research Institute, Pretoria.

Ahlrichs, J.S. and Bauer, M.E. 1983. Relation of agronomic and multispectral reflectance characteristics of spring wheat canopies. *Agronomy Journal*, 75: 987-993.

Ajai, D.S.K, Chaturuedi, G.S., Singh, A.K. and Sinha, S.K. 1983. Spectral assessment of leaf area index, chlorophyll content, and biomass of chickpea. *Photogrammetric Engineering and Remote Sensing*, 49: 1721-1727.

Angelici, G., Brynt, N. and Friendman, S. 1977. Techniques for land use change detection using Landsat imagery. *Proceedings of the American Society of photogrammetry,* Falls Church, Virginia, 217-228.

Anon, 1997. Plant Water Use. Washington State University. Available from: http://www.tfrec.wsu.edu/Orchard/pET/pETappl.html [Accessed: Sept 16, 2001].

Anon, 1998. Environmental and Natural Resources Committee, Parliament of Victoria Industrial chemicals, cosmetics and pharmaceuticals. Available from: http://www.parliament.vic.gov.au/default.htm [Accessed 06 Jun 2001].

Anon, 2000a. Sterile Seed to Restrict Wattle Spread. Wood SA and Timber Times. Available from: http://www.timbersa.co.za/MarketNews/sterilegene.htm [Accessed June 06, 2001].

Anon, 2000b. The leaf structure function relationships No.3. Rhodes Botany Fact Files.

Anon, 2001. Managing Water - the limiting resource for life. School of Bioresources Engineering and Environmental Hydrology, University of Natal, Pietermaritzburg. Available from: http://www.beeh.unp.ac.za [Accessed Aug 04, 2001].

Anon, 2002. Landsat: Geosciences Australia. Available from: http://www.auslig.gov.au [Accessed July 10, 2002].

Asrar, G., Fuchs, M., Kanemasu, E.T. and Hatfield, J.L. 1984. Estimating absorbed photosynthesis radiation of leaf area index from spectral reflectance in wheat. *Agronomy Journal,* 76: 300-306.

Asrar, G., Kanemasu, E.T., Jackson, R.D. and Pinter, P.J. 1985. Estimation of total above ground phytomass production using remotely sensed data. *Remote Sensing of Environment*, 17: 211-220.

Banner, A. and Lynham, T. 1981. Multispectral analysis of Landsat data for forest clear-cuts mapping - a trial of two procedures, *Proceedings of the 7th Canadian Symposium on Remote Sensing,* Winnipeg, Manitoba, Canada, 233-240.

Barclay, H.J., Trofymow, J.A. and Leach, R.I. 2000. Assessing bias from boles in calculating of leaf area index in immature Douglas-fir with the LI-COR canopy analyzer. *Agricultural and Forest Meteorology,* 100: 255-260.

Barden, J.A. 1977. Apple growth, photosynthesis, dark respiration, and specific leaf weight as affected by continuous and intermittent shade. *Journal of American Society of Horticultural Science,* 102(4): 391-394.

Baret, F. and Guyot, G. 1991. Potentials and limits of vegetation indices for LAI and APAR assessment. *Remote Sensing of Environment*, 35: 161-173.

Baret, F., Guyot, G., Begue, A. and Maurel, P. 1988. Complementarity of middle-infrared with visible and near-infrared reflectance for monitoring wheat canopies. *Remote Sensing of Environment*, 26: 213-225.

Barrett, E.C. and Curtis, L.F. 1976. Introduction to Environmental Remote Sensing. Chapman and Hall, London.

Battaglia, M., Cherry, M.L., Beadle, C.L. and Hingston, A. 1997. Leaf area index prediction in Eucalypt plantations accommodating the effects of water-stress and temperature. *Tree physiology*, 18: 521-528.

Battaglia, M. Beadle, C.L. and Sands, P.J. 1998. Process based forest productivity models and their application in forest management. *Forest Ecology and Management*, 102: 13-32.

Beadle, C.L., Cherry, M.L., Battaglia, M. and Hingston, A. 1998. Prediction of leaf area index in Eucalypt plantations: effects of water stress and temperature. *Tree Physiology*, 18: 521-528.

Beaumont, J.F., Ung, C-H. and Bernier-Cardu, M. 1999. Relating site index to ecological factors in black spruce stands: Tests of hypotheses. *Forest Science*, 45(4): 484-491.

Beymer, B.A. 2001. Rainfall interception analysis of a hardwood and pine forest. *Journal of Undergraduate Study and Independent Research,* 1:33-36.

Boden, D.I. 1991. Intensive site preparation on steep land: the effect of hydrological processes and growth of *Eucalyptus grandis* at 18 months. ICFR Annual Project Report, Pietermaritzburg, South Africa.

Borghetti, M. and Vendramin, G.G. 1986. Specific leaf area index distribution in a young Douglas-fir plantation. *Canadian Journal of Forest Research,* 16: 1283-1288.

Botkin, D.B. 1986. Remote Sensing of the Biosphere. National Academy of Sciences, Report of the Committee on Planetary Biology, National Research Council, Washington D.C., U.S.A.

Boyd, D.S., Foody, G.M. and Curran, P.J. 1999. The relationship between the biomass of Cameroonian tropical forests and radiation reflected in middle infrared wavelengths (3.0-5.0 μm). *International Journal of Remote Sensing,* 20: 912-920.

Boyd, D.S., Wicks, T.E. and Curran, P.J. 2000. Use of middle infrared radiation to estimate the leaf area index of boreal forest. *Tree Physiology,* 20: 755-760.

Bowers, S.A. and Hanks, R.J. 1965. Reflection of radiant energy from soils. *Soil Science,* 100: 130-138.

Bromilow, C. 1995. Problem Plants of South Africa. Bayer, Briza Publications.

Bunnik, N.J.J. 1981. Fundamentals of Remote Sensing. Relations between Spectral Signatures and Physical Properties of Crops. In: Application of Remote Sensing to Agricultural Production Forecasting (Eds) A. Berg, Balkema, A. and Rotterdam, A. pp. 47-81.

Burton, A.J., Pregitzer, K.S. and Reed, D.D. 2000. Leaf area and foliar biomass relationships in northern hardwood forests located along 800 km. Acid deposition gradient. *Forest Science,* 37(4): 1041-1059.

Calder. I. and Dye, P. 2000. Hydrological impacts of invasive alien plants. Available from: http://www.thewaterpage.com/hydro_impact_of_aliens.pdf [Accessed Oct 02, 2001].

Campbell, J.B. 1987. Introduction to Remote Sensing. The Guilford Press, London.

Carlson, R.E., Yarger, D.N. and Shaw, R.H. 1971. Factors affecting the spectral properties of leaves with special emphasis on leaf water status. *Agronomy Journal*, 63: 486-489.

Cermăk, J. 1989. Solar equivalent leaf area: an efficient biometrical parameter of individual leaves, trees and stands. *Tree Physiology*, 5: 269-289.

Clevers, J.G.P.W. 1988. The derivation of a simplified reflectance model for the estimation of leaf area index. *Remote Sensing of Environment*, 25: 53-69.

Clevers, J.G.P.W. 1989. The application of a weighed infrared vegetation index for estimating leaf area index by correcting for soil moisture. *Remote Sensing of Environment*, 29: 25-37.

Chance, J.E. 1981. Crop identification and leaf area index calculations with Landsat multitemporal data. *International Journal of Remote Sensing*, 2: 1-14.

Chason, J.W., Baldocchi, D.D. and Huston, M.A. 1991. A comparison of direct and indirect methods for estimating forest canopy leaf area. *Agricultural and Forest Meteorology*, 57: 107–128.

Chen, J.M. 1996. Optically-based methods for measuring seasonal variation of leaf area index in boreal conifer stands. *Agricultural and Forest Meteorology*, 51: 135-163.

Chen, J.M. and Black, T.A. 1992. Defining leaf area index for non-flat leaves. *Plant Cell Environment*, 15: 421-429.

Cherry, M., Hingston, A., Battaglia, M. and Beadle, C. 1998. Calibrating the LI-COR LAI-2000 for estimating leaf area index in Eucalypt plantations. CRCSPF, CSIRO and University of Tasmania. Available from: http://www.forestrytas.com.au/forestrytas/tasfor/tasfor-7.pdf [Accessed 20 Jul 2001].

Clough, B.F., Ong, J.E. and Gong, G.W. 1997. Estimating leaf area index and photosynthetic production in canopies of the mangrove *Rhizophora apiculata*. *Marine Ecology Progress Series*, 159: 285–292.

Computing Center for Water Research (CCWR). 1989. Estimation of mean annual precipitation (MAP) and other rainfall statistics at minute by minute of a degree grid points. Department of Agricultural Engineering University of Natal, Pietermaritzburg, South Africa.

Coops, N., Delahaye, A. and Pook, E. 1997. Estimation of Eucalypt forest leaf area index on the South Coast of New-South-Wales using Landsat MSS data. *Australian Journal of Botany,* 45(5): 757-769.

Coops, N.C., Waring, R.H. and Landsberg, J.J. 1998. Assessing forest productivity in Australia and New Zealand using a physiologically based model driven with averaged monthly weather data and satellite-derived estimates of canopy photosynthetic capacity. *Forest Ecology and Management,* 104:113-127.

Cornelissen, J.H.C., Castro, D.D. and Hunt, R. 1996. Seedling growth, allocation and leaf attributes in a wide range of woody plant species and types. *Journal of Ecology*, 84: 755-765.

Cracknell, A. and Hayes, L. 1991. Introduction to Remote Sensing. Taylor and Francis, Philadelphia.

Curran, P.J. and Williamson, H.D. 1985. The accuracy of ground data used in remote sensing investigations. *International Journal of Remote Sensing*, 6: 1637-1651.

Curran, P.J. and Williamson, H.D. 1987. GLAI estimation using measurements of red, near infrared and middle infrared radiance. *Photogrammetric Engineering and Remote Sensing*, 53(2): 181-186.

Curran, P.J. and Hay, A.M. 1986. The importance of measurement error for certain procedures in remote sensing at optical wavelengths. *Photogrammetric Engineering and Remote Sensing,* 40: 183-191.

Curran, P., Dawson, T.P. and Wicks, T.E. 1999. Geocomposition. Remote sensing and Process based Modeling. University of Southampton. High field, Southampton, U.K. and University of Oxford, Oxford, UK. Available from: http://www.geovista.psu.edu/sites/geocomp99/GC99/088/abs99.088.htm [Accessed 16 Sept, 2001].

Danson, F.M. and Plummer, S.E. 1995. Red-edge response of forest leaf area index. *International Journal of Remote Sensing*, 16(1): 183-188.

Davenport, M.L. and Nicholson, S.E. 1993. On the relationship between rainfall and the normalized difference vegetation index for diverse vegetation types of East Africa. *International Journal of Remote Sensing,* 14: 2369-2389.

Deblonde, G., Penner, M. and Royer, A. 1994. Measuring leaf area index with the LI-COR LAI-2000 in pine stands. *Ecology,* 75(5): 1507-1511.

De Beer H. 1986. Black Wattle. Farming in South Africa. Weeds A. 24/1986. Department of Agriculture and Water Supply, Pretoria.

Deering, D.W., Rouse, J.W., Haas, R.H. and Schell, J.A. 1975. Measuring forage production of grazing units from Landsat MSS data. *Proceedings of the 10th International Symposium on Remote Sensing of Environment,* II, 1169-1178.

Department of Water Affairs. 1986. Management of the water resources of the Republic of South Africa. Compiled by Department of Water Affairs, Pretoria, South Africa.

Di Bella, C.M., Rebella, C.M. and Paruelo, J.M. 2000. Evapotranspiration estimates using NOAA AVHRR imagery in the Pampa region of Argentina. *International Journal of Remote Sensing,* 21(4): 791-797.

Dicks, M. 2001. A Preliminary validation of the 3-PG Forest Growth and Water Use Model for *Acacia mearnsii* in Southern Africa. Report No. ENV-D-I-2000-16. CSIR.

Dobson, D. 2001. Director of South African Wattle Growers Union (SAWGU), Pietermaritzburg. Personal Communication.

Duke, J.A. 1981. Handbook of Legumes of World Economic Importance. Plenum Press. New York.

DWAF, 1996. How much water do alien plant invaders use? Working for Water Program Pamphlet: Government Printer.

Dye, P.J. 2001a. Modeling growth and water use in four *Pinus patula* stands with the 3-PG model. *South African Forestry Journal*, 191: 53-63.

Dye, P.J. 2001b. Evaluating the 3-PG Forest Growth Model. CSIR Environmentek, University of Natal, Pietermaritzburg (Personal communication).

Dye, P.J., Moses, G., Vilakazi, P., Ndlela, R. and Royappen, M. 2001. Comparative water use of wattle thickets and indigenous plant communities at riparian sites in the

Western Cape and KwaZulu-Natal. Available on: http://www.wrc.org.za [Accessed Jan13, 2001].

Eastman, J.R. 1995. Idrisi for Windows, User's Guide. Clarke University, U.S.A.

Eastman, J.R. 1999. Guide for GIS and Image Processing (Vol. 2). Clarke University, Worcester, MA, U.S.A.

Ellsworth, D.S. and Reich, P.B. 1993. Canopy structure and vertical patterns of photosynthesis and related leaf traits in a deciduous forest. *Oecologia*, 96(2): 169-178.

Elvidge, C.D. and Lyon, R.J.P. 1985. Estimation of the vegetation contribution to the 1.65/2.22 μm ratio in Airborne Thematic Mapper imagery for the Virginia Range, Nevada. *International Journal of Remote Sensing*, 6: 75-88.

Eklundh, L., Lars, H. and Kuus, A. 2001. Investigating relationships between Landsat ETM+ sensor data and leaf area index in boreal conifer forest. *Remote Sensing of Environment*, 78: 239-251.

ESRI, Inc., 2000. ArcGIS 8.1 (Software), Redlands, California, USA.

Erdas Imagine Inc. 1999. Geographic Imaging Simple. Atlanta, Georgia.

Evans, F. 1997. An Introduction to Remote Sensing. Available from: http://grenache.per.dms.csiro.au/research/remotesensing/whatis.html [Accessed: July 7, 2001].

Farrar, T.J., Nicholson, S.E. and Lare, A.R. 1994. The influence of soil type on the relations between NDVI, rainfall, and soil-moisture in the semiarid Botswana: 2, NDVI response to soil-moisture. *Remote Sensing of Environment*, 50(2): 121-133.

Fassnacht, K.S., Gower, J.M. and McMurtrie, R.E. 1994. A comparison of optical and direct methods of estimating foliage surface area index in forests. *Agricultural and Forest Meteorology*, 71: 1896-1900.

Fassnacht, K.S., Gower, S.T., MacKenzie, M.D., Nordheim, E.V. and Lillesand, T.M. 1997. Estimating the leaf area index of North Central Wisconsin forests using the Landsat Thematic Mapper. *Remote Sensing of Environment*, 61: 229-245.

Fey, M.V. and Schönau, A.P.G. 1982. Soils of Bloemendal Field Experiment Station. Report of Wattle Research Institute for 1981-1982.

Franklin, S.E., Hall, R.J., Moskal, L.M., Maudie, A.J. and Lavigne, M.B. 2000. Incorporating texture into classification of forest species composition from airborne multi-spectral images. *International Journal of Remote sensing*, 1: 61-79.

Fung, T. and Siu, W. 2000. Environmental quality and its changes, an analysis using NDVI. *International Journal of Remote Sensing*, 21(5): 1011-1024.

Genstat (4.2). 2000. 5th edition, Lawes Agricultural Trust.

Gholz, H.L. 1982. Environmental limits on aboveground net primary production, leaf area, and biomass in vegetation zones of the Pacific Northwest. *Ecology*, 63: 469-481.

Goel, N.S. and Thompson, R.L. 1984. Inversion of vegetation canopy reflectance models for estimating agronomic variables. V. Estimation of leaf area index and average leaf angle using measured canopy reflectance. *Remote Sensing of Environment*, 16: 69-85.

Goodchild, M.R., Parks, B.O. and Steyaert, L.T. (Eds) 1993. Environmental Modeling with GIS. Oxford University Press, New York, NY.

Goodchild, M.R., Steyaert, L.T., and Parks, B.O. (Eds) 1996. GIS and Environmental Modeling: Progress and Research Issues. GIS World Books, Fort Collins, CO.

Government Gazette 20615, 1999. Establishment of a pricing strategy for water use charges in terms of section 56(1) of the National Water Act, 1998. National water act, Act No 36 of 1998. Department of Water Affairs and Forestry. Available from: http://www.dwaf.gov.za/Documents/Notices/Pricestrat_English.doc [Accessed Dec 2, 2001].

Gower, S.T. and Norman, J.M. 1991. Rapid estimation of leaf area index in conifer and broad-leaf plantations. *Ecology*, 72(5): 1896-1900.

Gower, S.T., Kucharik, C.J. and Norman, J.M. 1999. Direct and indirect estimates of leaf area index, fapar and net primary production of terrestrial ecosystems. *Special Issues of EOS Remote sensing of the Environment,* 70(1): 29-51. Available from: http://sage.aos.wisc.edu/download/pubs/Abstracts/gower1999EOSabstract.htm [Accessed 01 Aug 2001].

Grantz, D.A., Zhang, X.J., Metheney, P.D. and Grimes, D.W. 1993. Indirect measurement of leaf area index in Pima cotton (*Gossypium barbadense* L.) using a commercial gap inversion method. *Agricultural and Forest Meteorology,* 67: 1-12.

Greenfell, A. 1976. Black Wattle (*Acacia mearnsii*) and Silver Wattle (*Acacia dealbata*). Agricultural Extension Service, Dohne Research Institute, Stutterheim, South Africa.

Grier, C.C. and Running, S.W. 1977. Leaf area of mature northwestern coniferous forests: relation to site water balance. *Ecology*, 58:893-899.

Hatfield, J.L., Asrar, G. and Kanemasu, E.T. 1984. Intercepted photosynthetically active radiation estimated by spectral reflectance. *Remote Sensing of Environment*, 14: 65-75.

Henderson, M., Fourie, D.M.C., Wells, M.J. and Henderson, L. 1987. Declared weeds and alien invader plants in South Africa. Department of Agriculture and Water Supply: Pretoria. Bulletin 413.

Herwitz, S.R., Peterson, D.L. and Eastman, J.R. 1990. Thematic mapper detection of changes in leaf area of closed canopy pine plantations in Central Massachusetts. *Remote Sensing of Environment,* 29: 129-140.

Holben, B.N., Tucker, C.J. and Fan, C.J. 1980. Spectral assessment of soybean leaf area and leaf biomass. *Photogrammetric Engineering and Remote Sensing,* 14: 651-656.

Hunt, M.A. 1999. Allometric relationships between stem variables and leaf area in planted *Eucalyptus nitens* and naturally regenerating *Acacia dealbata. New Zealand Journal of Forestry Science,* 29(2): 289-300.

ICFR and SAWGU. 1993. Establishment and re-establishment of wattle plantations from nursery seedlings and line-sowings. (Revised information booklet), 28p.

James, A.D. 1983. *Acacia mearnsii* de Wild: Handbook of Energy Crops. (Unpublished). Available from: http://www.newcrop.hort.purdue.edu/newcrop/duke_energy/Acaciamearnsii.htm [Accessed 05 May, 2001].

Jewitt, G.P.W. and Schulze, R.E. 1999. Verification of the ACRU model for forest hydrology and applications. *Water SA*, 25: 483-489.

Johnston, C.A. 2000. Geographic Information Systems in Ecology: Methods in Ecology. Blackwell Science, U.S.A.

Jordan, C.F. 1969. Derivation of leaf area index from quality of light on the forest floor. *Ecology*, 50: 663-666.

Justice, C.O. 1986. Monitoring East African vegetation using AVHRR data. *International Journal of Remote Sensing,* 6(8): 1335-1372.

Justice, C.O. and Townshend, J.R.G. 1981. Integrating ground data with remote sensing. In *Terrain Analysis and Remote Sensing*, edited by J.R.G. Townshend (London: George Allen and Unwin), pp. 38-58.

Kaufman, Y.J. and Remer, L.A. 1994. Detection of forests using MID-IR reflectance, an application for aerosol studies. *IEE Trans. Geosci. Remote Sens*., 32: 672-683.

Kauth, R.J. and Thomas, G.S. 1976. The tasseled cap - A graphic description of the spectral temporal development of agricultural crops as seen by Landsat. *Proceedings of the Symposium on Machine Processing of Remotely Sensed Data*, Perdue University, West Lafayette, Indiana, 41-51.

Knyazikhin, J.Y., Glassy, J. L., Privette, Y., Tian, A., Lotsch, Y., Zhang, Y., Wang, J. T., Morisette, P., Votava, R.B., Myneni, R. R., Nemani, S. and Running, W. 1999. MODIS Leaf Area Index (LAI) and Fraction of Photosynthetically Active Radiation Absorbed by Vegetation (FPAR) Product (MOD15) Algorithm Theoretical Basis Document. Available from: http://eospso.gsfc.nasa.gov/atbd/modistables.htm [Accessed July 3, 2001].

Kucharik, C.J., Norman, J.M., Mudock, L.M. and Gower, S.T. 1997. Characterizing canopy non-randomness with a multiband vegetation imager (MVI). *Journal of Geophysical Research,* 102(D24): 29:455-29,473. Available from: http://citeseer.nj.nec.com/context/889502/D [Accessed Sept 16, 2001].

Landsberg, J.J. and Waring, R.H. 1997. A generalized model of forest productivity using simplified concepts of radiation-use efficiency, carbon balance and partitioning. *Forest Ecology and Management,* 95: 209-228.

Lang, A.R.G. 1987. Simplified estimate of leaf area index from transmittance of the sun's beam. *Agricultural and Forest Meteorology*, 41: 179-186.

Lang, A.R.G. and Xiang, Y. 1986. Estimation of leaf area index from transmission of direct sunlight in discontinuous canopies. *Agricultural and Forest Meteorology*, 37: 229-243.

Leamer, R.W., Noriega, J.R. and Wiegand, C.L. 1978. Seasonal changes in two wheat cultivars. *Agronomy Journal,* 70: 113-118.

Le Maitre, D.C., Van Wilgen, B.W., Chapman, R.A. and Mckelly, D.H. 1996. Invasive plants and water resources in the Western Cape Province, South Africa: Modeling the consequences of a lack of management. *Journal of Applied Ecology,* 33: 161-172.

Leysen, M.M. and Goosens, R.E. 1991. Forest map updating in a GIS using high spatial resolution satellite data. In: EGIS'91, *Second European Conference on Geographical Information Systems,* Brussels, Belgium, April 2-5, 1991. Utrecht, The Netherlands: EGIS Foundation, 653-661.

LI-COR. 1990. LAI-2000 Plant Canopy Analyzer Instruction Manual. LI-COR Lincolin, Nebraska, USA.

Lillesand, T.M. and Kiefer, R.W. 2000 (4th ed). Remote Sensing and Image Interpretation. John Wiley & Sons, Inc. Singapore.

Lindsey, P. A. and Bassuk, N.L. 1992. A non-destructive image analysis technique for estimating whole-tree leaf area. *HortTechnology*. 2 (1): 66-72.

Little, E.L.Jr. 1983. Common Fuel Wood Crops: A Handbook for Their Identification. McClain Printing Co., Parsons. WV.

Lu, X.X., Wang, J. and Higitt, D.L. 2000. NDVI and its relationships with hydrological regimes in the Upper Yangtze. *Canadian Journal of Remote Sensing*, 26(5): 418-427.

Luckie, D.G. 1990. Advances in remote sensing technology for forest surveys and management. *Canadian Journal of Forest Research*, 20:464-483.

Lymburner, L., Beggs, P.J. and Jacobson, C.R. 2000. Estimation of canopy-average surface-specific leaf area using Landsat TM data. *Photogrammetric Engineering and Remote Sensing,* 66(2): 183-191.

Lyon, J.G., Yuan, D., Lunetta, R.S. and Elvidge, C.D. 1998. A change detection experiment using vegetation indices. *Photogrammetric Engineering and Remote Sensing,* 64(2): 143-150

Macdonald, I.A.W. 1984. Is the fynbos biome especially susceptible to invasion by alien plants? A re-analysis of available data. *South African Journal of Science*, 80:369-377.

Macdonald, I.A.W. and Jarman, M.L. (Eds) 1985. Invasive alien plants in the terrestrial ecosystems of Natal, South Africa. *South African National Scientific Programs.* Report No.118. CSIR. Pretoria.

MacFarlance, D.W., Green, E.J. and Burkhart, H.E. 2000. Population density influences assessment and application of site index. *Canadian Journal of Forestry Research,* 30: 1472-1475.

MacVicar, C.N., de Villiers, J.M., Loxton, R.F., Verster, E. and Von M Harmse, H.J. 1977. Soil Classification, a Binomial System for South Africa. Soil and Irrigation Research Institute, Department of Agricultural Technical Services, Pretoria, Science Bulletin 390, p 150.

Major, D.G., Schaalje, G.B., Asrar, G. and Kanemasu, E.T. 1986. Estimation of whole plant biomass and grain yield from spectral reflectance of cereals. *Canadian Journal of Remote Sensing*, 12(1): 47-54.

Maxwell, E.L. 1976. Multivariate system analysis of multispectral imagery. *Photogrammetric Engineering and Remote Sensing,* 42: 1173-1186.

McLeod, S.D. and Running, S.W. 1988. Comparing site quality indices and productivity in ponderosa pine stands of Western Montana. *Canadian Journal of Forest Research*, 18: 346-352.

McNaughton, K.G. and Jarvis, P.G. 1983. Predicting effects of vegetation changes on transpiration and evapotranspiration. In Water Deficits and Plant Growth, (Eds.) T.T. Kozlowski. Academic Press, London, pp 1-47.

McPherson, E.G. and Peper, P.J. 1998. Comparison of five methods for estimating leaf area index of open-grown deciduous trees. *Journal of Arboriculture* 24(2): 89-111.

Available from: http://wcufre.ucdavis.edu/comparison_of_five_methods_for_e.htm [Accessed May 10, 2001].

Miller, J.B. 1967. A formula for average foliage density. *Australian Journal of Botany*, 15: 141-144.

Miller, G.P., Fuchs, M., Hall, M.J., Asrar, G., Kanemasu, E.T. and Johnson, D.E. 1984. Analysis of seasonal multispectral reflectances of small grains. *Remote Sensing of Environment*, 14:153-157.

Misra, P.N., Wheeler, S.G. and Oliver, R.E. 1977. Landsat data from agricultural sites-crop signature analysis, *Proceedings of the 11th International Symposium on Remote Sensing of the Environment,* ERIM.

Mondi Forests, 2002. Management Plan - Paper Value Chain, Internal company document.

Monserud, R.A. 1984. Height growth and site index curves for in land Douglas-fir based on stem analysis date and forest habitat type. *Forest Science*, 20: 143-144.

Mthembu, S.L. 2001.Estimating Leaf Area Index (LAI) of Gum Tree (*Eucalptus grandis x camaldulensis*) using Remote Sensing Imagery and Licor-2000. M.Sc. Thesis, University of Natal, Pietermaritzburg, South Africa.

Nel, E.M., and Wessman, C.A. 1993. Canopy transmittance models for estimating forest leaf area index. *Canadian Journal of Forestry Research*, 23, 2579–2586.

Nelson, R. 1983. Detecting forest canopy change due to insect attack using Landsat MSS. *Photogrammetric Engineering and Remote Sensing*, 49: 1303-1314.

Nemani, R.L., Pierce, L.L. and Running, S. 1993. Forest ecosystem processes at the watershed scale: Sensitivity to remotely sensed leaf area index estimates. *International Journal of Remote Sensing,* 14(3): 2519-2534.

Nicholson, S.E. and Farrar, T.J. 1994. The influence of soil type on the relation between NDVI, rainfall, and soil-moisture in the semiarid Botswana: 1, NDVI response to rainfall. *Remote Sensing of Environment*, 50(2): 107-120.

Norman, J.M. and Campbell, G.S. 1989. Canopy structure. In: Plant Physiological Ecology: Field Methods and Instrumentation (Eds). R.W. Peary, J. Ehleringer, H.A. Mooney, and P.W. Rindel. Chapman and Hall, New York, New York, USA, pp 301-325.

Passiura, J.B. 1982. Hydraulic resistance of plants, constant or variable? *Australian Journal of plant physiology,* 11: 333-339.

Pearson, R.L. and Miller, L.D. 1972. Remote mapping of standing crop biomass for estimation of the productivity of the short grass prairie. *Eighth International Symposium on Remote Sensing of Environment,* University of Michigan, Ann Arbor, Mich., 1357-1381.

Peddle, D.R. and Johnson, R.L. 2000. Spectral mixture analysis of airborne remote sensing imagery for improved prediction of leaf area index in mountainous terrain, Kananaskis Alberta. *Canadian Journal of Remote Sensing,* 26(3): 177-188.

Peddle, D.R., Brunke, S.P and Hall, F.G. 2001. A comparison of spectral mixture analysis and ten vegetation indices for estimating boreal forest biophysical information from airborne data. *Canadian Journal of Remote Sensing,* 27(6); 627-635.

Perry, C.R. and Lautenschlager, L.F. 1984. Functional equivalence of spectral vegetation indices. *Remote Sensing of Environment,* 14: 169-182.

Perryman, A. 1996. Introduction to Remote Sensing and LARST Systems. Natural Resources Institute, Kent, U.K.

Peterson, D.L., Spanner, M.A., Running, S.W. and Teuber, K.B. 1987. Relationship of thematic mapper simulator data to leaf area index of temperate coniferous forests. *Remote Sensing of Environment,* 22: 323-341.

Phillips, J. 1973. The agricultural and related development of Tugela Basin and its influent surrounds. Natal Town and Regional Planning Report, Volume 19.

Pierce, L.L. and Running, S.W. 1988. Rapid estimation of coniferous forest leaf area index using portable integrating radiometer. *Ecology,* 69(6): 1762-1767.

Price, J.C. 1992. Estimating vegetation amount from visible and near infrared reflectances. *Remote Sensing of Environment,* 41: 29-34.

Puhr, C.B. and Donoghue, D.N.M. 2000. Remote sensing of upland conifer plantations using Landsat TM data: a case study from Galloway, southwest Scotland. *International Journal of Remote Sensing,* 21(4): 633-646.

Qi, J., Chehbouni, A., Huete, A.R., Kerr, Y.H. and Sorooshian, S. 1994. A modified soil adjusted vegetation index. *Remote sensing of Environment*, 48: 119-126.

Richardson, A.J. and Wiegand, C.L. 1977. Distinguishing vegetation from soil background information. *Photogrammetric Engineering and Remote Sensing*, 43: 1541-1552.

Rouse, J.W., Haas, R.H., Schell, J.A. and Deering, D.W. 1973. Monitoring vegetation systems in the Great Plains with ERTS. *Third ERTS Symposium,* NASA SP-351I: 309-317.

Rouse, J.W., Haas, R.H., Schell, J.A., Deering, D.W. and Harlan, J.C. 1974. Monitoring the vernal advancement of natural vegetation, NASA/ GSFC final Report, Greenbelt, MD, pp 371.

Rowntree, K.M. 1991. An assessment of the potential impact of alien invasive vegetation on the geomorphology of river channels in South Africa. *South African Journal of Aquatic Sciences,* 17:28-43.

Running, S.W., Peterson, D.L., Spanner, M.A. and Teuber, K.B. 1986. Remote Sensing of coniferous forest leaf area. *Ecology,* 67(1): 273-276.

Running, S.W., Loveland, T.R., Pierce, L.L., Nemani, R.R. and Hunt, E.R. 1995. A remote sensing based vegetation logic for global cover analysis. *Remote Sensing of Environment,* 51:39-48.

Runyon, J., Waring, R.H., Goward, S.N and Welles, J.M. 1994. Environmental limits on net primary production and light-use efficiency across the Oregon transect. *Ecological Applications*, 4: 226-237.

Sabins, F.F. 1997 (3rd ed). Remote Sensing: Principles and Interpretation. W.H. Freeman and Company, New York.

Sampson, D.A. and Allen, H.L. 1995. Direct and indirect estimates of leaf area index (LAI) for lodge pole and loblolly pine stands. *Trees*, 9: 119-122.

Schönau, A.R.G. 1969. A site evaluation study in black wattle. PhD Thesis, University of Stellenbosch, Unpublished.

Sellers, P.J. 1985. Canopy reflectance, photosynthesis and transpiration. *International Journal of Remote Sensing*, 6: 1335-1372.

Sherry, S.P. 1971. The Black Wattle (*Acacia mearnsii* De Wild.). City Printing Workers. University of Natal, Pietermaritzburg, South Africa.

Simmons, M. 1999. Acacia - An Introduction: Australian Plants Online. From "*Eucryphia*", newsletter of the Australian Plants Society (Tasmania), September 1999.

Singh, A. 1989. Digital change detection techniques using remotely sensed data. *International Journal of Remote Sensing*, 10: 9890-1003.

Smith, C.W. 2002a. Growth and yield prediction. In: Black Wattle: The South African Research Experience. Dunlop, R.W. and MacLenan, L.A. (ed) ICFR, Pietermaritzburg, pp 93-99.

Smith, C.W. 2002b. Institute of Commercial Forestry Research (ICFR), Pietermaritzburg. Personal Communication.

Smith, C.W. and Dunlop, R.W. 2002. Plantation establishment, re-establishment and regeneration. In: Black Wattle: The South African Research Experience. (Eds) Dunlop, R.W. and MacLennan, L.A. ICFR, Pietermaritzburg. pp: 37-46.

Smith, R.E., Moses, G. and Versfeld, D.B. 1992. Verification of heat pulse velocity technique for *Acacia mearnsii. South African Forestry Journal,* 163: 1-4.

Smith, N.J., Chen, J.M. and Black, T.A. 1993. Effects of clumping on estimates of stand leaf area index using the LI-COR LAI-2000. *Canadian Journal of Forest Research,* 23: 1940-1943.

Snowdon, P., Raison, J., Keith, H., Montagu, K., Bi, H., Ritson, P., Grierson, P., Adams, M., Burows, W. and Eamus, D. 2001. Protocol for Sampling Tree and Stand Biomass: National Carbon Accounting System Technical Report, No. 31, Australian Greenhouse Office.

Spanner, M.A., Pierce, L.L., Peterson, D.L. and Running, S.W. 1990. Remote sensing of temperate coniferous forest leaf area index. The influence of canopy closure, understorey vegetation and background reflectance. *International Journal of Remote Sensing*, 11: 95-111.

Spanner, M.A., Johnson, L., Miller, J., McCreight, R., Freemantle, J., Runyon, J. and Gong, P. 1994. Remote sensing of seasonal leaf area index across the Oregon transect. Ecological Applications, 4(2): 258-271.

Spurr, S.H. and Barnes, B.V. 1980. Forest Ecology. Wiley, New York.

Stein, R.1999. Focus Country Report: For the legal component of the IUCN global invasive species strategy for South Africa. Available from: http://psclasses.ucdavis.edu [Accessed Sept 4, 2001].

Stenberg, P., Linder, S., Smolander, H. and Flower-Ellis, J. 1994. Performance of the LAI-2000 plant canopy analyzer in estimating leaf area index of some Scots pine stands. *Tree Physiology,* 14: 981-995.

Stirton, C.H. 1987. Plant Invaders: Beautiful but Dangerous. Department of Nature and Environmental Conservation of the Cape Provincial Administration, Cape Town, South Africa.

Thomas, J.R., Namken, L.N. and Brown, R.G. 1971. Estimating leaf water content by reflectance measurements. *Agronomy Journal*, 63: 845-847.

Townshend, J.R.G., Gayler, J.R., Hardy, J.R., Jackson, M.J. and Baker, J. 1983. Preliminary analysis of Landsat-4 Thematic Mapper products. *International Journal of Remote Sensing*, 8: 817-828.

Tremble, 1994. GeoExplorer Operation Manual. Part Number (21281-00), Revision A. Trimble Navigation Limited, Sunnyvale, CA, U.S.A.

Tucker, C.J. 1977. Spectral estimation of grass canopy variables. *Remote Sensing of Environment,* 6: 11-26.

Tucker, C.J. 1979. Red and Photographic infrared combinations for monitoring vegetation. *Remote Sensing of Environment*, 8: 127-150.

van Laar, A. 1984. The estimation of the leaf area index for a mature *Pinus radiata* stand. *South African Forestry Journal*, 128: 8-11.

Veldtman, D.G., Rivers-Moore, N.A and Atkinson, P.R. 1995. Preliminary estimates of leaf area indices in Black Wattle (*Acacia mearnsii*). ICFR Annual Research Report, Pietermaritzburg, South Africa.

Versfeld, D.B., Le Maitre, D.C. and Chapman, R.A. 1998. Alien Invading Plants and Water Resources in South Africa: A Preliminary Assessment. WRC Report No. TT-99/98. CSIR No. ENV/S-C 97154.

Wang, Y.S., Miller, D.R., Welles, J.M. and Heisler, G.M. 1992. Spatial variability of canopy foliage in an oak forest measured with fisheye sensors. *Forest Science*, 38: 854-865.

Waring, R.H. 1985. Imbalanced forest ecosystems: assessment and consequences. *Forest Ecology and Management,* 12: 93-112.

Watts, W.R., Neilson, R.E. and Jarvis, P.G. 1976. Photosynthesis in *Sitka spruce* (*Picea sitchensis* [bong] Carr.) VII. Stomatal conductance and $14CO_2$ uptake in a forest canopy. *Journal of Applied Ecology,* 13: 623-638.

Weber, R.M. and Dunno, G.A. 2001. Riparian vegetation mapping and image processing techniques, Hopi Indian Reservation, Arizona. *Photogrammetric Engineering and Remote Sensing,* 67(2): 179-186.

Wells, J.M. 1990. Some indirect methods of estimating canopy structure. *Remote Sensing Reviews,* 5: 31-43.

Wiegand, C.L., Guasman, H.W., Cuellar, J.A., Gerbermann, A.H. and Richardson, A.J. 1974. Vegetation density as deduced from ERTS-1 MSS response, *Third ERTS Symposium*, NASA-SP-351, Vol. I, Sect. A, pp. 93-116.

Wolpert, J. 1999. Use of Aerial Imaging to Evaluate Vineyard Canopy Variability. University of California, Davis. Available from: http://www.avf.org/reports/9900v109.html [Accessed Aug 13, 2001].

Wulder. M.A., Ledrew, E.F., Lavigne, M.B. and Franklin, S.E. 1998. Aerial image texture information in the estimation of deciduous and mixed forest LAI. *Remote Sensing of Environment,* 64: 64-76.

Wullschleger, S.D., Meinzer, F.C. and Vertessy, R.A. 1998. A review of whole-plant water use studies in trees. *Tree Physiology,* 18: 499-512.

Yang, X., Miller, D.R. and Montogomery, M.E. 1993. Vertical distributions of foliage and biologically active radiation in a defoliated/ refoliated hardwood forest. *Agricultural and Forest Meteorology,* 67: 129-146.

Appendix 1

General characteristics of sample stands

Study site	Tree Age (yr)	Compart-ment No.	Latitude	Longitude	Altitude (m)	MAP (mm)	MedAP (mm)	MAT (°C)	Volume (m^3)	MAI (m^3ha^{-1} $annum^{-1}$)	Initial stocking (stems ha^{-1})	Final stocking (stems ha^{-1})
Bloemendal	4	014	29°33'	30°28'	819	875	854	18.0	73	18	2222	1981
	6	012	29°32'	30°28'	850	897	888	17.9	103	17	2222	1517
	8	009	29°32'	30°28'	850	897	888	17.9	114	14	2222	1455
	10	013	29°33'	30°28'	819	875	854	18.0	112	11	2222	1348
Mistley	3	A01	29°13'	30°37'	1134	1005	987	16.5	94	28	3000	1950
	5	B16	29°11'	30°39'	740	708	693	18.6	88	13	3000	1084
	7	B27	29°11'	30°39'	740	708	693	18.6	104	19	3000	1373
	11	C01A	29°13'	30°39'	1102	968	947	16.7	135	12	3000	1156
Seele	4	D27	29°14'	30°30'	1149	1105	1075	16.6	121	29	2222	1296
	7	E03	29°15'	30°31'	882	884	862	18.0	186	26	2222	1790
Mountain Home	8	D03	29°35'	30°16'	1244	1111	1064	16.0	160	20	2222	1650
	11	D01A	29°35'	30°16'	1244	1111	1064.1	16.0	198	17	2222	1728

MAP : Mean Annual Precipitation in mm.
MedAP : Median Annual Precipitation in mm.
MAT : Mean Annual Temperature in °C.
MAT : Mean Annual Increment in $m^3ha^{-1}annum^{-1}$.

Appendix 2

Sample Trees Biomass Determination

The main stages classically adopted for this type of study have been followed, that is:

- The sample trees were felled at ground level using a chainsaw.
- Tree height and height to the first limb carrying the live foliage were measured with a 50-meter measuring tape. The difference gives the crown length or crown depth.
- DBH and stem diameter at the base of the crown were measured using DBH tape and calipers.
- The crown was divided into three equal parts as upper, middle and lower crown zones.

Then the following parameters were measured:

A. Leaves

1. All leaves from the three crown zones were stripped by hand and placed in a plastic bag of known weight and the fresh weight was taken with a 30 kg spring balance in the field.
2. Small samples of leaves (replicated three times) representative of the upper, middle and lower crown zones were taken and placed in a zip-lock labeled bags and their fresh weight was determined with a more precise balance.
3. These small sample leaves were taken to the laboratory in a cooler box for leaf dry mass determination.
4. In the laboratory the leaf samples were dried to constant mass in an oven at 65^{o}C and the ratio of the wet and dry mass of these samples was used to calculate the dry leaf mass of the whole tree by multiplying it with the total wet leaf mass.
5. Other than the small leaf samples used for leaf dry mass determination ten random leaves from each of the three crown zones were picked, dipped in alcohol and preserved in a book or plant press to keep them flat.
6. The leaf area of the preserved flat leaves was measured with a LI-3100 Leaf Area Meter and they were dried to constant weight at 65^{o}C. Then the Specific Leaf Area

(SLA) of these sample leaves was determined as the ratio of leaf area to leaf dry mass.

7. The tree Leaf Area (LA) was calculated from the SLA and total leaf dry mass by using the equation:

   Leaf area (m2/kg)= Tree dry leaf mass (kg) x SLA (m^2/kg)

   and it was scaled up to the entire plot and canopy by taking the direct relationship of DBH and leaf area into consideration.
8. Finally the LAI was determined from the total leaf area and area measurement of the plot as:

   LAI= Total Leaf area of the trees in the plot / Plot area

B. Branches

1. Dry and live branches were weighed using a 30 kg spring balance in the field after being cut from the stem and put them separately.
2. Three sub-samples were taken for both dry and live branches with prunners of different size.
3. The samples were weighed in the field using a more precise 5 kg balance and were placed in plastic bags.
4. The samples were taken to the laboratory for drying.
5. Ratios of dry to wet mass were calculated for the sample branches dried in the laboratory.
6. The calculated ratios of dry to wet mass were used to scale up for branches on that particular tree by multiplying the total wet branch weight from the field by the ratio of dry to wet mass of the sample branches.

C. Bark

1. Each sample tree was debarked up to the pulpable part of the stem, i.e., up to 5cm diameter.
2. Three sub-samples were taken, weighed, placed into zip-lock bags, transported to the laboratory in a cooler box.

3. Samples were dried in the laboratory to constant weight at 65°C.
4. The ratio of dry to wet mass of the sample barks was calculated.
5. The ratio of dry to wet mass was used to scale up for tree bark weight by multiplying the total wet bark mass by the ratio of dry to wet sample bark.

D. Stem

1. Stem circumference (overbark and underbark) was measured at every 1.2m up to a diameter of 5 cm and the stem was cut at every 1.2m.
2. Fresh weight of the 1.2m stem chuncks up to a diameter of 5cm was taken in the field with a 30 kg spring balance and discs were cut every 1.2m with a chainsaw.
3. The discs were weighed fresh in the field, taken to the laboratory in plastic bags and dried to constant weight at 65°C.
4. Ratios of the dry to wet mass of the discs were calculated.
5. The dry weight was used to calculate the whole tree and plot stem dry weights by multiplying the total wet stem mass from the field by the ratio of the dry to wet mass of the sample discs dried.

Appendix 3

Scene Parameters

Scene ID	: 168-080 05-COT-2001
WRS identification	: 168-080
AcqDate	: 05-OCT-2001
AcqTime	: 07:39:01.128
Instrument	: ETM
Scene Size	: Quarter 3
Product format	: FAST
Processing Level	: 5
Number of spectral bands	: B1 B2 B3 B4 B5 B6L B7 B8 B6H
Scene Orientation Angle	: -8.29 [degrees]
Sun Angles [degrees]	: Azimuth: 57.12 Elevation 51.65
Number of Lines	: 3520
Number of Pixels per Line	: 3764
Vertical Pixel Resolution	: 30.0 [meters]
Horizontal Pixel Resolution	: 30.0 [meters]
Projection	: UTMS
Ellipsoid	: CLARKE 1880
Ephemeris	: from Definitive

Scene Center Location

Latitude	: S 029^{0}11'53"
Longitude	: E 030^{0}17'35"
Pixel Number	: 1882
Line Number	: 1760

Corner Location

Corner	Latitude	Longitude	Pixel No.	Line No.
1	S 028^{0}42'30"	E 029^{0}43'29"	1	1
2	S 028^{0}43'53"	E 030^{0}52'46"	3764	1
3	S 029^{0}39'35"	E 029^{0}41'40"	1	3520
4	S 029^{0}41'01"	E 030^{0}51'35"	3764	3520

Appendix 3 (Continued)

Scene Parameters

Scene ID	: 168-080 30-MAR-2002
WRS identification	: 168-080
AcqDate	: 30-MAR-2002
AcqTime	: 07:39:33.964
Instrument	: ETM
Scene Size	: Quarter 3
Product format	: FAST
Processing Level	: 5
Number of spectral bands	: B1 B2 B3 B4 B5 B6L B7 B8 B6H
Scene Orientation Angle	: -8.32 [degrees]
Sun Angles [degrees]	: Azimuth: 52.12 Elevation 42.90
Number of Lines	: 3520
Number of Pixels per Line	:3768
Vertical Pixel Resolution	: 30.0 [meters]
Horizontal Pixel Resolution	: 30.0 [meters]
Projection	: UTMS
Ellipsoid	: CLARKE 1880
Ephemeris	: from Definitive

Scene Center Location

Latitude	: S 029^{0}11'53"
Longitude	: E 030^{0}17'35"
Pixel Number	: 1882
Line Number	: 1760

Corner Location

Corner	Latitude	Longitude	Pixel No.	Line No.
1	S 028^{0}42'30"	E 029^{0}43'55"	1	1
2	S 028^{0}43'53"	E 030^{0}53'16"	3768	1
3	S 029^{0}39'35"	E 029^{0}42'05"	1	3520
4	S 029^{0}41'01"	E 030^{0}52'05"	3764	3520

Appendix 4a

Average Specific Leaf Area of Sample Trees

Study site	Tree Age (yr)	Tree No.	SLA (m^2kg^{-1}) of the crown zones Upper	Middle	Lower	Mean Tree SLA	Mean SLA (m^2kg^{-1})
Bloemendal	4	1	8.514	9.111	10.571	9.399	8.207
	4	2	7.962	8.169	9.200	8.444	
	4	3	7.031	7.678	8.992	7.900	
	4	4	6.525	6.817	7.912	7.085	
	6	1	7.509	8.343	9.018	8.290	7.401
	6	2	6.975	7.026	7.487	7.163	
	6	3	6.610	7.112	7.460	7.061	
	6	4	6.876	6.996	7.399	7.090	
	8	1	7.197	7.843	8.698	7.913	7.819
	8	2	6.352	7.664	8.025	7.347	
	8	3	7.748	8.187	8.645	8.193	
	8	4	7.786	7.928	7.758	7.824	
	10	1	7.313	7.784	7.846	7.648	7.834
	10	2	6.971	7.890	7.596	7.486	
	10	3	7.877	7.798	9.541	8.405	
	10	4	7.114	8.097	8.181	7.797	
Mistley	3	1	11.036	11.922	11.672	11.543	8.848
	3	2	8.869	9.176	9.514	9.186	
	3	3	7.434	7.728	7.980	7.714	
	3	4	6.480	6.905	7.461	6.949	
	5	1	9.809	10.274	10.164	10.082	8.119
	5	2	7.052	7.170	7.785	7.336	
	5	3	6.980	8.163	7.968	7.704	
	5	4	6.634	7.539	7.889	7.354	
	7	1	8.005	8.551	10.428	8.995	8.157
	7	2	7.166	8.512	9.828	8.502	
	7	3	7.222	8.577	9.037	8.279	
	7	4	6.146	6.793	7.623	6.854	
	11	1	7.579	9.768	9.416	8.921	8.104
	11	2	7.002	8.123	9.432	8.186	
	11	3	7.085	7.253	7.799	7.379	
	11	4	6.940	7.957	8.896	7.931	

Tree No1: stands for small size tree from the sample plot

Tree No2: Medium size

Tree No3: Large size

Tree No4: Very large size tree

The Upper SLA values are mean SLA values of ten randomly selected leaves from the upper crown zone, and the same applies to the middle and lower SLA values.

Appendix 4a (continued)

Average Specific Leaf Area of Sample Trees

Study site	Tree Age (yr)	Tree No	SLA (m^2kg^{-1}) of the crown zones Upper	Middle	Lower	Mean Tree SLA	Mean SLA (m^2kg^{-1})
Seele	4	1	7.909	7.487	9.893	8.430	8.360
	4	2	7.907	8.420	9.047	8.458	
	4	3	7.841	8.299	9.105	8.415	
	4	4	7.575	7.885	8.957	8.139	
	7	1	9.159	9.754	10.352	9.755	8.682
	7	2	8.035	8.976	10.381	9.131	
	7	3	7.882	8.217	9.864	8.654	
	7	4	7.060	7.111	7.398	7.190	
Mountain Home	8	1	8.416	10.058	9.295	9.256	8.558
	8	2	7.706	7.813	8.817	8.112	
	8	3	8.081	8.232	9.662	8.658	
	8	4	7.181	7.695	9.744	8.207	
	11	1	9.720	10.371	10.801	10.297	9.283
	11	2	8.483	9.294	12.184	9.987	
	11	3	7.385	7.295	8.902	7.861	
	11	4	7.968	9.228	9.768	8.988	

Tree No1: stands for small size tree from the sample plot

Tree No2: Medium size

Tree No3: Large size

Tree No4: Very large size tree

The Upper SLA values are mean SLA values of ten randomly selected leaves from the upper crown zone, and the same applies to the middle and lower SLA values.

Appendix 4b

Statistical Means of SLA, LA, LAI

	Parameter	Mean SLA (m^2kg^{-1})	Mean Tree LA (m^2)	Mean Plot LA (m^2)	Mean LAI
Over all sites	Site - Bloemendal	7.82	27.90	1065.66	3.30
	Mistley	8.31	56.60	1080.53	3.35
	Seele/Mountain Home	8.72	71.70	1535.11	4.75
	Age group - One	8.47	49.40	1105.90	3.42
	Two	8.07	42.90	1182.68	3.66
	Three	8.18	48.00	1239.63	3.84
	Four	8.41	67.90	1381.52	4.28
	Crown depth – Upper	7.63			
	Middle	8.23			
	Lower	8.99			
Within sites	Bloemendal				
	Age group - One	8.21	27.30		
	Two	7.40	20.00		
	Three	7.82	31.60		
	Four	7.84	32.60		
	Crown depth – Upper	7.27			
	Middle	7.78			
	Lower	8.40			
	Mistley				
	Age group - One	8.85	51.20		
	Two	8.12	42.80		
	Three	8.16	48.80		
	Four	8.10	83.70		
	Crown depth – Upper	7.59			
	Middle	8.40			
	Lower	8.93			
	Seele/Mountain Home				
	Age group - One	8.36	69.70		
	Two	8.68	65.90		
	Three	8.56	63.50		
	Four	9.28	87.50		
	Crown depth – Upper	8.02			
	Middle	8.51			
	Lower	9.64			

Appendix 4c
Sample Trees Leaf Area

Study site	Tree Age (yr)	Tree No	DBH (cm)	Tree height (m)	Crown depth (m)	Height to 1st limb (m)	SLA (m^2kg^{-1})	Total Leaves dry mass (kg)	LA (m^2)
Bloemendal	4	1	6.4	10.4	4.4	6.0	9.40	2.484	23.35
	4	2	8.8	13.4	6.3	7.1	8.44	3.429	28.95
	4	3	10.6	14.6	7.9	6.7	7.90	4.410	34.84
	4	4	12.4	14.6	7.2	7.4	7.09	3.131	22.18
	6	1	9.0	15.1	6.3	8.8	8.29	1.782	14.77
	6	2	11.1	17.8	6.2	11.6	7.16	1.767	12.65
	6	3	13.0	17.5	7.9	9.6	7.06	3.581	25.29
	6	4	15.0	17.4	7.8	9.6	7.09	3.842	27.24
	8	1	10.1	16.2	6.6	9.6	7.91	2.132	16.87
	8	2	12.0	17.4	7.8	9.6	7.35	2.800	20.57
	8	3	14.1	17.2	6.9	10.2	8.19	5.819	47.68
	8	4	15.9	17.7	9.3	8.4	7.82	5.260	41.15
	10	1	10.4	16.8	5.7	11.1	7.65	1.568	11.99
	10	2	12.6	17.8	6.2	11.6	7.49	3.094	23.16
	10	3	14.3	19.6	5.5	14.0	8.41	5.929	49.83
	10	4	17.1	18.8	7.6	11.2	7.80	5.799	45.21
Mistley	3	1	7.0	10.3	4.3	6.0	11.54	1.053	12.15
	3	2	9.0	14.1	4.9	9.2	9.19	2.068	19.00
	3	3	10.9	14.2	5.8	8.4	7.71	2.301	17.74
	3	4	13.2	16.2	7.8	8.4	6.95	5.199	36.13
	5	1	7.9	13.9	3.3	10.6	10.08	1.043	10.51
	5	2	10.3	15.9	3.9	12.0	7.34	1.880	13.80
	5	3	11.8	16.0	5.8	10.2	7.70	2.630	20.25
	5	4	13.2	15.6	7.2	8.4	7.35	4.591	33.74
	7	1	9.8	15.7	6.1	9.6	8.99	1.263	11.35
	7	2	11.5	16.0	6.4	9.6	8.50	1.914	16.27
	7	3	13.5	17.9	10.7	7.2	8.28	2.634	21.81
	7	4	15.6	19.2	6.0	13.2	6.85	5.363	36.74
	11	1	12.3	19.8	9.1	10.7	8.92	2.339	20.86
	11	2	14.8	19.2	9.1	10.1	8.19	2.592	21.23
	11	3	17.6	22.1	6.3	15.8	7.38	4.095	30.22
	11	4	19.8	21.7	6.7	15.0	7.93	7.754	61.49

Appendix 4c (Continued)

Sample Trees Leaf Area

Study site	Tree Age (yr)	Tree No	DBH (cm)	Tree height (m)	Crown depth (m)	Height to 1st limb (m)	SLA (m^2kg^{-1})	Total Leaves dry mass (kg)	LA (m^2)
Seele	4	1	9.3	15.6	4.4	10.8	8.43	2.408	20.30
	4	2	11.5	17.2	5.2	12.0	8.46	2.296	19.42
	4	3	13.8	18.2	8.6	9.6	8.42	4.456	37.52
	4	4	15.9	19.8	6.6	13.2	8.14	4.396	35.78
	7	1	9.1	17.6	5.6	12.0	9.76	0.961	9.38
	7	2	12.5	19.7	5.3	14.4	9.13	2.086	19.05
	7	3	15.3	22.2	7.8	14.4	8.65	4.482	38.77
	7	4	18.2	23.1	6.3	16.8	7.19	7.136	51.31
Mountain Home	8	1	10.8	15.8	7.4	8.4	9.26	0.688	6.37
	8	2	13.1	19.6	9.6	10.0	8.11	3.844	31.17
	8	3	15.6	20.1	8.1	12.0	8.66	3.695	32.00
	8	4	17.2	20.4	10.8	9.6	8.21	4.176	34.28
	11	1	9.3	14.4	8.0	6.4	10.30	1.576	16.23
	11	2	12.3	18.8	6.0	12.8	9.99	1.839	18.37
	11	3	15.0	22.8	6.0	16.8	7.86	2.632	20.69
	11	4	18.3	23.3	6.5	16.8	8.99	4.744	42.65

Appendix 5

Plant Area Index (PAI)

Study site	Tree Age (yr)	Replication	PAI	MTA	STDERR	Mean PAI	Mean STDERR
Bloemendal	4	1	3.39	57	0.012		
	4	2	3.31	58	0.024		
	4	3	3.35	54	0.042	3.35	0.026
	6	1	2.61	60	0.010		
	6	2	2.61	58	0.038		
	6	3	2.65	59	0.021	2.62	0.023
	8	1	2.68	56	0.013		
	8	2	2.75	54	0.007		
	8	3	2.93	56	0.019	2.79	0.013
	10	1	2.62	60	0.017		
	10	2	2.64	58	0.025		
	10	3	2.58	58	0.032	2.61	0.025
Mistley	3	1	3.23	60	0.025		
	3	2	3.27	59	0.029		
	3	3	3.30	59	0.04	3.27	0.031
	5	1	3.14	57	0.032		
	5	2	3.21	60	0.029		
	5	3	3.25	58	0.031	3.20	0.031
	7	1	3.27	61	0.028		
	7	2	3.30	61	0.025		
	7	3	3.36	62	0.034	3.31	0.029
	11	1	3.07	59	0.026		
	11	2	3.09	58	0.017		
	11	3	3.10	59	0.036	3.09	0.026
Seele	4	1	3.53	60	0.031		
	4	2	3.54	58	0.022		
	4	3	3.57	58	0.013	3.55	0.022
	7	1	3.79	59	0.029		
	7	2	3.80	59	0.038		
	7	3	3.79	60	0.048	3.79	0.038
Mountain Home	8	1	3.94	58	0.074		
	8	2	3.96	58	0.087		
	8	3	3.99	57	0.082	3.96	0.081
	11	1	4.64	57	0.061		
	11	2	4.59	57	0.068		
	11	3	4.63	57	0.062	4.62	0.064

MTA= Mean tilt angle in degrees

STDERR= Standard errors of measurements.

Each PAI value in the three replications is an average of twelve readings.

Appendix 6

General characteristics of sample trees (Biomass determination)

Study Site: Bloemendal

Tree Age (yr)	Tree No	DBH (cm)	Tree height (m)	Crown depth (m)	Height to 1st limb (m)	Bark (Wet, kg)	Bark (Dry, kg)	Dead Branch (Wet, kg)	Dead Branch (Dry, kg)	Live Branch (Wet, kg)	Live Branch (Dry, kg)	Stem (Wet, kg)	Stem (Dry, kg)
4	1	6.4	10.4	4.4	6.0	1.604	0.715	0.305	0.268	1.638	0.802	9.612	6.129
4	2	8.8	13.4	6.3	7.1	6.323	3.230	0.585	0.505	12.297	6.243	26.519	17.667
4	3	10.6	14.6	7.9	6.7	7.157	3.866	1.344	1.198	24.416	12.499	38.893	25.384
4	4	12.4	14.6	7.2	7.4	9.815	4.350	3.371	2.775	11.842	5.714	45.586	26.946
6	1	9.0	15.1	6.3	8.8	6.980	3.648	3.101	2.669	15.111	9.371	36.553	25.888
6	2	11.1	17.8	6.2	11.6	10.476	5.356	4.429	3.778	9.600	5.025	53.717	37.393
6	3	13.0	17.5	7.9	9.6	17.010	8.002	5.041	4.128	32.088	17.553	87.073	59.057
6	4	15.0	17.4	7.8	9.6	18.144	8.989	7.522	5.942	15.113	7.758	94.041	62.564
8	1	10.1	16.2	6.6	9.6	10.669	5.081	4.718	3.888	10.445	5.505	42.477	28.677
8	2	12.0	17.4	7.8	9.6	11.036	5.419	3.990	3.257	1.644	10.958	68.090	46.562
8	3	14.1	17.2	6.9	10.2	24.928	11.991	3.699	2.864	42.145	21.909	96.707	65.700
8	4	15.9	17.7	9.3	8.4	23.693	11.304	11.985	9.751	36.388	19.163	116.791	79.846
10	1	10.4	16.8	5.7	11.1	12.561	6.191	8.686	7.459	18.839	10.350	57.394	39.824
10	2	12.6	17.8	6.2	11.6	14.064	7.390	16.092	13.298	25.149	14.374	83.654	58.375
10	3	14.3	19.6	5.5	14.0	28.144	14.063	10.216	8.925	26.406	16.418	131.586	94.813
10	4	17.1	18.8	7.6	11.2	29.515	14.930	10.590	9.741	39.175	22.410	156.669	112.295

Tree No1: stands for small size tree from the sample plot

Tree No2: Medium size

Tree No3: Large size

Tree No4: Very large size tree

Appendix 6 (continued)

General characteristics of sample trees (Biomass determination)

Study Site: Mistley

Tree Age (yr)	Tree No	DBH (cm)	Tree height (m)	Crown depth (m)	Height to 1st limb (m)	Bark (Wet, kg)	Bark (Dry, kg)	Dead Branch (Wet, kg)	Dead Branch (Dry, kg)	Live Branch (Wet, kg)	Live Branch (Dry, kg)	Stem (Wet, kg)	Stem (Dry, kg)
3	1	7.0	10.3	4.3	6.0	5.250	2.325	0.432	0.337	13.623	5.795	16.375	7.520
3	2	9.0	14.1	4.9	9.2	6.912	2.960	0.529	0.430	12.921	6.096	45.203	21.090
3	3	10.9	14.2	5.8	8.4	11.381	5.054	2.582	2.138	13.000	5.809	61.505	30.000
3	4	13.2	16.2	7.8	8.4	17.235	7.272	1.125	0.898	29.059	11.525	58.309	29.768
5	1	7.9	13.9	3.3	10.6	4.593	2.138	1.857	1.554	7.606	3.568	25.016	15.144
5	2	10.3	15.9	3.9	12.0	10.280	4.406	1.956	1.673	10.836	5.107	51.332	30.908
5	3	11.8	16.0	5.8	10.2	11.055	5.123	2.905	2.494	14.442	7.116	67.679	41.959
5	4	13.2	15.6	7.2	8.4	14.254	6.588	2.929	2.397	28.831	13.860	85.746	51.120
7	1	9.8	15.7	6.1	9.6	10.179	5.182	5.326	4.382	19.381	10.184	47.849	29.906
7	2	11.5	16.0	6.4	9.6	14.571	7.128	8.464	7.096	17.363	8.850	57.835	35.549
7	3	13.5	17.9	10.7	7.2	15.835	7.587	3.788	3.122	43.873	23.701	97.157	63.060
7	4	15.6	19.2	6.0	13.2	29.413	14.106	16.889	13.329	43.308	21.115	161.457	98.655
11	1	12.3	19.8	9.1	10.7	17.654	8.114	2.376	1.828	24.341	12.757	99.733	62.354
11	2	14.8	19.2	9.1	10.1	30.336	15.605	3.000	2.283	44.425	26.174	151.617	97.202
11	3	17.6	22.1	6.3	15.8	41.835	21.052	16.351	13.855	43.529	22.105	223.121	143.549
11	4	19.8	21.7	6.7	15.0	52.028	26.718	36.378	31.157	70.671	38.126	324.147	173.231

Tree No1: stands for small size tree from the stand plot

Tree No2: Medium size

Tree No3: Large size

Tree No4: Very large size tree

Appendix 6 (continued)

General characteristics of sample trees (Biomass determination)

Study Site: Seele and Mountain Home

Tree Age (yr)	Tree No	DBH (cm)	Tree height (m)	Crown depth (m)	Height to 1st limb (m)	Bark (Wet, kg)	Bark (Dry, kg)	Dead Branch (Wet, kg)	Dead Branch (Dry, kg)	Live Branch (Wet, kg)	Live Branch (Dry, kg)	Stem (Wet, kg)	Stem (Dry, kg)
4	1	9.3	15.6	4.4	10.8	7.853	3.273	0.619	0.508	11.461	5.141	46.760	24.993
4	2	11.5	17.2	5.2	12.0	12.474	5.006	4.644	3.837	18.915	8.163	81.384	39.681
4	3	13.8	18.2	8.6	9.6	17.946	7.675	1.185	0.968	28.000	12.997	108.940	59.171
4	4	15.9	19.8	6.6	13.2	23.265	10.004	4.476	3.662	25.337	11.904	147.969	78.076
7	1	9.1	17.6	5.6	12.0	7.920	3.295	2.070	1.677	8.634	4.150	43.785	24.439
7	2	12.5	19.7	5.3	14.4	14.884	6.732	2.339	1.981	15.145	7.638	93.499	51.860
7	3	15.3	22.2	7.8	14.4	26.972	12.416	6.214	5.311	23.646	11.504	197.224	104.276
7	4	18.2	23.1	6.3	16.8	38.182	15.906	9.560	8.052	30.388	15.089	217.162	144.186
8	1	10.8	15.8	7.4	8.4	9.571	4.753	3.710	2.852	13.950	6.784	54.318	30.807
8	2	13.1	19.6	9.6	10.0	20.683	9.790	2.212	1.683	31.877	16.345	117.592	70.504
8	3	15.6	20.1	8.1	12.0	23.854	11.445	2.706	2.009	33.820	16.461	156.976	88.105
8	4	17.2	20.4	10.8	9.6	30.585	12.537	6.274	4.972	37.018	16.978	209.245	127.714
11	1	9.3	14.4	8.0	6.4	7.880	3.789	0.305	0.255	8.747	4.962	39.272	24.301
11	2	12.3	18.8	6.0	12.8	17.891	8.982	2.667	2.215	9.352	4.939	93.559	59.450
11	3	15.0	22.8	6.0	16.8	33.068	15.980	11.611	9.472	24.288	13.212	195.113	126.432
11	4	18.3	23.3	6.5	16.8	41.445	17.800	7.430	6.065	32.048	16.830	236.815	148.258

Tree No1: stands for small size tree from the sample plot

Tree No2: Medium size

Tree No3: Large size

Tree No4: Very large size tree